FEM based Virtual Prototyping and Design of Third Harmonic Excitation System

for

Low Voltage Brushless Alternators

Thesis submitted in partial fulfillment of the requirements
for the award of the Degree of
Doctor of Philosophy in Engineering
under the Faculty of Engineering

by

Jiji K. S.
(Reg. No. 3679)

under the guidance of
Prof. (Dr.) Jayadas N. H. (Guide)
Prof. (Dr.) C. A. Babu (Co-Guide)

School of Engineering
Cochin University of Science and Technology,
Kochi - 682 022

May 2015

FEM based Virtual Prototyping and Design of Third Harmonic Excitation System

for

Low Voltage Brushless Alternators

Ph.D Thesis under the Faculty of Engineering

Author
Jiji K. S.
Research Scholar
School of Engineering
Cochin University of Science and Technology.

E-mail: jijiks@gectcr.ac.in

Under the supervision of
Dr. Jayadas N. H.
Dr. C. A. Babu

School of Engineering,
Cochin University of Science and Technology,
Kochi - 682 022.

School of Engineering
Cochin University of Science and Technology, Kochi - 682 022

Certificate

Certified that the thesis titled **FEM based Virtual Prototyping and Design of Third Harmonic Excitation System for Low Voltage Brushless Alternators** is a bona-fide record of the research work carried out by Jiji K. S. under our supervision in Faculty of Engineering, Cochin University of Science and Technology. The work presented in this thesis or part thereof has not been presented for any degree from any other institution.

Dr. Jayadas N. H. (Supervising Guide)
Associate Professor,
Division of Mechanical Engineering

Dr. C. A. Babu (Co-Guide)
Professor,
Division of Electrical Engineering

Declaration

It is declared that the thesis titled **FEM based Virtual Prototyping and Design of Third Harmonic Excitation System for Low Voltage Brushless Alternators** is a bona-fide record of the research work carried out by me under the guidance and supervision of Prof. (Dr.) Jayadas N. H. (Guide), Associate Professor, Division of Mechanical Engineering and Prof. (Dr.) C. A. Babu, (Co-Guide), Professor, Division of Electrical Engineering, School of Engineering, Cochin University of Science and Technology, Cochin - 682 022. This work or any part thereof has not been presented for the award of any degree from any other institution.

<div align="right">

Jiji K. S.
Reg. No. 3679
Research Scholar
School of Engineering
Cochin University of Science and Technology.

</div>

Curriculum Vitae

Jiji K. S. was born in Ernakulam District of Kerala, India in 1968. She obtained her B. Tech Degree in Electrical Engineering securing third rank, from Kerala University in the year 1990 and further completed M. Tech in Computer and Information Science from Cochin University of Science and Technology, Kochi in the year 2004. She is having 8 years of industrial experience in the areas of Alternator Design, Quality Assurance and Materials Management in Kerala Electrical & Allied Engineering Company Ltd., Kasaragod Unit, Kerala. She got selected through PSC, Govt. of Kerala for appointment as Lecturer in Electrical Engineering in 1999. Since then, she has been teaching in Government Engineering Colleges in Kerala. Presently she is working as Assistant Professor in Electrical Engineering Department at Government Engineering College, Thrissur, Kerala. She has so far published two research papers in international journals and presented more than fifteen papers in international/national conferences. Her areas of interest include Computational Electromagnetics, Special Electrical Machines and Finite Element Analysis of Electro-magnetic Devices.

Acknowledgement

At the outset, I thank God Almighty for providing me the opportunity, willpower and knowledge for successful completion of this research work.

I would like to express my profound gratitude to Dr. Jayadas N. H., Associate Professor and Head, Division of Mechanical Engineering, School of Engineering, Cochin University of Science and Technology, for his valuable guidance, timely advice, suggestions and personal attention as supervising guide and also for being a source of constant inspiration and motivation during the course of this research work. Heartfelt thanks are due to him for all the encouragement and freedom given to me for pursuing research on my line of thought. I was able to successfully complete the work and deliver this thesis only because of his able guidance and immense patience.

I am much grateful to my co-guide, Dr. C. A. Babu, Professor, Division of Electrical Engineering, Cochin University of Science and Technology, for his guidance, valuable suggestions, continuous encouragement and constant support, in this research work. I express my sincere thanks to him for the support given to me during critical phases of the research work.

I place on record my deep sense of gratitude to Dr. V. N. Narayanan Nampoothiri, Professor, Division of Mechanical Engineering, Cochin University of Science and Technology, and member of the Doctoral Committee, for continuous support throughout the period of research.

I am extremely thankful to Cdr. (Retd) K. Shamsudeen, Managing Director, Kerala Electrical and Allied Engineering Co. Ltd.,

Abstract

Salient pole brushless alternators coupled to IC engines are extensively used as stand-by power supply units for meeting industrial power demands. Design of such generators demands high power to weight ratio, high efficiency and low cost per KVA output. Moreover, the performance characteristics of such machines like voltage regulation and short circuit ratio (SCR) are critical when these machines are put into parallel operation and alternators for critical applications like defence and aerospace demand very low harmonic content in the output voltage. While designing such alternators, accurate prediction of machine characteristics, including total harmonic distortion (THD) is essential to minimize development cost and time.

Total harmonic distortion in the output voltage of alternators should be as low as possible especially when powering very sophisticated and critical applications. The output voltage waveform of a practical AC generator is replica of the space distribution of the flux density in the air gap and several factors such as shape of the rotor pole face, core saturation, slotting and style of coil disposition make the realization of a sinusoidal air gap flux wave impossible. These flux harmonics introduce undesirable effects on the alternator performance like high neutral current due to triplen harmonics, voltage distortion, noise, vibration, excessive heating and also extra losses resulting in poor efficiency, which in turn necessitate de-rating of the machine especially when connected to non-linear loads. As an important control unit of brushless alternator, the excitation system and its dynamic performance has a direct impact on alternator's stability and reliability.

The thesis explores design and implementation of an excitation

system utilizing third harmonic flux in the air gap of brushless alternators, using an additional auxiliary winding, wound for $1/3^{rd}$ pole pitch, embedded into the stator slots and electrically isolated from the main winding. In the third harmonic excitation system, the combined effect of two auxiliary windings, one with $2/3^{rd}$ pitch and another third harmonic winding with $1/3^{rd}$ pitch, are used to ensure good voltage regulation without an electronic automatic voltage regulator (AVR) and also reduces the total harmonic content in the output voltage, cost effectively.

The design of the third harmonic winding by analytic methods demands accurate calculation of third harmonic flux density in the air gap of the machine. However, precise estimation of the amplitude of third harmonic flux in the air gap of a machine by conventional design procedures is difficult due to complex geometry of the machine and non-linear characteristics of the magnetic materials. As such, prediction of the field parameters by conventional design methods is unreliable and hence virtual prototyping of the machine is done to enable accurate design of the third harmonic excitation system.

In the design and development cycle of electrical machines, it is recognized that the use of analytical and experimental methods followed by expensive and inflexible prototyping is time consuming and no longer cost effective. Due to advancements in computational capabilities over recent years, finite element method (FEM) based virtual prototyping has become an attractive alternative to well established semi-analytical and empirical design methods as well as to the still popular trial and error approach followed by the costly and time consuming prototyping. Hence, by virtually prototyping the alternator using FEM, the important performance characteristics of the machine are predicted.

Design of third harmonic excitation system is done with the help of results obtained from virtual prototype of the machine. Third harmonic excitation (THE) system is implemented in a 45 KVA

experimental machine and experiments are conducted to validate the simulation results. Simulation and experimental results show that by utilizing third harmonic flux in the air gap of the machine for excitation purposes during loaded conditions, triplen harmonic content in the output phase voltage is significantly reduced. The prototype machine with third harmonic excitation system designed and developed based on FEM analysis proved to be economical due to its simplicity and has the added advantage of reduced harmonics in the output phase voltage.

Key words: Brushless Alternators, Finite Element Method, Third harmonic excitation, Total harmonic distortion, Triplen harmonics, Virtual prototyping.

Contents

List of Figures

List of Tables

List of Abbreviations

ABS	American Bureau of Shipping
AC	Alternating Current
AVR	Automatic Voltage Regulator
BEM	Boundary Element Method
BIS	Bureau of Indian Standards
BSI	British Standards Institution
BV	Bureau Veritas
CAD	Computer Aided Design
DC	Direct Current
DG	Diesel Generator
EMF	Electro Motive Force
FDM	Finite Difference Method
FE	Finite Element
FEA	Finite Element Analysis
FEM	Finite Element Method
FVM	Finite Volume Method
IACS	International Association of Classification Societies
IC	Internal Combustion
IEC	International Electro-technical Commission
ISO	International Organisation for Standardisation
KVA	Kilo Volt Ampere
LR	Lloyds Register
MMF	Magneto Motive Force
MoM	Method of Moments

MVP	Magnetic Vector Potential
NEMA	National Electrical Manufacturer's Association
NR	Newton Raphson
OCC	Open Circuit Characteristic
p.f.	power factor
p.u.	per unit
PMBL	Permanent Magnet Brushless
PMG	Permanent Magnet Generator
PMSG	Permanent Magnet Synchronous Generator
PWM	Pulse Width Modulation
r.m.s.	Root mean square
SCR	Short Circuit Ratio
THD	Total Harmonic Distortion
THE	Third Harmonic Excitation
THW	Third Harmonic Winding
TVD	Transient Voltage Dip
TVR	Transient Voltage Rise
VP	Virtual Prototyping
VR	Voltage Regulation

List of Symbols

A	Magnetic vector potential
A_F	Current density of field winding
$\hat{A}$	Approximate solution of A
B	Magnetic flux density
B_{rad}	Radial component of flux density
B_{tan}	Tangential component of flux density
B_1	Fundamental component of flux density
B_3	Third harmonic flux density
C_l	Leakage coefficient
D	Electric flux density
E	Electric field strength
H	Magnetic field strength
I_d	Direct axis current
I_m	Maximum value of AC current
I_q	Quadrature axis current
J	Jacobian Matrix
L_i	Net iron length of core
L'	Core length
N_i	Shape function
P	Point in the analysis domain
R	Residue
V_1	rms value of fundamental voltage
V_n	rms value of nth harmonic voltage
W	Weight function

X_d	Direct axis reactance
X_q	Quadrature axis reactance
f	Frequency
f_3	Third harmonic frequency
k_c	Carter's coefficient
l_e	Effective length of conductor
l_g	Length of air gap
l'_g	Equivalent air gap length considering saturation
n	Order of harmonic component
$\hat{n}$	Outward unit vector
t	time
w_p	Width of pole
x	Distance along stator frame
Γ	Domain boundary
Λ	Air gap permeance
Λ_0	Mean value of permeance
$\hat{\Lambda}_n$	Peak amplitude of n_{th} harmonic component of permeance
Λ_P	Permeability over a pole pitch
Φ_s	Phase angle between stator current and voltage
Θ	Current linkage
β	Angle dependant on the winding construction
δ	Current density
ϵ	Electric permittivity
ζ	Shape function in terms of area coordinates
μ	Magnetic permeability
ν	Magnetic reluctivity
ξ_i	Area coordinates
ρ	Electric charge density
σ	Electric conductivity
τ_p	Pole pitch
υ	Air gap MMF
υ_F	Field winding MMF
υ_s	Instantaneous value of stator MMF
$\upsilon_{s,1}$	Instantaneous value of fundamental stator MMF

$\hat{v}_{s,1}$	Peak amplitude of fundamental stator MMF
$v_{s,n}$	Instantaneous value of nth harmonic stator MMF
ϕ_T	Total flux
ϕ_U	Useful flux
ψ	Flux linkage
ψ_d	Direct axis flux linkage
ψ_q	Quadrature axis flux linkage
ω	Angular frequency
ω_m	Mechanical speed of rotor

Chapter 1

Introduction

1.1 Overview of Brushless Alternators

Low voltage brushless alternators are primarily used as standby
power supply units with internal combustion (IC) engines as
prime movers. Of late, these are also being used as booster power
plants to meet peak load requirements of industrial consumers in
order to reduce cost. Power generation from renewable energy
sources which is gaining importance currently also demand dis-
tributed generation. In view of the fact that embedded generation
even of modest rating can contribute to peak load management,
widely dispersed generating sets have scope for inclusion in power
plant scheduling programs by power utilities. In this scenario, it
is obvious that output parameters, operating characteristics and
performance of small generating sets have gained importance in
recent years.

An alternating current (AC) generator set intended for commer-
cial purpose generally consists of a suitably governed IC engine as
prime mover, usually a diesel engine, directly coupled to a brush-
less alternator. The brushless alternator comprises of a main

alternator, an exciter machine, a three phase rotating bridge rectifier and an automatic voltage regulator (AVR) as shown in the block schematic in Figure 1.1. The main alternator is of salient pole construction, usually of four poles, chosen based on size and speed of prime mover which is also a trade off between capital cost and running cost. In a low voltage brushless alternator, main machine is a salient pole synchronous generator with a rated voltage below 1000 V.
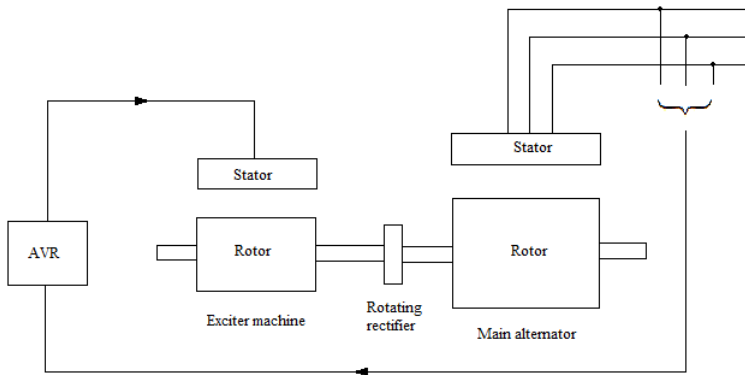
Fig. 1.1: Block schematic of brushless alternator

The exciter machine, which provides excitation to the main field through a diode bridge mounted on the rotating shaft, is an inverse design multi-pole machine with a 3-phase wound rotor mounted on the same shaft of the main alternator (Darabi, 2004; Cosovic *et al.*, 2011). To make the alternator self generating and self regulating, a part of the output power from main alternator is fed back to the exciter field winding. Conventionally, excitation power for an alternator is provided from the terminal voltage through a step down transformer or an independent supply source, often a permanent magnet generator (PMG) mounted on the same shaft of main alternator.

By varying the amount of direct current (DC) through stationary

exciter field coils, 3-phase output from rotating exciter armature is varied. This exciter output is rectified by rotating rectifier assembly, mounted on the shaft, and resultant DC supplies rotating field of the main alternator and alternator output is taken from 3-phase main AC winding embedded into the stator slots of the alternator. As a result, by controlling small DC exciter current, output voltage of the main alternator is controlled.

1.2   Applications

Typical applications of low-voltage brushless alternators are in standby power generating units, for peak-shaving or continuous base load operation in stationary power stations, in auxiliary power units as well as shaft generator systems in ships or offshore platforms. These generators are suitable for operation with prime movers like diesel/gas engines, gas turbines and steam turbines.

1.3   Standards Followed

Low voltage brushless alternators are manufactured as per the requirements set by several standardising organisations such as International Electro-technical Commission (IEC), National Electrical Manufacturers Association (NEMA), British Standards Institution (BSI), International Organisation for Standardisation (ISO) and Bureau of Indian Standards (BIS). The alternator in the scope of this study is conforming to the standards IEC 60034-1: 2004 for rating and performance of rotating electrical machines with rated voltage not exceeding 1000 V AC and Indian standard IS 4722: 2001-Specification for rotating electrical machines (second revision). In marine and offshore applications, the additional design criteria of the applicable classification society are also followed. These societies include American Bureau of

Shipping (ABS), Bureau Veritas (BV) and Lloyds Register (LR) which are members of the International Association of Classification Societies (IACS). In addition to the set standards, different customer specifications are also considered in the alternator design.

1.4   Operational Modes

Brushless alternators powered by IC engines are mainly employed in three main roles *viz.,* base load, peak-shaving and stand-by.

- For base load or primary duty in locations where there is no utility supply; or as an independent power source to ensure continuity of supply, where power supply system available is susceptible to frequent burn-outs/black-outs.

- For peak-shaving duty to supplement power and/or to reduce the cost of electricity supply from a utility source during peak hours.

- For stand-by duty to power critical loads during outage of mains power for short periods.

These modes of operation fall into two categories *viz.,* continuous duty where generators are required to run continuously and intermittent duty, where generators are put to operation only for short duration of time.

1.5   Performance Criteria

Certain types of loads have direct bearing on the sizing of generating plant and demand specific quality of supply. Hence, performance parameters need to be clearly defined and specified for

each application. The supply characteristics required for highly sophisticated and sensitive loads will be quite different from those that need to be specified for less sensitive loads such as general purpose, domestic and industrial systems. In all such systems, some or all of the following performance parameters need to be defined.

- Step load acceptance

- Transient and steady state voltage and frequency regulation

- Waveform characteristics (harmonic limitation)

To meet performance criteria specified for transient frequency and voltage characteristics on sudden application and rejection of connected loads, the key area the generator manufacturer must consider is the generator's automatic excitation control system.

1.6 Role of Excitation System in Machine Performance

The basic function of an excitation system is to precisely provide necessary direct current to the field winding of the synchronous generator for keeping the generator output voltage within tolerable limits. The excitation system should be able to automatically adjust the field current for maintaining the required terminal voltage, even under varying load conditions. Thus, the excitation system has a powerful impact on generator dynamic performance ensuring quality of generated voltage and energy delivered to the consumers. Main functions of the excitation system are to:

- provide variable DC current to main field winding with short time overload capability

- control the terminal voltage with suitable accuracy

- ensure stable operation within acceptable tolerance limits

- guarantee transient stability subsequent to a fault

- sustain the machine within permissible operating range

1.7   Generator Excitation Characteristics

Brushless alternator excitation system is designed in such a way that the terminal voltage of the alternator under all load conditions is within the rated value. The terminal voltage drop on load application is due to the effects of armature reaction and stator leakage reactance and is largely affected by the power factor (p.f.) of the load as shown in Figure 1.2.
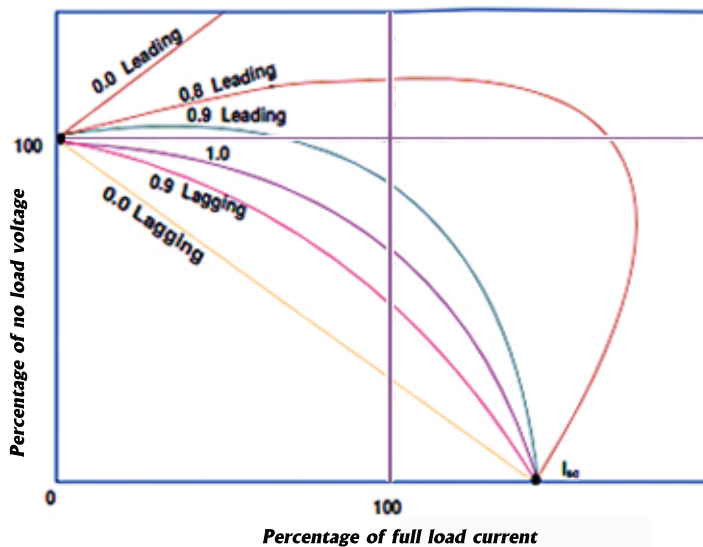
Fig. 1.2: Voltage characteristics of alternators (*Source: NPTEL Website, IIT, Madras*)
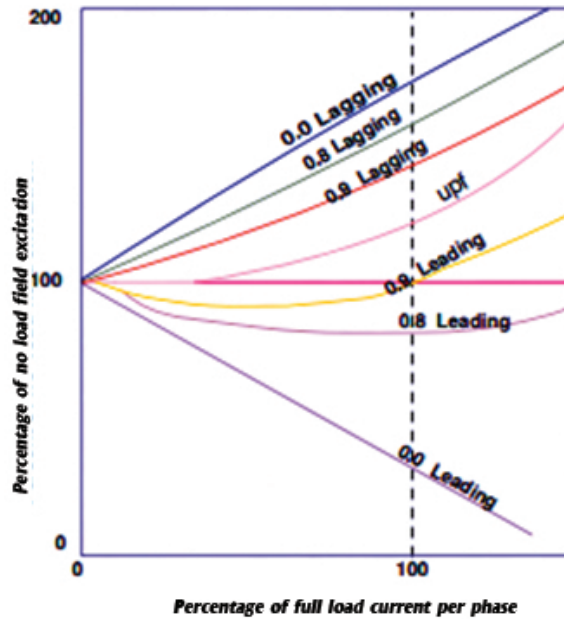
Fig. 1.3: Typical excitation curves of alternators (*Source: NPTEL Website, IIT, Madras*)

Therefore, to keep the output voltage constant over the entire operating range, the excitation current has to be varied over a wide range as shown in Figure 1.3. In order to maintain constant output voltage at a p.f. of 0.8 lagging for which the machine is normally designed, the per unit (p.u.) excitation required at full rated output is 1.9. Thus, the range of excitation required for rated kilo volt ampere (KVA) output at power factors between 0.9 leading and 0.8 lagging is 1.1 to 1.9 p.u. The excitation voltage required to circulate these currents through the generator field coils therefore need to have the same spread.

Owing to the changes in field winding resistance arising from off-load to on-load variations and transient conditions such as

switching on of large induction motors with high in-rush currents at low starting power factors, it is necessary to provide excitation current much above the steady state range. Typically, excitation current of the order 4 times that required for steady state operation is ensured to maintain output voltage within acceptable limits under all operating conditions. Therefore, excitation system of an alternator has an important role in deciding the performance characteristics of the machine.

1.8   Performance Characteristics

The principal interacting characteristics of brushless alternators under steady state are armature current, terminal voltage, short circuit ratio, load power factor and efficiency of the machine. When a diesel generator (DG) set is under operation, any change in the active load demand need to be met by response from the prime mover fuel governor, in order to adjust the input torque so as to keep the system speed/frequency constant. The excitation system of the alternator should simultaneously regulate the field current in order to maintain the terminal voltage at its rated value. When several DG sets operate in parallel, each generator is required to deliver proportionate share of the total load. Under such conditions, the active and reactive power demands of the electrical system need to be shared between the generators, in proportion to their ratings.

1.8.1   Voltage Characteristics

Relating to voltage at the output terminals of the alternator, specifications of the machine normally include voltage modulation, voltage stability under a constant load, voltage waveform characteristics, phase voltage balance, voltage regulation

(VR) from no load to full load and transient voltage dip/rise (TVD/TVR).

Voltage Regulation (VR)

The inherent voltage regulation of the machine is a characteristic which is dependent on magnitude and p.f. of the load. The requirement for close inherent voltage regulation makes a machine uneconomical to manufacture since it generally involves long air gap and higher machine dimensions (Mahon, 1992). Hence, all modern machines are equipped with a well designed excitation system with automatic voltage control equipment which serves to maintain a constant terminal voltage, irrespective of any disturbing influence such as speed/load change and temperature rise. Typically, voltage regulation of the brushless alternator from no load to full load is to be kept in the tolerance band of $\pm 1\%$.

Transient Voltage Dip/Rise (TVD/TVR)

One of the important requirements for an alternator is its ability to accept/reject sudden heavy loads, with minimum disturbance to its terminal voltage, especially when the machine is operating in a small group providing an independent power source. As these machines do not have the back-up of an infinite bus-bar such as a large utility power supply, all the watt-less current demanded by the load needs to be met by the alternator. Therefore, heavy loads, especially that of poor p.f., when suddenly switched on to a finite power source, cause an instantaneous dip in the alternator output voltage. The transient voltage dip from normal voltage is determined by sub-transient reactance of the machine. The reverse process occurs when load is disconnected and there is a transient voltage rise which again is proportional to the sub-transient reactance of the machine. The rate of

recovery to normal voltage is governed by the characteristics of the excitation system.

Voltage Waveform Characteristics

Performance specifications for low voltage brushless alternators include limits for form/crest factors and waveform deviation from the sinusoidal, expressed as total harmonic distortion (THD) (Fuchs and Masoum, 2011). The standards and some user specifications set limits on the harmonic content in the output voltage.

Output Voltage Harmonics in Brushless Alternators

The output voltage waveform of an Industrial AC brushless alternator is not perfectly sinusoidal. The time variation of the induced electro-motive force (EMF) in a conductor of the stator winding in an AC generator has the same form as the space distribution of the flux density in the air gap (Kemp, 1952). Therefore, only a sinusoidal wave of the air gap flux density can result in a sine-wave induced EMF. Several factors such as shape of the rotor pole face, core saturation, slotting and style of coil disposition render realisation of a sinusoidal air gap flux wave commercially non-viable. The symmetric air gap flux density wave results in the absence of even harmonics, leaving a space distribution comprising of only fundamental and harmonics which are odd multiples of the fundamental (Langsdorf, 1955).

The flux harmonics introduce undesirable effects on the alternator performance such as high neutral current due to triplen harmonics, voltage distortion, noise, vibration, excessive heating and extra losses resulting in poor efficiency, which necessitates oversizing of the machine especially when connected to non-linear

loads (Fitzgerald *et al.*, 1983).

Harmonic reduction in output voltage can be achieved in machines by properly shaping the pole profile, introducing fractional slot winding and the effect of slot harmonics can be reduced by skewing either stator or the rotor (Knight and Karmaker, 2005). Over and above this, selected harmonics can be eliminated by short chording the winding. Ignoring slot harmonics, in general 3rd, 5th and 7th harmonics are the dominant harmonics, but with different percentage of each, in various conditions (Langsdorf, 1955).

Although different modified winding configurations are suggested to reduce voltage harmonics, it is impossible to achieve a winding in which all the winding factors other than that for fundamental are zero. Several authors (Charmers, 1964; Hughes, 1970; Centner and Hanistsch, 2006; Knight, 2009) have considered the problem of producing an improved magneto-motive force (MMF) waveform using unconventional windings, the latest being a novel design in which both the winding arrangement and the slot pattern are unconventional (Kocabas, 2009). This winding method introduces both non-uniform conductor and slot distributions and is applicable only for 3-phase single layer AC windings with number of slots being multiples of 12.

Total Harmonic Distortion (THD)

Total harmonic distortion is an important figure of merit used to quantify the level of harmonics in voltage or current waveforms. THD is defined as the ratio of the root mean square (r.m.s.) value of all harmonics (V_n, $n = 2\,to\,\infty$) to the r.m.s. value of the fundamental voltage (V_1), *i.e.*,

$$THD = \frac{\sqrt{\sum_{n=2}^{\infty} V_n^2}}{V_1} \qquad (1.1)$$

The permissible level of harmonic content of the no-load voltage of synchronous generators is limited by the requirements of IEC 60034-1 which specifies a maximum THD of 5% for all ratings of brushless alternators. Calculation of THD takes into account both even and odd harmonics. The contribution of even harmonics is negligible because harmonics of this order do not exist in machines. In voltages measured across lines, the third harmonics and its multiples known as triplen harmonics are absent. However, in the phase voltage to which single phase loads are connected, all odd harmonic components including the triplen harmonics are present.

1.9   The Research Problem

Design inputs for low voltage brushless alternators are the specifications/requirements put forward by the customers in addition to general guidelines as per different standards (IEC 60034; IS 4722). Out of the important output parameters, voltage regulation and total harmonic distortion in the output phase voltage are critical when the alternator is intended for powering sophisticated and sensitive single phase loads. The voltage regulation of the alternator is kept within the specified tolerance band with the help of a well designed excitation system. In this backdrop, the present study investigates the effectiveness of an improved excitation system for low voltage brushless alternators, utilising third harmonic power in the air gap of the machine for excitation control under loaded conditions. The objectives of the study are to:

- devise and implement a novel third harmonic excitation (THE) system for low voltage salient pole brushless alternators.

- design the third harmonic winding in the excitation system

using finite element method (FEM) modelling and virtual prototyping (VP).

- predict the characteristics/parameters of the brushless alternator by virtual prototyping, using finite element (FE) model.

- analyse the effectiveness of third harmonic excitation system in keeping voltage regulation within tolerance limits and reducing the output voltage harmonics, of the brushless alternator.

1.10   Research Focus

Among the important output parameters of brushless alternators, voltage regulation and total harmonic distortion in the output phase voltage are significant when the machine is put to service for powering single phase loads. Voltage regulation of the alternator is kept within specified tolerance band with the help of a well designed excitation system. In the present study, an excitation system is designed for low voltage brushless alternators, which utilises triplen harmonic content in the air gap flux of the machine for excitation control under loaded conditions.

The basic design of a rotating electrical machine, *i.e.*, the dimensioning of the magnetic and electric circuits, is usually carried out by applying analytical equations. However, accurate performance of the machine is usually evaluated using numerical methods. Of the different numerical methods available, FEM is the most acceptable one in industry as it offers an efficient and accurate means of predicting the magnetic field distribution, taking full account of non-linearity of the iron material and induced currents in electrically conducting parts of the machine. Hence, in the present study, virtual prototyping of the brushless alterna-

tor is done by modelling using FEM software, Ansys Maxwell 2D
(Ansys Maxwell 2D V14 Documentation manual). With this soft-
ware, the effect of a single parameter on dynamic performance of
the machine can be effectively studied by parametric modelling.
Furthermore, some tests on machines which are not feasible un-
der laboratory circumstances can be virtually performed. The
software employed in the analysis has an adaptive mesh gener-
ation algorithm, which iteratively increases the mesh density to
keep the error due to discretisation, within a user specified norm.

Even though, the real field problems in rotating electrical ma-
chines are three dimensional (3D) in nature, the field properties
are invariant along the depth of the machine structure. Hence,
2D FEM formulation is sufficient for analysis of synchronous
machines thereby considerably reducing the computational time
(Bianchi, 2005). By FEM, governing equation of electromagnetic
field distribution existing in the geometry of the machine is solved
for magnetic vector potential (MVP) A, having component only
along z-axis. From the computed value of A, the magnetic flux
density B having components in the (x, y) plane is calculated.
From the estimated value of B at each and every point in the 2D
machine structure, various electromagnetic parameters *viz.,* total
and useful flux, leakage coefficient, B_{max} and B_{av} in the machine
parts, saturation factor, winding inductance, open circuit char-
acteristics (OCC) and direct (d) axis as well as quadrature (q)
axis reactances are derived.

The proposed excitation system is an improvement over the con-
ventional systems, which effectively reduces THD in the output
phase voltage, by utilizing triplen flux harmonics for excitation
control in brushless alternators. In the present study, FE mod-
elling of a brushless alternator of 45 KVA capacity was done us-
ing geometrical data, material properties, winding data, period
of symmetry and the boundary conditions. Virtual prototype of
the machine with third harmonic winding (THW) was subjected

to detailed analysis for EMF induced per turn of THW and based on this, number of turns of the third harmonic winding was selected. FE model of the machine with third harmonic winding was analysed for harmonic content in the output phase voltage to ascertain the effect of third harmonic excitation winding as a damper of triplen harmonics in the output voltage.

An experimental machine was designed and developed, with third harmonic excitation implemented in a 45 KVA, 415 V, 3-phase, 4 pole brushless alternator. The main winding is a full pitched concentric winding and the third harmonic excitation winding is wound for $1/3^{rd}$ pitch with number of turns per harmonic pole obtained from analysis of the FE model. Since THW is wound for $1/3^{rd}$ pitch, only the triplen harmonic flux in the air gap of the machine links with it. The no load excitation for the machine are provided by a $2/3^{rd}$ pitched auxiliary winding placed in the stator slots along with the main winding. To keep the voltage regulation of the machine within the specified tolerance band of $\pm 1\%$, the additional excitation requirements of the machine under loaded conditions are supplied by the third harmonic winding. Since third harmonic flux is utilised for meeting excitation requirements, there is a reduction in the triplen harmonics in the output phase voltage of the machine. The simulation results of the virtual prototype were validated by experiments conducted on the prototype machine. The experimental results clearly indicated that third harmonic excitation system is effective in keeping VR of the machine within the specified tolerance band and also in reducing THD in the output phase voltage.

The thesis is organised systematically with the following sections: Chapter 1 introduces the research topic along with brief background information, statement of the research problem, research objectives and focus. Chapter 2 reviews the literature on different modelling methods for synchronous generators, application of FEM for parameter prediction of electrical machines and evolu-

tion of third harmonic excitation systems. Chapter 3 deals with the aspects of finite element formulation of the field problem in brushless alternators. Chapter 4 looks into virtual prototyping aspects of the brushless alternators and analyses the performance parameters/characteristics. In Chapter 5, a study of the conventional excitation systems is done and the effectiveness of improved excitation system utilising third harmonic power is tested. Design aspects of the third harmonic excitation system are also detailed in this chapter. Chapter 6 deals with comparison of results from the virtual prototype and the experimental machine. The last chapter (Chapter 7) of the thesis presents the summary and the scope for further research. Bibliography is presented towards the end of the thesis.

Chapter 2

Literature Review

2.1   Introduction

A comprehensive literature survey was conducted to study the various approaches existing for design and analysis of electro-magnetic devices. Electro-magnetic field analysis, virtual prototyping and parameter prediction are the most important activities in machine design and development cycle. Hence, field simulation has attracted lot of attention these days and different methodologies are adopted by designers for accurate performance prediction of machines being developed.

Design of rotating electrical machines with high power to weight ratio demands accurate determination of electromagnetic field properties across the machine geometry. The conventional methodology adopted by the designers in early days was computation of the field parameters by the reluctance method followed by expensive prototyping. This was replaced by sophisticated computational methods with the advent of computers. The evolution of these methods is reviewed in section 2.2.

As an important control unit of the brushless alternator, the excitation system and its dynamic performance has direct impact on the stability and reliability of the alternator. The literature on different types of excitation systems are extensively reviewed in section 2.3.

In machines designed for mission-critical and sophisticated applications, certain output parameters and performance characteristics are significant. Hence, accurate prediction of machine parameters during design stage itself minimises cost and time incurred towards development. Virtual prototyping is a method usually adopted for parameter prediction in electrical machines during the machine design process. FEM is a numerical method being used for virtual prototyping of brushless alternators for accurate prediction of machine parameters. The applications of FEM in brushless alternator modelling and analysis are reviewed under sections 2.4 and 2.5.

For a brushless alternator, among the important machine parameters, output voltage harmonics play an important role. THD if allowed beyond certain limits, introduces ill effects in the machine performance like reduced efficiency, excessive temperature rise and increased neutral current. Hence, employing methods to minimize THD in the output voltage of the machine and accurate prediction of the same is very important in the machine development process. The literature on different methods for reduction of output voltage harmonics in brushless alternators is reviewed in sections 2.6 and 2.7. Various winding configurations implemented in alternators for minimisation of THD in the output voltage are also reviewed.

The literature reported on third harmonic excitation systems are reviewed in section 2.8 and the knowledge gaps identified are also presented.

2.2 Analysis of Electrical Machines

Evaluation of electrical machine behaviour under various operating conditions has always been a challenging issue. Depending on the requirements, various approaches are possible for performance evaluation and in certain cases, different methods are to be combined to get satisfactory results. When traditional methods are used for the analysis of electrical machines, there are lots of approximations made and the magnetic field calculations are only fairly accurate (Yilmaz, 2008). The analytic methods for the performance prediction in electric machinery are based on the rough idea of the magnetic field distribution in the machine core and the air gap. Therefore, the results are not reliable for prediction of dynamic behaviour of the machine. Because of these reasons, lot of research is undertaken for parameter predictions associated with numerical field computations (Tandon *et al.*, 1980; Chari, 1983).

Originally, the theory of electrical machines was based on construction of equivalent circuits and their analysis. The conventional methods used for machine analysis were construction of vector diagram, symbolic method, circle diagram method (Heyland, 1906; Blondel, 1913; Behrend, 1921) and method of symmetric components (Fortescue, 1918; Lyon, 1937). Subsequently, theory and analysis of electrical machines was developed in the framework of generalised theory of electric machines, which was stimulated by the problems arose during the construction of synchronous generators and power systems. The first works concerned with the mathematical theory of electrical machines appeared in the middle of 1920's, 1930's and 1940's. Among the authors, Park (1928; 1929; 1933), Kron (1939; 1942) and Petrov (1963) made valuable contributions for development of the theory. A significant contribution to the development of the mathematical theory was made by Park in a set of three papers (Park, 1928;

1929; 1933). These papers presented not only the general two-axes equations of the synchronous machine, but they indicated how the equations can be applied to many important practical problems. Park's transformation provided the development of Kron's generalised theory, which was published in a series of papers and books (Kron, 1942; 1951; 1957). Kron (1957) suggested the model and equations for generalised (primitive) electrical machine. The generalised electric machine is an idealised two-pole machine with two pairs of windings on the stator and two pairs of windings on the rotor. A variety of constructions are available for electric machines and any electrical machine with a circular field in the air gap could be reduced to the generalised electric machine. Later, Blondel (1913), Steinmetz (1916) and Kostenko (1962) extended and advanced the theory of steady-state operation of electric machines.

The next important step in the development of mathematical theory of electrical machines was the creation of mathematical models describing the transient processes. Initial studies of transient processes in power systems were conducted in the beginning of 1920's and the results of this work were published by Doherty and Nickle (1927; 1930), Longley (1930), and Rudenberg (1942). A large contribution to the development of the theory of transient processes was made by Adkins (1957), White and Woodson (1959) and Kostenko (1962). On the basis of the generalised electric machine, the general theory of electrical machines was explained by Adkins (1957) and many examples of its application for analysis of individual machines were demonstrated. In the fundamental work of White and Woodson (1959) the equations for generalised electric machine were derived. On the basis of these equations, almost all electro-mechanical converters were analysed and a good deal of attention was paid to the dynamic modes of operation of electro-mechanical devices. But, all the analytic methods for machine modelling could give only approximate results owing to complex geometry of the machine and

presence of non-linear magnetic materials.

2.2.1 Numerical Methods for Field Analysis

With the ever increasing need for improved efficiency, high reliability and economic design for electro-magnetic devices, the necessity for accurate modelling of the geometry, non-linear material characteristics and disposition of sources as well as induced currents was recognised. Advancements in computer technology, software engineering and graphics have ushered the development and analysis of sophisticated models enabling accurate prediction of electro-magnetic field parameters (Salon *et al.*, 1999; Sykulski, 2006; Zhou, 2012)

The development of numerical methods for electrical machine analysis started with the finite difference method (FDM) which was followed and overtaken by finite element method. Pioneering works in electro-magnetic field analysis using numerical methods were carried out during 1970's and Demerdash and Nehl (1979) evaluated the methods of finite differences and finite elements as applied to non-linear magnetic field problems in electrical machines. The evaluation was done on the aspects of effectiveness, numerical accuracy, computer storage and execution time requirements of the two methods and finite element method was found to be superior. Results derived from the finite element analysis had the tendency to converge asymptotically to corresponding experimental test data as the fineness of the discretisation mesh was increased. But, with finite difference scheme, the results strongly indicated that there are lower bounds beyond which inherent numerical error could not be decreased by an increase in the degree of fineness of the corresponding discretisation mesh. Awad *et al.* (2000) proposed a method for modelling steady state performance of large turbo-alternators, including effects of magnetic saturation. To avoid the superpo-

sition limitations of the conventional d-q approach, a sectoral model of a pole of the machine was developed and solved iteratively. Monorchio *et al.* (2004) described a hybrid technique that combines FEM, FDM and the integral equation based method of moments (MoM) in time domain to analyse complex electromagnetic problems related to thin wire antennas. This method is applicable to electro-magnetic waves in high frequency domain and not for low frequency domain of electrical machines.

Of the several methods propagated, FEM has gained increasing acceptance from industry for modelling rotating electrical machines with complicated geometry and non-linear material properties. The formulation of FEM and its application to magnetic field analysis has been adequately detailed by Chari and Silvester (1971), Rafinejad *et al.* (1976), Sarma (1979), Tandon *et al.* (1983), Belforte and Chiampi (1984), and Brauer (1993). To keep up with more stringent design requirements that the industry demands, designers of electrical machines have turned to computer aided design (CAD) and especially to finite element techniques for design and analysis of electrical machines (Chang *et al.*, 2003; Premkumar, 2006; Trowbridge and Sykulski, 2006; Yilmaz and Krein, 2008; Guptha *et al.*, 2009). Finite element method has evolved as the fastest and the surest way to the prediction of machine parameters at the design stage. Electro-magnetic field solution is only the first step in the analysis process and further the machine parameters are derived from the field solutions by post-processing. The availability of affordable desk-top computing power and the arrival of powerful menu-driven softwares have largely contributed to the acceptance of such methods in the design process.

Chiricozzi and Napoli (1978) developed a method for machine modelling by FEM based on state-variable approach, for accounting the saturation effect in the iron parts and eddy currents in the rotor winding. The method was based on assumptions that mag-

netic field is produced by a step current impressed to the rotor slot bar and the stator windings have three phase linear current density which is a deviation from reality under actual situations.

Chari *et al.* (1981) presented the method of determining internal state of a synchronous machine during steady state load operation. A two dimensional (2D) finite element model was employed to compute the excitation values and direct and quadrature axes reactances. The authors employed realistic representation of stator currents by allowing actual instantaneous coil currents in the slots and discarded harmonic components of phase currents. This is a compromise between the sinusoidal current sheet representation which is simple for analysis and the coil current representation in which the analytical solution is complex.

Ashtiani and Lawther (1983) described a possible technique for using FEM to directly obtain values of the load angle and field current in an alternator from the knowledge of terminal operating conditions. The novelty of the method was that even in presence of non-sinusoidal flux linkages, the terminal parameters could be related to nodal MVPs which is important for analysis of salient pole machines. The disadvantage of the method is that resulting set of equations was non-symmetric and hence faced difficulty for solving.

Benefit assessment of finite element based saturation model of the synchronous generator is done by Schulz *et al.* (1987) and the saturation representation of the machine model is improved by non-linear magnetic finite element analysis (FEA). A comparison of finite element algorithm and conventional algorithm is done based on B-H characteristics of the magnetic material.

An improved model for the transient analysis of saturated salient pole synchronous motors was presented by Ojo and Lipo (1989) with the aid of saturation factors obtained by test or with finite elements. Park's equations (Park 1929) for the synchronous ma-

chine were modified to independently account for the saturation of d and q-axes magnetic flux linkages in the region of stator teeth and rotor pole face as well as saturation of total flux linking the stator core.

Small salient pole synchronous generators are normally skewed in order to eliminate slot ripples from the induced EMF and current waveforms. Williamson *et al.* (1995) outlined a technique which enables two dimensional FE analysis to be applied to skewed machines which involves representing the continuous skew in a series of discrete steps. Each two dimensional slice corresponds to a different position along the axis of the machine and non-linear field solution is performed for each slice at each time step. The disadvantage of this method is that deep bar effect is not automatically included in the field solution since magneto-static field solutions are used.

According to IEEE standard 115-1995, the d-axis dynamic reactances and time constants can be computed from 3-phase short circuit tests and the negative sequence reactance can be derived from the line to line short circuit test. Susnjic (1997) reported on numerical simulation of the sudden short circuit in the q-axis by which the q-axis parameters of the synchronous generator were predicted. Arjona and McDonald (1999) presented a steady state model that describes synchronous reactance over the whole operating region of the machine, taking into account main and cross axis magnetic saturation. The analysis presented saturation as a function of total air gap ampere-turns of the machine. Wamkeue *et al.* (2003) proposed a 2D time stepped finite element method to simulate the line to line and 3-phase short circuit tests for parameter prediction of large hydro-generators. In the FE model generated, the stator and rotor windings were not taken into account because of their small physical dimensions in comparison with the overall machine geometry. But, this method suffered a discrepancy of shift in the time axis between the computed and

experimental parameters, which, as explained by the authors, is
due to the difficulty in matching of the initial rotor angle during
simulation with that in the experiment.

Amaya *et al.* (2003) reported on synchronous machine parameter
identification by simulation using FEM. By finite element anal-
ysis of the machine, the reactances and time constants in the d
and q-axes were obtained. Compared to the test procedures for
calculation of reactances and time constants, the results are more
accurate as it also considered the effect of saturation. Shima *et
al.* (2003) described a method for calculating the steady and
transient state leakage flux distributions, based on FEM. The
method analysed the leakage inductances that represent the cor-
responding leakage fluxes with magnetic saturation taken into
account. Kolondzovski (2004) explained the calculation of syn-
chronous generator reactances by FEA and compared results with
analytic solutions and experimental results. The magnetic flux
pattern in the machine was plotted and the prediction of transient
and sub-transient reactances of the machine was done. Kolond-
zovski and Petkovska (2005) reported on the determination of
synchronous generator characteristics like open circuit character-
istic (OCC), flux and flux density distribution in the air gap of
the machine, by finite element analysis.

Petkovska *et al.* (2008) described two different methods based on
FEM for computation of steady state and transient d-axis and q-
axis parameters. First method combined the results of magneto-
static FEM analysis as well as Matlab/Simulink simulation and
transient performance characteristics were predicted. Using the
machine parameters obtained by simulation of FE model of the
machine, the mathematical model of the synchronous genera-
tor in Matlab/Simulink environment was developed. Simulating
this model for 3-phase symmetrical short circuit, the time depen-
dant transient characteristics were also predicted. In the second
method, the transient analysis of the 2D FE model of the machine

was done using the FE software, which took into account the end winding effects and saturation of core in the machine. The results obtained by time stepping FE method proved to be more precise and in close agreement with the experimental results. Okafor *et al.* (2009) applied FEM for prediction of magnetic flux pattern and the magnetisation curve of DC machines. The author presented variational formulation for Poisson's equation which governs the approximating function, and the functional minimisation using first order triangular finite elements.

The properties of permanent magnet brushless (PMBL) alternators like high power to weight raatio, small size, high efficiency, high reliability, variable speed operation and good dynamic performance make them suitable for aircraft and automobile applications. Due to stringent performance requirements like highly competitive costs, low acoustic noise, high efficiency and unique operating conditions, design of PMBL machines is challenging and designers are constantly in search of effective methodologies for design and performance prediction of such machines. Hence, a wide variety of designs for such machines are proposed by researchers. Spooner and Williamson (1996) designed and constructed two small multi-pole radial flux permanent magnet test machines for use as a direct coupled generator in wind turbines. The authors later proposed a modular design of permanent magnet generators for wind turbine. Chen *et al.* (2000) proposed the methodology for design and finite element analysis of an outer rotor permanent magnet generator for directly coupled wind turbine applications. Comanescu *et al.* (2003) reported on the design and analysis of a 42 V permanent magnet generator for automotive applications.

Bhim Singh and Jally Ravi (2006) proposed a method based on FEM for design and analysis of a 3 KVA, 28 V PMBL alternator for light combat aircraft. Main objective of the design was to maximise the efficiency and minimise the volume of the al-

ternator. The preliminary design was done based on analytic equations and FE model developed based on these dimensions was subjected to simulation. The simulation results were verified for critical values of flux density in various parts of the machine.

Chan *et al.* (2005) studied the performance of a permanent magnet synchronous generator (PMSG) with inset rotor construction by using a time stepped coupled field circuit FEM. The focus was on the effect of inverse saliency on voltage regulation. The study was limited to linear R-L loads and only steady state operation was considered. Further, Chan *et al.* (2010) applied time stepping finite element analysis to study steady state and transient performance of the PMSG when supplying an isolated resistive load, at constant speed.

Synchronous reluctance machines are used in applications requiring high dynamics, high efficiency and high flux weakening capacity (Welchko, 2003). A permanent magnet is sometimes buried in rotor flux barriers for the purpose of saturating iron bridges and increasing the power factor. The anisotropy of the rotor causes a high content of flux density harmonics which results in increased iron losses. Barcaro and Bianchi (2010) developed an analytical model for the machine which on validation by FEM shows the dependence of flux density harmonics on the rotor geometry. A number of authors have presented models for calculating iron losses in synchronous machines with anisotropic rotor (Mi, 2003; Magnussen, 2004; Yamazaki, 2006; Roshen, 2007).

Shima *et al.* (2002) analysed the leakage flux distributions in a salient pole synchronous machine using finite elements. The authors presented a method for calculation of steady state and transient state leakage flux distributions in the machine. The method analysed leakage inductances that represent leakage fluxes with magnetic saturation also taken into account. The leakage inductances were divided into the self-leakage, gap leakage, and winding-differential leakage inductances. Cross-magnetizing in-

ductances were also calculated. Weak magnetic influence of the damper circuits on the armature in the d-axis was quantitatively illustrated through values of the winding-differential leakage inductances.

Chebak *et al.* (2010) presented the method for optimal design of a high speed slot-less permanent magnet synchronous generator with soft magnetic composite stator yoke and rectifier load, by FEM. Lidenholm and Lundin (2010) estimated the parameters of hydro-power generator through field simulation of the standard tests. The 3-phase short circuit test, slip test and the field decrement test were implemented using a time stepping finite element software. The simulation results shown compliance with the measured values of the hydro-power generator. Iamamura *et al.* (2012) conducted a study on rotor static eccentricities of turbo alternator using air gap flux sensors, by FEM. The method also took into account the eddy currents in damper bars while operating at rated load conditions.

Tessarolo *et al.* (2012) used time stepping finite element analysis for predicting generator performance with different damper cage designs. The results of FE analysis as a method to predict generator performance was assessed against test results for various damper cage design alternatives. FE simulations gave accurate results even without model tuning if continuous end rings were used to short circuit the damper bars. Laldin *et al.* (2013) proposed an analytical design model of a salient hybrid synchronous machine that utilizes a field winding as well as permanent magnets for excitation. The model was designed for use in a multi-objective design process to establish the trade off between mass and loss. The methodology validation was done by using a finite element model of the machine. The calculated parameters include resistances, inductances, and the back-emf of the machine.

2.2.2 Circuit Coupled FEM

Intensive efforts are being undertaken to explore suitable methods to couple finite element machine models with external circuit equations for analysing power electronic drives in time domain. There are situations where properties of the machine significantly affect behaviour of the external circuit (Krause, 2013). The trends and accomplishments in coupled field circuit problems have been presented by Tsukerman *et al.* (1993). There are two different approaches to couple finite element models with circuit equations: the direct method in which equations of FE model and circuit model are handled as a single system and the indirect method in which the finite element model of the machine is handled as a separate system which communicates with the circuit model with the aid of coupling coefficients. Direct coupling was used in conjunction with time domain simulation by Hecht (1990) and Sadowshi *et al.* (1993). Drawback of direct coupling is that the circuit equations are to be so formulated that the sparse matrix solution technique still works when the circuit models are added in parallel with the FE model, which limits the freedom with circuit modelling. Vaananen (1996) proposed a method for coupling FE models with circuit equations based on indirect coupling. In this method, FE model is handled as a circuit theoretical multi-port element which is treated in same way as ordinary non-linear circuit elements within the Newton-Raphson (N-R) iteration of the circuit equations.

Fixed parameter models give good insight into the operation of the system as a whole, but are not accurate enough for design optimisation. FE models give an exact representation of the magnetic field inside the machine, enabling iron saturation and skin effect to be accounted with great accuracy. However, they are expensive to time step at the rate demanded by the fast transients caused by the converter (Preston *et al.*, 1991). Williamson

and Volschenk (1995) proposed a hybrid technique which used a circuit model and a FE model for representation of the generator feeding rectifier load. The circuit model was time stepped until changes in flux linkage indicated that the parameters needed updation. Using the known orientation of rotor and the known set of currents, the field model was run and the circuit model parameters were updated. In this way, expensive field solutions were carried out only when needed, rather than at a frequency dictated by the fast acting transients generated by the converter. This method is suitable for analysis of machines in which currents flow in well defined paths, for *e.g.*, conductors of a winding and bars of a damper cage. But, the method poses restriction to accommodate eddy currents induced in massive iron structures such as solid rotors in certain alternators.

Fu and Ho (2010) presented a general formulation of 2D FEM for computation of magnetic field and electric circuit coupled problems. The authors extended the concept of windings to include group of solid conductors and all excitations including stranded windings and solid conductors were regarded as special cases of the basic winding.

2.3   Excitation Systems in Alternators

Excitation system in brushless alternators has an important role on machine dynamic performance, ensuring the quality of generated voltage. More precisely, in brushless alternators, it is the role of the excitation system to keep voltage regulation within a specified tolerance band over the entire operating range. Hence, all modern machines are equipped with a well designed excitation system with automatic voltage control equipment as shown in Figure 2.1 which serves to maintain a constant terminal voltage under all load conditions.
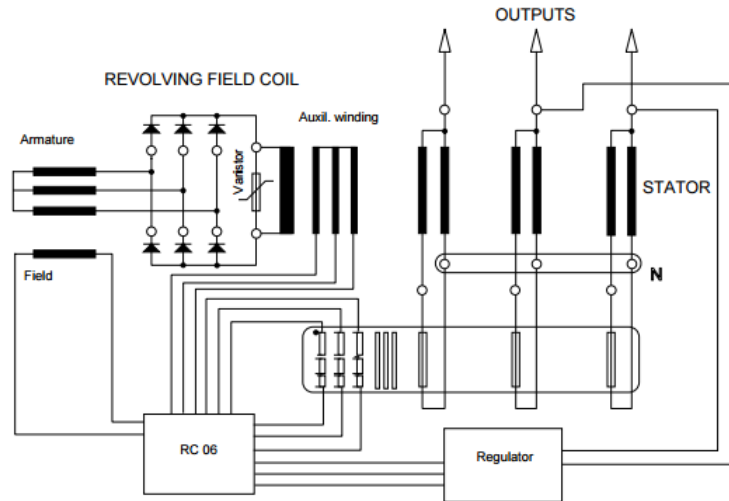
Fig. 2.1: Schematic of brushless excitation systems (*Source: Operation manual, BHEL EML, Kasaragod*)

2.3.1 Brushless Excitation Systems

The brushes and slip ring assembly for feeding power to the rotating field of conventional synchronous generators results in spark at the brushes, increased losses and frequent maintenance. To overcome these disadvantages, the concept of brushless alternators was introduced in 1980's. Since then, there was a continuous up-gradation of the technology and today, all modern brushless alternators are designed to be self generating and self regulating, for maintaining the quality of power generated. To meet this requirement, different configurations of the excitation system are presently available.

Shibata *et al.* (1983) introduced the concept of a brushless, self-excited 3-phase synchronous generator. Subsequently, Shibata *et al.* (1990) developed brushless and exciter-less, single-phase

and 3-phase synchronous generators. In the 3-phase generator, the stator armature winding was connected electrically with the secondary winding of a transformer and the rotor was provided with a bridge type field winding. In the single-phase generator, armature winding was electrically connected with the excitation power-supplied winding through a capacitor and the rotor was provided with a balanced 2-phase field winding. In these generators, AC excitation current flows in the armature winding simultaneously with the load current and thus, the generator was made brushless and exciter-less.

Inoue *et al.* (1992) proposed a brushless self-exciting 3-phase synchronous generator which comprised 3-phase armature windings on the stator, one field winding, one exciting winding on the rotor with five times as many poles as that of the armature winding and a 3-phase reactor connected to the terminal of the armature windings. By utilising the 5th space harmonic component of armature EMF, small voltage regulation for various loads and no oscillatory tension occurring at the rotor shaft were realised. The basic constitution, principle of operations, and exciting characteristics were also described.

A new variable speed synchronous generator system was proposed by Nonaka and Kawaguchi (1992) which consisted of a brushless self-excited synchronous machine and a voltage source pulse width modulated (PWM) frequency changer. In this generator, the field current was obtained by superimposing another field on the stator rotating field, which was achieved by control of the PWM converter so that AC voltages are induced and half rectified in the rotor field windings. This generator did not require an exciter or additional exciting equipment and in order to superimpose the additional field on the stator field, two modulation schemes of the PWM converter of the frequency changer were provided.

Nonaka and Kesamaru (1994) described a new brushless genera-

tor without a rotating exciter, and having a stator with two independent windings designed for different pole numbers, the first being single-phase load winding and the second, exciter DC winding. This generator had the advantage of presenting an almost constant output voltage for large load variations and different speeds.

More recently, Chan and Lai (2001) analysed the steady state behaviour of a single-phase self excited generator where the equations were derived using the symmetrical component method. Detailed discussions of excitation control systems for brushless synchronous generators were presented by Godhwani and Basler (1996) and Erceg *et al.* (1999). Erceg proposed digitally controlled excitation systems for the synchronous brushless generators. The control system had two feedback loops: one based on generator's voltage and the other based on excitation current of the exciter. Besides basic function of a voltage controller, the digital system had more control functions like limits of minimal and maximal exciter current, compensation of the voltage, voltage/frequency characteristic, and possibility of communicating with higher system levels. Different methods for control of field excitation for better voltage regulation in generators were proposed by Rabelo *et al.* (2004) and Boldea (2005).

Brown and Haydock (2003) presented a new brushless synchronous alternator which combined permanent magnet and wound coil excitations to provide a single stage brushless alternator. The design procedure followed was based on lumped parameter magnetic circuit model. Singh *et al.* (2012) proposed a synchronous generator with asynchronous excitation and uncontrolled rectifier bridge. The terminal voltage of the machine was regulated through the field current. The methodology for modelling the machine neglected harmonics due to saliency as well as rotor field winding resistance and assumed the rotor speed to be constant.

2.3.2   Brushless Exciter Modelling

Complete study of dynamic transient performance of brushless alternators needs development of a total gen-set system model for which modelling the exciter machine is essential. Conventional models of brushless exciters employ transfer functions, the parameters of which usually decided by test, and the use of such models is limited to small disturbances. Kabir and Shuttleworth (1994) proposed a brushless exciter model which uses d-q parameters rather than a transfer function. The model was based on steady state phasor diagrams, by the two-axis approach.

Darabi and Tindall (2002) reported on a methodology for prediction of self and mutual inductances of a brushless exciter of gen-set alternator for different rotor angle positions, by using FEM. A real time model for the exciter, the load and the diode bridge mounted on the rotor was proposed which was analysed for parameter identification using a FE package. Subsequently, Darabi *et al.* (2004) presented the model of a small brushless generating set linking the finite element and time stepping circuit model of the main alternator as well as load, the real time model of the analog AVR and a model based on the self and mutual inductances of the exciter machine along with the diode bridge rectifier. The complete model was used to study the transient and steady state performance of the whole generating set under different load conditions including synchronous operation in parallel with the mains. But, the composite model had the limitation that the diesel engine dynamics was not included for complete gen-set investigation.

Recently, Griffo *et al.* (2013) proposed the design methodology and characterisation of a 3-phase brushless exciter for air-craft generator. The authors evaluated a 3-phase AC main exciter for a wound field synchronous starter generator for air-crafts, capable of operating in both starting and generating modes. The

output capabilities of the machine were predicted in all operating conditions using 3D finite element model together with lumped parameter circuit approach.

2.4 Virtual Prototyping and Parameter Prediction of Electrical Machines

Electrical machines and devices experience transient electromagnetic disturbances during operation either in a stand-alone mode or in conjunction with a system or network to which other electrical apparatus are connected. Some of the more common disturbances are switching transients, system faults, lightning surges, and electromagnetic interference in communication lines. Such occurrences result in over-voltages, which impair the dielectric strength of the insulation, or current surges which causes overheating and high mechanical stress in structural members, thus affecting the performance and reliability of electrical machines. The severity of the disturbance is further enhanced by saturation of iron parts and flow of induced currents in conducting media. To achieve design integrity and assure reliability of operation, it is essential to evaluate the impact of these transient effects on machine performance at the design stage. As a necessary first step, the designer has to determine the magnetic field distribution accurately and in detail enabling performance prediction of machines.

The performance analysis of synchronous generators employs steady state two axis (d-q) model, transient two axis model or finite element model. When harmonic effects are neglected and linear passive loads are considered, the steady state performance of the machine can be computed using two axis model. Saturation effects may be taken into consideration using appropriate values of synchronous reactances.

Conventionally, field computation in rotating electrical machines under steady state and transient conditions are carried out by closed form and analog methods for simplified machine representation (Chari *et al.*, 1982). Numerical methods for solving transient field problems have become popular these days and techniques based on time-step integration procedures using either explicit or implicit solution algorithms or a combination of the two (Hughes and Liu, 1978) have been developed. In these methods, the solution to the field problem is expressed as a product of functions in space and time. The function in space is determined using an established finite element (Silvester and Chari, 1970) or finite difference technique (Fuchs and Erdelyi, 1973) and the function in time is evaluated by a time stepping procedure (Myers, 1971). Other methods applied to the solution of transient electromagnetic field problems are the state-space technique as reported by Demerdash and Lau (1976) which uses a finite difference model, the model analysis technique described by Konrad *et al.* (1976) and the Fourier transform technique discussed by Lawrenson and Miller (1978).

Owing to rapid advances in computational magnetics, FEM has become a popular and powerful tool for performance analysis of electrical machines. FEM is useful for dealing with irregular geometries, complex material properties, local saturation, harmonic effects and circuit non-linearities. Nonaka *et al.* (1991) presented the magnetic field analysis of brushless 4-pole, 3-phase synchronous generator in which the rotor of the generator consisted of short circuited field coils with diodes. The characteristics of this generator were analysed using finite element method. Zhou Ji *et al.* (2000) presented a method for determination of power angle curves of synchronous machines including saturation and cross magnetizing effect, by FEM. The authors compared two methods where in the first, the saturated power angle curve was determined directly by FEM and in the second method the saturated reactances were calculated by FEM and subsequently

the saturated power angle curves determined indirectly based on calculations.

Among different machine parameters, iron loss is an important parameter directly affecting the efficiency and temperature rise of the machine. Hence iron loss prediction is an important issue in the machine design process. Due to complexities in the machine structure, flux distribution and variation of flux under rotor movement, prediction of iron losses in rotating electrical machines is cumbersome. Ma *et al.* (2003) investigated on the prediction of iron losses in the core of rotating machines, by FEM. By this method, accurate prediction of iron losses was possible by considering the influence of flux vector rotations and flux density harmonics. Later, Nakahara *et al.* (2004) extended this method by computing the additional losses in metal portions other than the steel laminations.

Petkovska *et al.* (2008) presented a methodology for FEM coupling for transient performance analysis of a salient pole synchronous generator. The methodology focused on time-stepped simulation of transients during 3-phase bolted short circuit at the generator terminals. The analysis was based on the combined solution of magnetic field equations and circuit equations of windings. Ranlof *et al.* (2010) presented a permeance model that was employed to estimate the no load damper current loss and voltage waveform harmonics in large turbo-generators. The computed harmonics were compared with the time-stepped FE calculations and influence of pole to pole damper bar connections and number of damper bars, on the voltage waveform was also analysed.

Merkhouf *et al.* (2012) conducted a study on loss calculation by simulation of core loss models including finite element model, to predict the magnetic core losses in hydro-electric machines. Petrinic *et al.* (2012) reported on a methodology based on FEM for determination of synchronous generator load condition pa-

rameters, awareness of which gives insight into the possible operational problems and helps prevention during design stage itself. Calvano *et al.*, (2013) introduced a technique based on integral formulation of non-linear magneto-static model for investigations on the influence of end effects on flux linkages of a large turbine alternator.

2.5   Modelling Methods for Virtual Prototyping of alternators

Different analytic methods are available for modelling magnetic field problems to obtain closed form solutions (Mukhopadhyay, 2007). Some of these analytic solutions are obtained assuming certain situations, thereby making the solutions applicable to idealised situations. Analytic solutions have an inherent advantage of being exact and they make it possible to observe behaviour of the solution when there is variation in problem parameters. However, analytic methods have the limitation that solutions are available only for problems with simple configurations. This poses difficulty in the electro-magnetic analysis of rotating electrical machines as the geometry is very complex and the magnetic materials used are non-linear. In general, analytic models of rotating electrical machines support fast simulation but at the cost of limited accuracy and flexibility.

When the complexities of analytic formula became intractable, non-analytic graphical, experimental and analog methods are used for solution of the field problem. Application of graphical methods is a cumbersome and tedious process and is limited to linear problems with constant material characteristics. Owing to the effect of temperature and humidity variations and their effect on measurements, the experimental and analog methods can not be relied upon for accurate and consistent results. Hence all these

methods are applicable only for limited cases where the geometry of the problem domain is simple and the material characteristics are linear.

The practical field problems in rotating electrical machines involve complicated domains with regard to geometry, material constitution, loads and non-linearities which forbid the use of analytic solutions and the only alternative is to find solution using numerical methods.

2.5.1   Lumped Parameter Models

In lumped parameter models, the inherently distributed nature of the electro-magnetic interaction inside the generator is lumped into a fairly limited set of equations. The field variables in the problem domain are computed by solving these equations.

Permeance Model

The rotating field method determines air gap flux density in an electrical machine and the same is calculated as product of MMF and a permeance function. A calculation scheme that uses this approach to derive the air gap flux density is referred to as a permeance model (Knight *et al.*, 2002; Ranlof *et al.*, 2010).

The permeance model uses Amperes law to solve for magnetic fluxes and magnetic fields. Simplifying assumptions must be made, and hence this method cannot always give accurate results. For very simple problems, its results are often reasonably accurate, but for electrical machine analysis, the geometry being complex, the results are unreliable.

The permeance model when applied for electrical machine analysis, has several limitations as given below:

- Fringing of flux in non-linear air gap is either ignored or approximated with fringing factors.

- Since reluctance is inversely proportional to permeability, prediction of non-linear B-H effects in steel is difficult.

- Losses in steel can be represented by use of complex reluctance. However, obtaining values of complex reluctance is often very difficult.

- Most real world devices have complicated geometries with multiple flux paths that are difficult to analyse. However, magnetic circuits can be constructed with series and parallel reluctances to more accurately model such devices.

  For many magnetic devices, the necessity of assuming flux paths makes the reluctance method inaccurate. Thus, the reluctance method cannot be accurately applied to model many electro-magnetic devices.

Equivalent Circuit (EC) Alternator Model

In studies of the electro-magnetic interaction between alternators and other electrical equipments, the alternators are frequently represented by a set of electrical circuit equations. A long tradition of elaborate refinement and adaptation of such circuit representations to fit almost any problem of interest, makes this the most established and accessible form of alternator analysis. A number of factors determine the nature of an alternator EC model (Yilmaz and Krein, 2008). Some of the most important factors of EC modelling are briefly discussed below (Ranlof, 2011).

- Model quantities can be represented with physical units (V, A and W) or, alternatively, units are eliminated from the

calculations by expressing all quantities in terms of fractions of specified base values. The latter approach called per unit (p.u.) representation is convenient in power systems with many different voltage levels, and also facilitates the comparison of electrical equipments with dissimilar power ratings.

- The armature can be modelled by its three physical stationary armature phases A, B, and C or, alternatively, by means of fictitious rotor-fixed windings. A stator-fixed representation is usually referred to as a phase domain model, while the rotor-fixed representation is called a d-q-0 or two-axis model. The d-q-0 representation brings about numerous modelling advantages, such as time-independent circuit inductances and decoupling of d and q-axis circuits if iron saturation is neglected. The level of modelling detail should be adjusted to the problem at hand and to the required accuracy of results.

Limitations of the EC method in practical rotating machine analysis are:

- d-q-0 models are fundamental wave models, *i.e.*, they only consider the dominating space fundamentals of the magnetic flux density waves inside the generator.

- Linear EC models either neglect iron saturation or represent the effect by parameter values appropriate at the studied point of operation (saturated parameters).

The limitations imposed by analytic methods, their restriction to homogeneous, linear and steady state problems, are overcome by the use of numerical methods.

2.5.2 Numerical Models

Since the distribution of electro-magnetic field in electrical machines is represented by the second order partial differential equation, the magnetic field parameters at each and every point in the machine can be determined by solving this governing equation. For solution of the governing partial differential equations, numerical methods have come into prominence and have become more attractive with advancements in computational capabilities. The most commonly used numerical techniques in electro-magnetics are the moment method or the boundary element method (BEM), finite difference method (FDM) and the finite element method. Most electromagnetic problems are governed by either partial differential equations or integral equations. Partial differential equations are usually solved by using FDM or FEM whereas; integral equations are solved conveniently by using the moment method also known as BEM. Although numerical methods give approximate solutions, the solutions are sufficiently accurate for engineering purposes. The problem of solving field equations by means of digital computing can be tackled with a variety of numerical methods as detailed below:

Method of Moments (MoM) or Boundary Element Method (BEM)

The method of moments (MoM) or BEM is a numerical computational method of solving linear partial differential equations which have been formulated as integral equations (*i.e.*, in boundary integral form). It has applications in many areas of engineering and science including fluid mechanics, acoustics, electromagnetics, fracture mechanics and plasticity.

BEM requires calculation of only boundary values, rather than values throughout the problem space and hence it is significantly

more efficient in terms of computational resources for problems with a small surface/volume ratio. Conceptually, it works by constructing a mesh over the modelled surface. However, for many problems, BEM is significantly less efficient than volume discretisation methods like FDM, FEM and finite volume method (FVM). Boundary element formulations typically give rise to fully populated matrices. This means that the storage requirements and computational time will tend to grow according to the square of the problem size. In contrast, finite element matrices are typically banded (elements are only locally connected) and the storage requirements for the system matrices typically grow linearly with the problem size. Compression techniques can be used to ameliorate the problems associated with the BEM, though at the cost of added complexity and with a success rate that depends heavily on the nature and geometry of the problem.

BEM is applicable to problems for which Green's functions can be calculated which usually involve fields in linear homogeneous media. This places considerable restrictions on the range and generality of problems suitable for boundary elements.

Finite Difference Method (FDM)

Among the various numerical methods employed for solution of partial differential equations, FDM has gained popularity mainly due to its simplicity and computational economy. The underlying principle of this method is to convert the partial differential equations describing the boundary value problem into difference equations and solving these by iterative methods. The continuous problem domain is discretised into a set of uniformly/non-uniformly spaced discrete points, generally termed as grid points, and the derivative terms in the governing differential equation and in its boundary conditions are represented by their appropriate finite difference forms using Taylor's series expansion, re-

sulting in an algebraic equation for each grid point in the computational domain. The difference equation is written for each node in the problem domain to obtain a set of simultaneous equations, solution of which yields field variables in the problem domain (Salon and Chari, 1999). FDM when applied to rotating electrical machines for field analysis, poses the following difficulties (Trowbridge, 1993).

- The discretisation schemes in FDM have fixed topology which cause considerable difficulties when complex boundaries as that of rotating electrical machines are modelled.

- The extension of FDM for a higher order approximation by including higher order terms in the Taylor's series expansion involves considerable complications.

The above difficulties are overcome in the Galerkin's weighted residual approach (Finlayson and Scriven, 1966; Finlayson, 2013) which forms the basis of FEM.

Finite Element Method (FEM)

For electromagnetic analysis of electrical machines, FEM has emerged as the most widely applied numerical method. Its popularity is linked to its ability to handle the complicated calculation geometries presented by rotating machinery. FEM allows the field solution to be obtained even with time variable fields and with materials that are non-homogeneous, anisotropic or non-linear. Using FEM, the whole analysis domain is divided into elementary sub-domains, called finite elements, and the field equations are applied to each of them. By FEM, a meticulous local analysis of the field problem is carried out, highlighting dangerous field gradients, magnetic field strength and saturation. It also allows a good estimation of performance characteristics of the electromagnetic device by virtual prototyping, which permits

a designer to reduce substantially, the number of prototypes during the machine design and development process.

Finite Element method with its inherent ability to accurately represent even intricate geometries, is used to evaluate magnetic field distributions very accurately. Accurate evaluation of the magnetic field distribution, in-turn, leads to accurate estimation of field related machine parameters.

2.6 Prediction of THD by FEM

There is a growing demand for a method to predict the magnitude of various harmonics under no-load and full load conditions of operation, from design data. In machines with loads applied from line to neutral, the third harmonic voltage is of greatest interest because of its large magnitude with respect to other harmonics (Angst and Oldenkamp, 1956). Grabner *et al.* (2003) investigated on the non-linear dependency of air gap magnetic flux density of synchronous generators with fractional slot windings at various operational states, by FEA.

Finite element modelling of the machine combined with harmonic analysis allows designers to rapidly investigate the source of flux density harmonics during machine design process. In comparison with analytical methods, the simulation time for finite element analysis is significant, especially in large synchronous machines where the physical size of the machine is such that, carrying out time-stepped FEA of even a machine that is not skewed is prohibitively expensive in the initial design stages. Standard 2D FEA using multi-slice approach significantly increases time and costs involved. Application of domain decomposition and parallel computation techniques has shown that multi-slice FEA of machines with ratings in excess of 1 MW is possible. Zhan and Knight (2008) studied the effect of axial skew on the flux density

and open circuit voltage harmonics in large synchronous machines and presented an approach that combines the advantages of FEA with the low simulation time of analytical models. Using distinct magneto-motive-force (MMF) and permeance functions for each harmonic source, the approach gives designers the ability to trace harmonics in the open circuit voltage to design parameters.

Time stepping FEM for prediction of machine parameters are time consuming and simulation time depends principally on two factors, *viz.*, mesh complexity and step size. Mesh complexity can be reduced with the use of symmetry where only one pole pair of the geometry needs to be modelled for analysis. Step size determines how far the machine rotates between solutions and hence determines the number of solutions in a single revolution of the machine which in turn determines the validity of harmonics analysed. Therefore, to allow the critical analysis of high order harmonics, a low time step is required, which increases the computational time required for analysis.

To calculate the higher harmonic sequences in machines quantitatively, Ide *et al.* (1992) proposed a method based on FEM considering rotor movement. The rotor movement was accounted by using a slip surface on the moving boundary (Preston *et al.*, 1988) and the slip surface was placed at the centre of the air gap. Nodes on the slip surface were arranged at the same pitches in the direction of rotor movement and elements constructed by these nodes were divided into 8 for one stator slot pitch. The non-linearity of the iron core was accounted by Newton-Raphson method. The authors neglected eddy currents flowing in the iron core as stator and rotor cores were laminated. Damper currents were also neglected, because a no-load steady state condition was assumed. This method had the limitation that rotor movement was considered only for a span of stator slot pitch of the synchronous generator. Later, Hargreaves *et al.* (2010) proposed a method for prediction of open circuit voltage distortion in salient

pole synchronous generators with damper windings.

It is very important for the designer of salient pole synchronous generators to be able to predict the no-load voltage waveform accurately, since knowing in advance the harmonic content of the no-load voltage is important for satisfying standard requirements. Several authors attempted the prediction of harmonics by applying analytical, numerical and combined methods. Knight *et al.* (2002) presented a combined analytical and FE modelling method for calculation of harmonics including the effects of damper bar currents. Schwery and Samek (2002) came up with a transient FEM for prediction of no-load voltage waveform. Later, Schmidt *et al.* (2002) applied a fast analytical method whose output can be used as a criterion for selection of number of slots in salient pole synchronous generators.

Keller *et al.* (2006) presented a combined analytical and FE method for prediction of no-load voltage waveform of laminated salient pole synchronous generators. The method took into account the saturation effects and by FEM simulations, the magnetic coupling of electrical conductors of the machine like damper bars, field and stator windings, for different rotor positions were calculated. By solving the governing differential equations, damper bar currents and no load voltage were calculated. The methodology assumed the field current to be constant and the eddy current at the end region effects were neglected.

Shanming *et al.* (2001) investigated the effects of parameters and operating conditions on the waveform and harmonic content in the output voltage of synchronous generators. The results were compared for multi-loop and FEM methods and the effects of magnetic circuit geometry, saliency, saturation, winding layouts as well as slotting on the space harmonics were studied. Kim and Sykulski (2002) carried out harmonic analysis of the output voltage in synchronous generators using FEM taking account of the rotor movement. A 2D FE model was used for calculating

the stator coil flux linkages and rotor movement was accounted by moving band technique. Rotor movement can be implemented by different schemes such as slip surface (Ide *et al.*, 1992), moving band technique (Sadowski *et al.*, 1992), lagrange multipliers (Lombard and Meunier, 1993), incomplete shape functions approach (Biddlecombe, 1998) and lockstep mesh (Rapetti *et al.*, 2000) and novel technique based on integral formulation to treat the motion in the analysis of electric machinery was proposed by Calvano *et al.* (2012).

As reported by Premkumar (2006), FEM enables accurate estimation of the magnetic field in electrical machines and devices and therefore makes possible accurate estimation of various flux related parameters, the induced voltage magnitude being one among them. The author described a method for computation of turbo-generator induced voltage waveform and its harmonic content, at the design stage. FE approach has been used for the accurate estimation of magnetic field in the turbo-alternator at no load. Harmonic components computed from the air gap induction profile were used to arrive at the harmonic voltage magnitudes.

Yonghong *et al.* (2008) presented a methodology based on tooth flux method for prediction of harmonics in the no load electromagnetic field of synchronous generators. In the steady state, flux distributions over one slot pitch in the stator occur periodically and it is sufficient to analyse one period of such flux distributions for calculating induced voltages. Hence, in tooth flux method, the stator tooth was taken as the smallest analysis unit and by FEM with rotor movement through one stator tooth pitch, the magnetic vector potential in the centre of the stator slot was calculated. The flux waveforms of each stator tooth for different rotor positions were calculated and based on this, the flux linkage of the fundamental windings and the third harmonic windings were computed. In this method, the effects of the magnetic circuit geometry, saliency, saturation, windings and slotting

on the flux harmonics were studied.

Hargreaves *et al.* (2010) studied the influence of machine geometry on the open circuit voltage distortion in salient pole synchronous machines with damper bars, by magneto-static FEA. Transient analysis of the machine was achieved by shifting the position of stator conductors keeping the rotor stationary. The method incorporated magnetic non-linearity and modelled damper bar currents.

THD in the output voltage of alternators cause ill effects in the performance of these machines. Hence, out of the different design modifications available for reduction of harmonics, the designer has the liberty to choose the design option based on the order of the harmonic to be eliminated/reduced. This decision is taken based on the simulation results of the FE model of the machine.

2.7 Methods for Reduction of Harmonics in Salient Pole Alternators

Wakileh (2003) has reported on the impact of harmonics on rotating electric machines. Formulae for the induced emf, pitch factor and distribution factor were extended to include the effect of harmonics, thus allowing the computation of total harmonic distortion. Methods for reducing harmonics in rotating machines were also discussed and numerical examples were provided to show the effect of winding distribution and chording on the phase voltage waveform. The advantage of using distributed and chorded windings to reduce harmonics was also demonstrated. Harmonic reduction in the output voltage of salient pole alternators is achieved by conventional methods like properly shaping the pole profile, introducing fractional slot winding and the effect of slot harmonics is reduced by skewing either stator or the rotor (Knight *et al.*, 2009). In addition to this, selected

harmonics are eliminated by short chording the winding. Ignoring slot harmonics, 3rd, 5th and 7th harmonics are the dominant harmonics with different percentage of each in various conditions.

2.7.1   Winding Modifications

The familiar method for reducing space harmonic content of MMF produced by a distributed poly-phase AC winding, is by chording, although by itself this can selectively eliminate only one of the major low order harmonics. To achieve a winding in which all the winding factors other than the fundamental are zero has been proved to be impossible. Several authors have reported on the use of unconventional windings for producing an improved MMF waveform. Charmers (1964) used interspersed windings for an odd number of slots per pole per phase. Even though this has a significant effect on the harmonic winding factors, it also brings about a slight reduction in that of the fundamental. Hughes (1970) divided the conventional 60° phase spread winding into two parallel connected star delta windings, each with a phase spread of 30°, thereby effectively producing a 6-phase machine fed from a 3-phase supply with an improved winding factor of 0.987. Thus, with interspersed windings, a reduction, but not elimination, of harmonics is brought about.

Use of non-uniformly distributed (or graded) windings, in which the number of conductors per phase per slot in a double layer winding varied linearly, was proposed by Krebs (1948) and later refined by Smith and Layton (1963) who allowed the number of conductors per slot to vary sinusoidally, resulting in the elimination of all non-slot harmonics with a fundamental winding factor of 0.904. Centner and Hanistsch (2006) described a stator design with two different slot shapes for use with fractional slot windings without changing the phase spread. The work by Kocabas (2009) described a novel extension to this work in which both the

winding arrangement and the peripheral slot pattern were unconventional. It was shown that the MMF waveform can be greatly improved by the introduction of both non-uniform conductor and slot distributions. There was no discrete phase spread for each phase and the phase spreads were interspersed with one other. The novel slot positions and the number of conductors per slot were calculated for one phase using Newton-Raphson optimisation method to eliminate a given number of target harmonics. Once a targeted space harmonic is eliminated from one phase, it will not produce a rotating field in the overall winding and there will not be any corresponding adverse effects. The winding factor was checked after optimisation and a high value for the fundamental was confirmed. In this method, the number of targeted space harmonics that can be eliminated depends solely on the number of slots. But, this method has the limitations that the design is to be customized for different models of machines and different slot designs are needed to accommodate different numbers of conductors. The method is applicable for any conventional 3-phase single layer AC winding having number of slots in multiples of 12.

2.8 Third Harmonic Excitation of Brushless Alternators

In certain configurations of brushless excitation systems, auxiliary windings are used for powering AVR. Different schemes of this concept are used by different authors, the latest being the use of a winding for harvesting third harmonic power for excitation.

Darabi (2005) reported on the use of auxiliary windings for powering AVR of a brushless synchronous generator and the voltage induced in the auxiliary winding was used for excitation control in the machine. Shaogang *et al.* (2007) proposed the tooth

flux method for calculation of third harmonic flux in the air gap of synchronous generators. This method was based on the calculation of flux in each of the tooth in the machine stator, for different rotor positions. According to the coupling relationship between the coils and tooth, the winding flux linkage was calculated and then the EMF induced in the winding was estimated as proportional to the change in flux linkages. But, this method is useful for calculation of the third harmonic voltage only under steady state operation of the machine. Further, the authors described a method for prediction of magnitude and waveform of harmonic winding voltage in synchronous generator by computation of the electromagnetic field, by tooth flux method.

Podgornovs and Zviedris (2007) proposed a methodology where an auxiliary winding is placed in the armature of a machine to use the third harmonic energy of a magnetic field and it was concluded that the energy of magnetic field third harmonic is enough to provide supply of synchronous motor excitation winding in no-load operation.

Chicco *et al.* (2011) reported on the explicit role of the triplen harmonics in unbalanced 3-phase systems with distorted waveforms and the triplen harmonics contribute to the neutral current when 3-phase systems power single phase loads. Abdulla *et al.* (2014) has developed third harmonic model for salient pole synchronous generator in symmetrical component domain, under balanced load.

2.9   Conclusion

The main feature of a brushless alternator excitation system is the ability to keep voltage regulation within the specified tolerance bands. Output parameters of brushless alternators like THD and winding inductances play important role in the per-

formance of the machine. Prediction of these parameters in the design stage helps to save cost and time for machine development. Hence, virtual prototyping is adopted for advance prediction of machine parameters and of the different methods available, FEM proves to be an accurate method as it accounts for the material non-linearities. The details of research related to parameter estimation of machines using FEM, as reported in literature is summarized in Table 2.1.

After the extensive literature review, it is observed that application of third harmonic excitation system for improvement in THD and voltage regulation in brushless alternators has not so far been reported. The main objective of the present research work is to use FEM based virtual prototype of an alternator to design the third harmonic winding in the brushless excitation system and to ascertain the effectiveness of the third harmonic excitation system as a damper of triplen harmonics in the output phase voltage of the alternator.

Table 2.1: Summary of literature on parameter estimation of machines using FEM

Reference	Method used	Parameter estimated
[4]	$2D\,FEM$	X_d, X_q
[6]	$2D\,FEM$	$Load\,angle,\ field\,current$
[18]	$3D\,magnetostatic\,FEM$	$End\,winding\,inductances$
[20]	$Time\,stepped\,2D\,FEM$	$Induced\,voltage\,and\,current\,wave forms$
[24]	$3D\,magnetostatic\,FEM$	$Magnetic\,flux\,and\,flux\,density\,distribution$
[26]	$2D\,FEM$	X_d, X_q
[34]	$2D\,FEM$	$Self\,and\,mutual\,inductances$
[37]	$Time\,stepped\,2D\,FEM$	$Voltage\,and\,current\,wave forms$
[57]	$2D\,FEM$	$THD\,in\,no-load\,output\,voltage$
[65]	$2D\,FEM$	$Magnetic\,flux\,output\,voltage\,wave forms$
[67]	$2D\,FEM$	$Power\,angle\,characteristics$
[72]	$2D\,FEM$	$Damper\,bar\,currents, voltage\,wave form$
[73]	$2D\,FEM$	$Output\,voltage\,Harmonics$
[76]	$2D\,FEM$	$Output\,voltage\,harmonics$
[79]	$2D\,FEM$	$Steady\,state\,and\,transient\,reactances$
[80]	$2D\,FEM$	$Air\,gap\,flux\,density\,distribution, OCC$
[92]	$2D\,FEM$	$Iron\,losses$
[95]	$2D\,FEM$	$Magnetic\,core\,losses$
[104]	$2D\,FEM$	$Air\,gap\,flux\,density, OCC$
[108]	$Time\,stepped\,2D\,FEM$	X_d, X_q
[109]	$2D\,FEM$	$Load\,parameters$
[111]	$2D\,FEM$	OCC
[113]	$2D\,FEM$	$Telephone\,harmonic\,factor$
[118]	$Time\,stepped\,2D\,FEM$	$Output\,voltage\,harmonics$
[132]	$2D\,FEM$	$Output\,voltage\,harmonics$
[134]	$2D\,FEM$	$Output\,voltage\,harmonics$
[141]	$2D\,FEM$	$Flux\,density\,plot$
[145]	$Time\,stepped\,2D\,FEM$	$Field\,and\,phase\,current\,wave forms$
[155]	$Time\,stepped\,2D\,FEM$	$Short\,Circuit\,fault\,simulation$
[158]	$Time\,stepped\,2D\,FEM$	$Output\,voltage\,wave form\,and\,harmonics$
[159]	$Time\,stepped\,2D\,FEM$	$Phase\,voltage\,and\,current\,wave forms$
[163]	$2D\,FEM$	$Output\,voltage\,harmonics$

Chapter 3

Finite Element Formulation of the Field Problem

3.1   Introduction

Computer aided analysis of field distribution has become the most effective method for performance prediction of electrical machines. A typical electro-magnetic field problem is described by defining the geometry, material properties, currents, boundary conditions and the governing field equations. Solution of the governing equation, yields the primary variable, *i.e.*, MVP at each and every point in the problem domain. From the primary variable, the secondary variables like magnetic flux, flux density, induced emf, inductances and other machine parameters are derived. Combining analytical methods with FEM solution, performance characteristics of the machine like THD are calculated.

FEM was originally used to study problems in structural me-

55

chanics. Its employment for solution of electro-magnetic vector field problems presented by electric machinery became popular in 1980's. Today, FE analysis is a widely applied tool in electrical machine analysis, and the method finds its application for studying problems of electro-magnetic, thermal, mechanical,coupled or multi-physics nature.

To start with the electrical machine design process, it is necessary to have the basic design of the machine. This involves dimensioning of the magnetic and electric circuits which is usually carried out by applying analytical equations. Subsequently, actual performance of the machine is accurately predicted using the FEM model and based on the results, fine tuning of the design is done. With FEA, the effect of a single parameter on the dynamic performance of the machine can be studied and some tests which are not feasible in laboratory circumstances can be virtually performed.

3.2   Analytic Design of Electrical Machines

Design of an electrical machine basically involves dimensioning of the electric and magnetic circuits and quantitative determination of magnetic flux in the machine. In the design of magnetic circuit, the precise dimensions for machine parts are determined, the required current linkage for the magnetic circuit and the magnetizing current are calculated. Further, the magnitude of losses occurring in the magnetic circuit are estimated.

Design of magnetic circuit is based on Ampere's law which states that sum of magnetic potential differences calculated around the magnetic circuit is equal to surface integral of the current densities over surface S of the magnetic circuit, where surface S indicates the surface penetrated by the main flux (Say, 1952; Pyrhonen *et al.*, 2009). Ampere's law can be rewritten as:

$$v_{tot} = \sum v_i = \oint_l H \cdot dl = \oint_S J \cdot dS = \sum I = \Theta \qquad (3.1)$$

i.e., Sum of magnetic potential differences, v_{tot} around the magnetic flux path is equal to the sum of magnetizing currents in the circuit, that is the current linkage Θ. The integration path S is the main flux path of the machine.

Analytical methods using classical magnetic field equations can only estimate magnetic flux magnitude and distribution within the machine. Magnetic leakage and changes in material permeability cannot be accommodated using classical fundamental equations. Analytical calculation methods work fine if testing a prototype is practical.

3.3   Governing Equations for Electro-magnetic Fields in Electrical Machines

Electro-magnetic phenomena in electrical machines is described by Maxwell's equations and constitutive relationships (Chari and Silvester, 1980; Sadoku, 2000; Zhou, 2012). The quantities involved in the phenomena are the following:

- Electric field strength, E

- Magnetic field strength, H

- Electric flux density, D

- Magnetic flux density, B

- Current density, δ

- Electric charge density, ρ

Maxwell's equations are written in differential form as:

$$\nabla \times H\left(P,t\right) \;=\; \delta\left(P,t\right) + \frac{\partial D\left(P,t\right)}{\partial t} \tag{3.2}$$

$$\nabla \times E\left(P,t\right) \;=\; -\frac{\partial B\left(P,t\right)}{\partial t} \tag{3.3}$$

$$\nabla.B\left(P,t\right) \;=\; 0 \tag{3.4}$$

$$\nabla.D\left(P,t\right) \;=\; \rho\left(P,t\right) \tag{3.5}$$

The constitutive relationships are:

$$B\left(P,t\right) \;=\; \mu\left(P\right)H\left(P,t\right) \tag{3.6}$$

$$D\left(P,t\right) \;=\; \epsilon\left(P\right)E\left(P,t\right) \tag{3.7}$$

$$\delta\left(P,t\right) \;=\; \sigma\left(P\right)E\left(P,t\right) \tag{3.8}$$

Combining Maxwell's equations and the constitutive relationships, the quasi-stationary electromagnetic field distribution in the machine structure is described by the governing equation known as Poisson's equation (Chari and Salon, 2000), as given by:

$$\frac{1}{\mu}\nabla^2 A_z \;=\; -\delta_z \tag{3.9}$$

$$\frac{\partial^2 A_z}{\partial x^2} + \frac{\partial^2 A_z}{\partial y^2} \;=\; -\mu\delta_z \tag{3.10}$$

Solution of the non-linear partial differential equation by FEM yields magnetic vector potential A_z from which the magnetic flux density B having components only in the (x,y) plane is computed using the relation:

$$B\left(P,t\right) = \nabla \times A\left(P,t\right) \tag{3.11}$$

In 2D magneto-static problems, the difference between vector potentials in two points (x_1, y_1) and (x_2, y_2) represents the flux

through a surface having unitary length in z-direction with the sides of the coil parallel to z-axis. (Bargallo, 2006). In a coil with sides 1 and 2, the flux per unit length ϕ is given by:

$$\phi = A_1 - A_2$$

The flux linked with the coil is given by:

$$\psi = \frac{1}{S} \int A \cdot dS$$

As per Faraday's law, induced e.m.f. in the conductor can be obtained by numerical derivation of the flux linkage. Thus, from the value of the primary variable obtained from the field simulation, all secondary variables are derived and hence machine parameters like induced voltage, inductances, d and q-axes reactances, saturation factor are computed (Bianchi, 2001) based on the fundamental electro-magnetic principles.

3.4 FE Formulation of Electro-magnetic Field Problems

Design optimisation of electrical machinery is a challenging job for the designer because it demands competitive price, high power to weight ratio and high degree of reliability in operation. This necessitates virtual prototyping and parameter estimation of the machine under development. But, complex geometry together with presence of non-linear magnetic materials pose difficulty in analysis and prediction of magnetic field pattern in such machines.

In order to predict the performance of electrical machines accurately at the design stage, magnetic field mapping of the machine structure is necessary which requires accurate modelling of the machine. Conventional methods are based on approximations and hence inaccurate. FEM offers an efficient and accurate means of predicting the magnetic field distribution in machines, taking into account non-linearity of the iron material.

3.4.1 Formulation of Brushless Alternator Field Problem

3D analysis of the synchronous generator involves dividing the whole structure by 3D finite elements which require heavy processing and results in long computation time. The magnetic field existing in the machine structure can be approximated to be 2D since there exists a symmetry due to repetition of the physical phenomena, plane by plane. This happens as the currents flow in a direction parallel to the z-axis and the transverse sections to this axis always present same geometry and the same materials, point by point (Bargello, 2006) Considering planar symmetry of the field problem as shown in Figure 3.1, the field properties of the machine are invariant along the z-axis and the dimensionality of the problem can be reduced to two, thereby considerably reducing the computational time (Bianchi, 2005; Bargello, 2006; Pyrhonen *et al.*, 2009). Hence, the brushless alternator field problem under the present study is reduced to 2D field analysis without compromising the accuracy of results.

Study of the 2D field problem with planar symmetry has been detailed as follows:

1. The current density vector δ has z-axis component only. *i.e.*,

$$\delta = [0, 0, \delta_z] \tag{3.12}$$
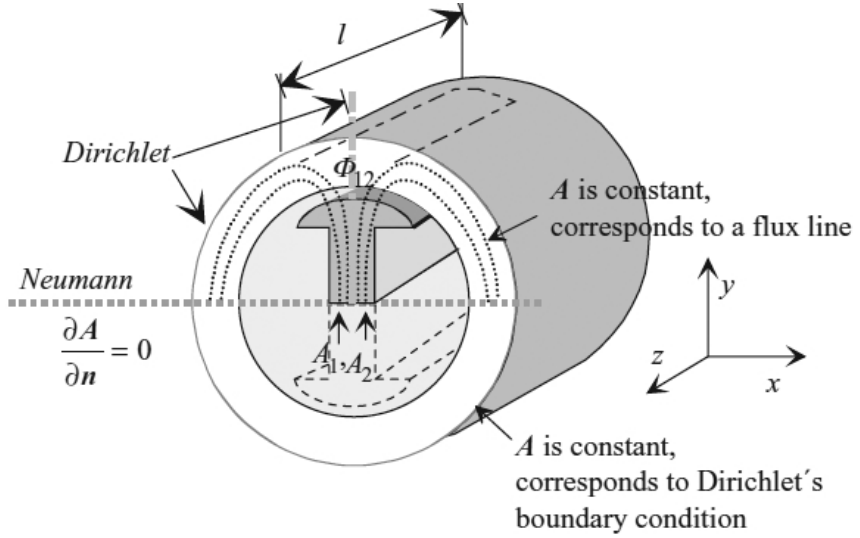
Fig. 3.1: 2D field and boundary conditions for a salient pole synchronous machine(*Source: Pyrhonen et al. (2009)*)

2. The magnetic vector potential A is parallel to the vector δ, thus it has z-axis component only. *i.e.,*

$$A = [0, 0, A_z] \qquad (3.13)$$

As regards the divergence of the magnetic vector potential, Coulomb's gauge is adopted, *i.e.,* $div A = \nabla \cdot A = 0$

3. The flux density vector B has components only in the (x,y) plane and is derived from A using the formula:

$$B = curl A = \nabla \times A = \nabla \times [0, 0, A_z]$$
$$= \left[\frac{\partial A_z}{\partial y}, -\frac{\partial A_z}{\partial x}, 0 \right] \qquad (3.14)$$

4. With a constant magnetic permeability, the magnetic field distribution along the cross section of a synchronous machine is described by the two dimensional Poisson's as given

in Equation 3.10. MVP can be determined from Poisson's equation, at each point in the problem domain if the current density δ is fixed and the value of A_z is known on the boundary Γ of the domain, *i.e.*, in a part of the domain, say Γ_1 , the value of A_z is assigned, and in the remaining part of the boundary, say Γ_2 , the value of the derivative of A_z normal to the boundary line is assigned.

5. Since the flux lines are tangential to the outer boundary of the machine structure, no flux lines cross the boundary. Hence homogeneous Dirichlet's condition (Bianchi, 2005) is assigned, fixing the MVP, $A_z = 0$ along the outer boundary.

6. The magnetic behaviour in the machine structure has periodic symmetry among pole pairs around the z-axis. The machine under study being 4-pole, the domain under analysis is reduced to one fourth on account of the periodic symmetry of the field pattern, which further reduces the computational time for field analysis. Therefore, along the axes of periodic symmetry, the periodic boundary conditions are applied. Since the flux density components cannot be discontinuous across the symmetry axis, the flux lines must be normal to the axis. Hence the Neumann's boundary condition, *i.e.*, $\frac{\partial A}{\partial n} = 0$, is applied along the symmetry axis (Bianchi, 2005).

3.4.2   Formulation by Galerkin's Method

Let $\hat{A}$ be the approximate solution of the magnetic vector potential. Substituting the approximate solution $\hat{A}$ in Equation (3.10), the residue R can be made available as (Silvester *et al.*, 1996; Bianchi, 2005; Virjoghe *et al.*, 2012):

$$R = \frac{1}{\mu}\frac{\partial^2 \hat{A}}{\partial x^2} + \frac{1}{\mu}\frac{\partial^2 \hat{A}}{\partial y^2} + \delta \qquad (3.15)$$

The weighted integral form for 2D solution is:

$$\iint_\Omega R \cdot W \, dx \, dy = 0 \qquad (3.16)$$

where W is the weight function (Finlayson and Scriven, 1966; Finlayson, 2013). Substituting the value of R in the weighted integral form,

$$-\iint_\Omega W \left(\frac{1}{\mu} \frac{\partial^2 \hat{A}}{\partial x^2} + \frac{1}{\mu} \frac{\partial^2 \hat{A}}{\partial y^2} \right) dx \, dy = \iint_\Omega W \delta \, dx \, dy \qquad (3.17)$$

Integrating L.H.S. of Equation (3.17) by parts,

$$-\iint_\Omega \frac{1}{\mu} \left(\frac{\partial W}{\partial x} \frac{\partial \hat{A}}{\partial x} + \frac{\partial W}{\partial y} \frac{\partial \hat{A}}{\partial y} \right) dx \, dy - \oint_c \frac{1}{\mu} W \frac{\partial \hat{A}}{\partial \hat{n}} \, dc$$
$$= \iint_\Omega W \delta \, dx \, dy \qquad (3.18)$$

where $\hat{n}$ is the outward unit vector on boundary c.

Discretisation of the problem domain in Equation (3.18) is performed using 2D finite elements. Six noded triangular elements are used for discretisation of the problem domain which has three nodes at the vertices of the triangle, three mid-side nodes and the variable interpolation within the element is quadratic in x and y (Bastos and Sadowski, 2003). For $'M'$ triangular elements,

$$\sum_M \left[\frac{1}{\mu^e} \iint_{\Omega^e} \left(\frac{\partial W^e}{\partial x} \frac{\partial \hat{A}^e}{\partial x} + \frac{\partial W^e}{\partial y} \frac{\partial \hat{A}^e}{\partial y} \right) \right] dx \, dy$$
$$- \frac{1}{\mu^e} \frac{\partial \hat{A}^e}{\partial \hat{n}} \oint_c W^e \, dc = \delta \iint_{\Omega^e} W^e \, dx \, dy \qquad (3.19)$$

Geometry of the machine discretised with second order triangular elements are shown in Figure 3.2.
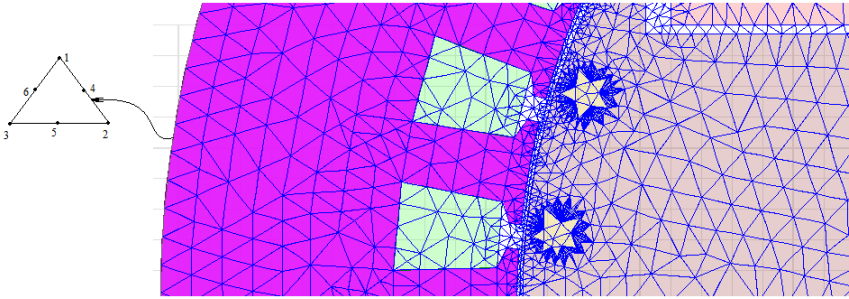
Fig. 3.2: Geometry of the machine discretised with triangular elements

The approximate solution of A at any point (x,y) in the element is represented in terms of the nodal values of A and the shape functions,

$$\hat{A}^e_{(x,y)} = \begin{bmatrix} N_1 & N_2 & N_3 & N_4 & N_5 & N_6 \end{bmatrix} \begin{bmatrix} A_1 \\ A_2 \\ A_3 \\ A_4 \\ A_5 \\ A_6 \end{bmatrix} \qquad (3.20)$$

Three digit numbering is given for each node of the second order triangular element, where α, β and γ are integers satisfying the relation, $\alpha + \beta + \gamma = n$, and n is the order of the interpolation function for the element (Chari and Silvester, 1980; Hoole, 1989; Humphries, 1997; Salon *et al.*, 1999). Triple-subscript designation is used for the interpolation functions, so that $\zeta_{\alpha\beta\gamma}(\xi_1, \xi_2, \xi_3)$ will denote the shape function for node $P(\alpha, \beta, \gamma)$ in terms of the area coordinates ξ_1, ξ_2, ξ_3. As per Silvester's method (Chari and Salon, 2000), the interpolation function for an nth order triangular element is derived by the formula:

$$\zeta_{\alpha\beta\gamma}(\xi_1, \xi_2, \xi_3) = \zeta_\alpha(\xi_1)\zeta_\beta(\xi_2)\zeta_\gamma(\xi_3) \qquad (3.21)$$

where

$$\zeta_\alpha\left(\xi_1\right) = \prod_{i=1}^{\alpha} \frac{n\xi_1 - i + 1}{i}, \alpha \geq 1 \qquad (3.22)$$

The interpolation functions for the six noded second order triangular element, with $n = 2$ and three-digit notation for each of the nodes, $\zeta_{200}, \zeta_{020}, \zeta_{002}$ for the three vertices and $\zeta_{101}, \zeta_{110}, \zeta_{011}$ for the three mid-side nodes respectively are evaluated by the formula:

For node 1,

$$\alpha = 2, \beta = 0, \gamma = 0$$

$$\zeta_\alpha = \zeta_2 = \xi_1\left(2\xi_1 - 1\right)$$

$$\zeta_\beta = \zeta_0 = 1$$

$$\zeta_\gamma = \zeta_0 = 1$$

i.e.,

$$N_1 = \zeta_{200} = \zeta_2\left(\xi_1\right)\zeta_0\left(\xi_2\right)\zeta_0\left(\xi_3\right) = \xi_1\left(2\xi_1 - 1\right) \qquad (3.23)$$

Shape functions for the remaining nodes are derived as:

$$N_2 = \zeta_{020} = \xi_2\left(2\xi_2 - 1\right) \qquad (3.24)$$
$$N_3 = \zeta_{002} = \xi_3\left(2\xi_3 - 1\right) \qquad (3.25)$$
$$N_4 = \zeta_{101} = 4\xi_3\xi_1 \qquad (3.26)$$
$$N_5 = \zeta_{110} = 4\xi_1\xi_2 \qquad (3.27)$$
$$N_6 = \zeta_{011} = 4\xi_2\xi_3 \qquad (3.28)$$

As per the iso-parametric interpolation formula,

$$\begin{bmatrix} 1 \\ x \\ y \\ \hat{A} \end{bmatrix} = \begin{bmatrix} 1 & 1 & 1 & 1 & 1 & 1 \\ x_1 & x_2 & x_3 & x_4 & x_5 & x_6 \\ y_1 & y_2 & y_3 & y_4 & y_5 & y_6 \\ A_1 & A_2 & A_3 & A_4 & A_5 & A_6 \end{bmatrix} \begin{bmatrix} N_1 \\ N_2 \\ N_3 \\ N_4 \\ N_5 \\ N_6 \end{bmatrix} \qquad (3.29)$$

in which the natural derivatives are:

$$\frac{\partial N}{\partial \xi_1} = \begin{bmatrix} 4\xi_1 - 1 \\ 0 \\ 0 \\ 4\xi_2 \\ 0 \\ 4\xi_3 \end{bmatrix} \tag{3.30}$$

$$\frac{\partial N}{\partial \xi_2} = \begin{bmatrix} 0 \\ 4\xi_2 - 1 \\ 0 \\ 4\xi_1 \\ 4\xi_3 \\ 0 \end{bmatrix} \tag{3.31}$$

$$\frac{\partial N}{\partial \xi_3} = \begin{bmatrix} 0 \\ 0 \\ 4\xi_3 - 1 \\ 0 \\ 4\xi_2 \\ 4\xi_1 \end{bmatrix} \tag{3.32}$$

Then, the magnetic vector potential A is expressed as:

$$\hat{A} = \sum_{i=1}^{6} N_i\,(x, y)\, A_i \tag{3.33}$$

In Galerkin's weighted residual method, weight function is the shape function itself.*i.e.*,

$$W^e = \begin{bmatrix} N_1 \\ N_2 \\ N_3 \\ N_4 \\ N_5 \\ N_6 \end{bmatrix} = \begin{bmatrix} \zeta_{200} \\ \zeta_{020} \\ \zeta_{002} \\ \zeta_{101} \\ \zeta_{110} \\ \zeta_{011} \end{bmatrix} \tag{3.34}$$

The shape function logic is concerned with computation of the partial derivatives of the shape functions with respect to x and y at any point in the element. For this purpose, a generic scalar function, $w\left(\zeta_1, \zeta_2, \zeta_3\right)$ is considered that is quadratically interpolated over the triangle by,

$$
\begin{aligned}
w &= w_1 N_1 + w_2 N_2 + w_3 N_3 + w_4 N_4 + w_5 N_5 + w_6 N_6 \\
&= \begin{bmatrix} w_1 & w_2 & w_3 & w_4 & w_5 & w_6 \end{bmatrix} N^T
\end{aligned}
\tag{3.35}
$$

where w stands for $1, x, y$ or A . Taking partials of Equation (3.35) with respect to x and y and applying the chain rule twice yields,

$$
\begin{bmatrix} \frac{\partial N_i}{\partial x} & \frac{\partial N_i}{\partial y} \end{bmatrix} = \begin{bmatrix} \frac{\partial N_i}{\partial \xi_1} & \frac{\partial N_i}{\partial \xi_2} & \frac{\partial N_i}{\partial \xi_3} \end{bmatrix} P
\tag{3.36}
$$

In matrix form,

$$
\begin{bmatrix} \frac{\partial w}{\partial x} \\ \frac{\partial w}{\partial y} \end{bmatrix} = \begin{bmatrix} \frac{\partial \xi_1}{\partial x} & \frac{\partial \xi_2}{\partial x} & \frac{\partial \xi_3}{\partial x} \\ \frac{\partial \xi_1}{\partial y} & \frac{\partial \xi_2}{\partial y} & \frac{\partial \xi_3}{\partial y} \end{bmatrix} \begin{bmatrix} \sum_{i=1}^6 w_i \frac{\partial N_i}{\partial \xi_1} \\ \sum_{i=1}^6 w_i \frac{\partial N_i}{\partial \xi_2} \\ \sum_{i=1}^6 w_i \frac{\partial N_i}{\partial \xi_3} \end{bmatrix}
\tag{3.37}
$$

Transposing both sides of Equation (3.37) while exchanging sides yields,

$$
\begin{bmatrix} \sum_{i=1}^6 \omega_i \frac{\partial N_i}{\partial \xi_1} & \sum_{i=1}^6 \omega_i \frac{\partial N_i}{\partial \xi_2} & \sum_{i=1}^6 \omega_i \frac{\partial N_i}{\partial \xi_3} \end{bmatrix} \begin{bmatrix} \frac{\partial \xi_1}{\partial x} & \frac{\partial \xi_1}{\partial y} \\ \frac{\partial \xi_2}{\partial x} & \frac{\partial \xi_2}{\partial y} \\ \frac{\partial \xi_3}{\partial x} & \frac{\partial \xi_3}{\partial y} \end{bmatrix} = \begin{bmatrix} \frac{\partial \omega}{\partial x} & \frac{\partial \omega}{\partial y} \end{bmatrix}
\tag{3.38}
$$

Making $w = 1, x, y$ and stacking the results row-wise,

$$
\begin{bmatrix} \sum_{i=1}^6 \frac{\partial N_i}{\partial \xi_1} & \sum_{i=1}^6 \frac{\partial N_i}{\partial \xi_2} & \sum_{i=1}^6 \frac{\partial N_i}{\partial \xi_3} \\ \sum_{i=1}^6 x_i \frac{\partial N_i}{\partial \xi_1} & \sum_{i=1}^6 x_i \frac{\partial N_i}{\partial \xi_2} & \sum_{i=1}^6 x_i \frac{\partial N_i}{\partial \xi_3} \\ \sum_{i=1}^6 y_i \frac{\partial N_i}{\partial \xi_1} & \sum_{i=1}^6 y_i \frac{\partial N_i}{\partial \xi_2} & \sum_{i=1}^6 y_i \frac{\partial N_i}{\partial \xi_3} \end{bmatrix} \begin{bmatrix} \frac{\partial \xi_1}{\partial x} & \frac{\partial \xi_1}{\partial y} \\ \frac{\partial \xi_2}{\partial x} & \frac{\partial \xi_2}{\partial y} \\ \frac{\partial \xi_3}{\partial x} & \frac{\partial \xi_3}{\partial y} \end{bmatrix} = \begin{bmatrix} \frac{\partial 1}{\partial x} & \frac{\partial 1}{\partial y} \\ \frac{\partial x}{\partial x} & \frac{\partial x}{\partial y} \\ \frac{\partial y}{\partial x} & \frac{\partial y}{\partial y} \end{bmatrix}
\tag{3.39}
$$

But, $\frac{\partial x}{\partial x} = \frac{\partial y}{\partial y} = 1$ and $\frac{\partial 1}{\partial x} = \frac{\partial 1}{\partial y} = \frac{\partial x}{\partial y} = \frac{\partial y}{\partial x} = 0$ because x and y are independent coordinates. Since $\sum_{i=1}^{6} N_i = 1$, the entries of the first row of the coefficient matrix are equal to a constant C, which can be scaled to unity because the first row of the right hand side is null. Therefore, Equation (3.39) gets reduced to,

$$
\begin{bmatrix}
1 & 1 & 1 \\
\sum_{i=1}^{6} x_i \frac{\partial N_i}{\partial \xi_1} & \sum_{i=1}^{6} x_i \frac{\partial N_i}{\partial \xi_2} & \sum_{i=1}^{6} x_i \frac{\partial N_i}{\partial \xi_3} \\
\sum_{i=1}^{6} y_i \frac{\partial N_i}{\partial \xi_1} & \sum_{i=1}^{6} y_i \frac{\partial N_i}{\partial \xi_2} & \sum_{i=1}^{6} y_i \frac{\partial N_i}{\partial \xi_3}
\end{bmatrix}
\begin{bmatrix}
\frac{\partial \xi_1}{\partial x} & \frac{\partial \xi_1}{\partial y} \\
\frac{\partial \xi_2}{\partial x} & \frac{\partial \xi_2}{\partial y} \\
\frac{\partial \xi_3}{\partial x} & \frac{\partial \xi_3}{\partial y}
\end{bmatrix}
=
\begin{bmatrix}
0 & 0 \\
1 & 0 \\
0 & 1
\end{bmatrix}
$$
(3.40)

The coefficient matrix of equation (3.40) is called the Jacobian matrix denoted by $\mathbf{J}$. For compactness, Equation (3.40) is written as

$$
\mathbf{JP} =
\begin{bmatrix}
1 & 1 & 1 \\
J_{x1} & J_{x2} & J_{x3} \\
J_{y1} & J_{y2} & J_{y3}
\end{bmatrix}
\begin{bmatrix}
\frac{\partial \xi_1}{\partial x} & \frac{\partial \xi_1}{\partial y} \\
\frac{\partial \xi_2}{\partial x} & \frac{\partial \xi_2}{\partial y} \\
\frac{\partial \xi_3}{\partial x} & \frac{\partial \xi_3}{\partial y}
\end{bmatrix}
=
\begin{bmatrix}
0 & 0 \\
1 & 0 \\
0 & 1
\end{bmatrix}
$$
(3.41)

Solving this system gives,

$$
\begin{bmatrix}
\frac{\partial \xi_1}{\partial x} & \frac{\partial \xi_1}{\partial y} \\
\frac{\partial \xi_2}{\partial x} & \frac{\partial \xi_2}{\partial y} \\
\frac{\partial \xi_3}{\partial x} & \frac{\partial \xi_3}{\partial y}
\end{bmatrix}
= \frac{1}{2J}
\begin{bmatrix}
J_{y23} & J_{x32} \\
J_{y31} & J_{x13} \\
J_{y12} & J_{x21}
\end{bmatrix}
= \mathbf{P}
$$
(3.42)

in which $J_{xji} = J_{xj} - J_{xi}$, $J_{yji} = J_{yj} - J_{yi}$ and

$J = \frac{1}{2} det\mathbf{J} = \frac{1}{2}\left(J_{x21}J_{y31} - J_{y12}J_{x13}\right)$

Substituting into Equation (3.37):

$$
\frac{\partial w}{\partial x} = \sum_{i=1}^{6} w_i \frac{\partial N_i}{\partial x} = \sum_{i=1}^{6} \frac{w_i}{2J}\left(\frac{\partial N_i}{\partial \xi_1}J_{y23} + \frac{\partial N_i}{\partial \xi_2}J_{y31} + \frac{\partial N_i}{\partial \xi_3}J_{y12}\right)
$$
(3.43)

$$\frac{\partial w}{\partial y} = \sum_{i=1}^{6} w_i \frac{\partial N_i}{\partial y} = \sum_{i=1}^{6} \frac{w_i}{2J} \left(\frac{\partial N_i}{\partial \xi_1} J_{x32} + \frac{\partial N_i}{\partial \xi_2} J_{x13} + \frac{\partial N_i}{\partial \xi_3} J_{x21} \right)$$

(3.44)

The shape function derivatives are,

$$\frac{\partial N_i}{\partial x} = \frac{1}{2J} \left(\frac{\partial N_i}{\partial \xi_1} J_{y23} + \frac{\partial N_i}{\partial \xi_2} J_{y31} + \frac{\partial N_i}{\partial \xi_3} J_{y12} \right) \qquad (3.45)$$

$$\frac{\partial N_i}{\partial y} = \frac{1}{2J} \left(\frac{\partial N_i}{\partial \xi_1} J_{x32} + \frac{\partial N_i}{\partial \xi_2} J_{x13} + \frac{\partial N_i}{\partial \xi_3} J_{x21} \right) \qquad (3.46)$$

in which the natural derivatives $\frac{\partial N_i}{\partial \xi_j}$ can be read off Equations (3.30) to (3.32). Use of the **P** matrix defined in Equation (3.42), yields Equations (3.45) and (3.46) in compact form as,

$$\left[\begin{array}{cc} \frac{\partial N_i}{\partial x} & \frac{\partial N_i}{\partial y} \end{array} \right] = \left[\begin{array}{ccc} \frac{\partial N_i}{\partial \xi_1} & \frac{\partial N_i}{\partial \xi_2} & \frac{\partial N_i}{\partial \xi_3} \end{array} \right] \mathbf{P} \qquad (3.47)$$

These differentials are substituted in the weighted integral form of Equation (3.18) and the second term in the equation,

$\oint_c \frac{1}{\mu} W \frac{\partial \hat{A}}{\partial \hat{n}} \, dc = 0$ as the component of $\hat{A}$ along the outward unit vector $\hat{n}$ on boundary c is zero. Also,

$$\iint_\omega W \delta \, dx \, dy = \frac{\delta}{3} \begin{bmatrix} 0 \\ 0 \\ 0 \\ 1 \\ 1 \\ 1 \end{bmatrix} \Delta = \frac{\delta \Delta}{3} \begin{bmatrix} 0 \\ 0 \\ 0 \\ 1 \\ 1 \\ 1 \end{bmatrix} \quad (3.48)$$

Product of the current density, δ and area of the triangle, Δ gives the total current flowing through the triangle. Hence, the governing partial differential equation of the field form represented by Equation (3.18) gets reduced to the matrix form,

$$[S][A] = [I] \qquad (3.49)$$

where $[S]$ is the stiffness matrix which depends only on the nodal coordinates of the triangular element and $[I]$ is the forcing function at the nodes of the triangular element. Several triangles when used to discretise the problem domain under analysis, results in a $k \times k$ matrix equation, where k is the total number of nodes. Each triangle used for discretisation may have a different constant permeability and applied current density (zero or non-zero). With advanced software/hardware, matrices with thousands of rows/columns and millions of matrix entries are solved within a few minutes. In general, both storage requirements and computation time are proportional to the number of unknowns (k) to a power between 2 and 3.

The stiffness matrix gives a relationship between the nodes in an element and some of the nodes are part of neighbouring elements. By enumerating the nodes and adding all the matrices together, stiffness matrix for the problem domain is obtained. From Equation (3.49), the unknown nodal values of A are calculated.

After computation of all nodal vector potentials, magnetic flux density in each triangle is calculated using the equation,

$$B = \sqrt{\left(\frac{\partial A}{\partial x}\right)^2 + \left(\frac{\partial A}{\partial y}\right)^2} \qquad (3.50)$$

Since permeability in iron parts of the machine is non-linear and field dependent, the solution to the field problem can not be obtained by solving matrix equation for discretised field region, only once. As solution to the problem is piecewise continuous, permeability of different sub-regions or finite elements spanning the iron parts cannot be determined *a priori* (Trowbridge, 1990). Therefore, solution of non-linear equations is done by Newton-Raphson (N-R) method (Wait, 1979).

N-R method is based on derivatives of the function or quantity to be updated, and the procedure yields rapid convergence, with the

error in a given step decreasing as square of error in the previous step. The acceptable limit of error for convergence is fixed as 0.5%. Application of this procedure consists of finding a change in the potential as a result of change in the permeability, which again varies as a function of the potential, the flow chart given in Figure 3.3.

Therefore, matrix Equation 3.49 gets modified to,

$$\nu(A)[S][A] - [I] = 0 \qquad (3.51)$$

where $\nu(A)$ is a matrix of field dependent non-linear reluctances. Differentiating Equation 3.51 by each of the nodal potential A_k,

$$J = \nu(A)[S] + \frac{\partial \nu}{\partial A_k}[S][A] \qquad (3.52)$$

where J is the Jacobian matrix of derivatives. Further expanding the derivative $\frac{\partial \nu}{\partial A_k}$ by chain rule of differentiation,

$$\frac{\partial \nu(A)}{\partial A_k} = \frac{\partial \nu(A)}{\partial |B|^2} \cdot \frac{\partial |B|^2}{\partial A_k} \qquad (3.53)$$

From Equation (3.50), for the two dimensional region, flux density B in each element is defined in terms of the x, y derivatives of vector potential A as,

$$B^2 = \left(\frac{\partial A}{\partial x}\right)^2 + \left(\frac{\partial A}{\partial y}\right)^2 \qquad (3.54)$$

Substituting for B in the derivative term of B with respect to A_k in Equation (3.53), and performing the necessary algebraic operations,

$$\frac{\partial \nu}{\partial A_k} = 2\frac{\partial \nu}{\partial |B|^2}\left[\left(\frac{\partial A}{\partial x}\right)\frac{\partial}{\partial A_k}\left(\frac{\partial A}{\partial x}\right) + \left(\frac{\partial A}{\partial y}\right)\frac{\partial}{\partial A_k}\left(\frac{\partial A}{\partial y}\right)\right]$$
$$= 2\frac{\partial \nu}{\partial |B|^2}\left((S)(A)\right)^T \qquad (3.55)$$

Substituting the result from Equation (3.55) into Equation (3.52), the Jacobian is obtained as,

$$J = \nu(A)(S) + 2\frac{\partial \nu(A)}{\partial |B|^2}((S)(A))((S)(A))^T \qquad (3.56)$$

The N-R algorithm can then be written as,

$$(J)\delta(A) = -(R) \qquad (3.57)$$

where (R) is the residual vector given in terms of vector potential at start of the iteration as,

$$\nu(A)(S)(A) - (I) \qquad (3.58)$$

Solving the set of algebraic equations resulting from Equation (3.57) in each iterative step of the N-R scheme, the changes in vector potential A are obtained. The new vector potential in the $(k + 1)^{th}$ iterative step is found in terms of its value in the kth step as follows:

$$(A)^{k+1} = (A)^k + (\delta A)^k \qquad (3.59)$$

From the vector potential obtained in $(k + 1)^{th}$ iteration, flux density B is calculated and new value of derivative of the reluctivity with respect to B^2 is found from material characteristic curve. Finite element solution is once again obtained as described in Equations (3.51) through (3.58) and the new value of vector potential is computed. When magnitude of the residual vector given by Equation (3.58) is less than an acceptable limit, the iterative process is discontinued and solution vector is saved and used for post-processing.

3.5   Conclusion

In this chapter, The basic steps to solve the governing Poisson's equation using quadratic triangular finite elements are de-

scribed. By this method, the continuous partial differential equation describing electro-magnetic field distribution in the problem domain is replaced with a set of discrete algebraic equations which are then solved by standard procedures. The resulting matrix has a banded and symmetric structure which minimises the computational overhead.

Finite element formulation of electromagnetic fields in rotating electrical machines with linear triangular elements is less computationally intensive. But, to get accurate computation of field variables, elements in the air gap of the machine has to be dense and the resulting matrices are large necessitating huge computer storage. To improve accuracy of computation, quadratic triangular elements are used where the field variable at six nodes of each element are computed and then interpolated to estimate the field variable at each and every point in the analysis domain. Isoparametric elements used for discretisation help modelling complex geometry of the machine accurately.
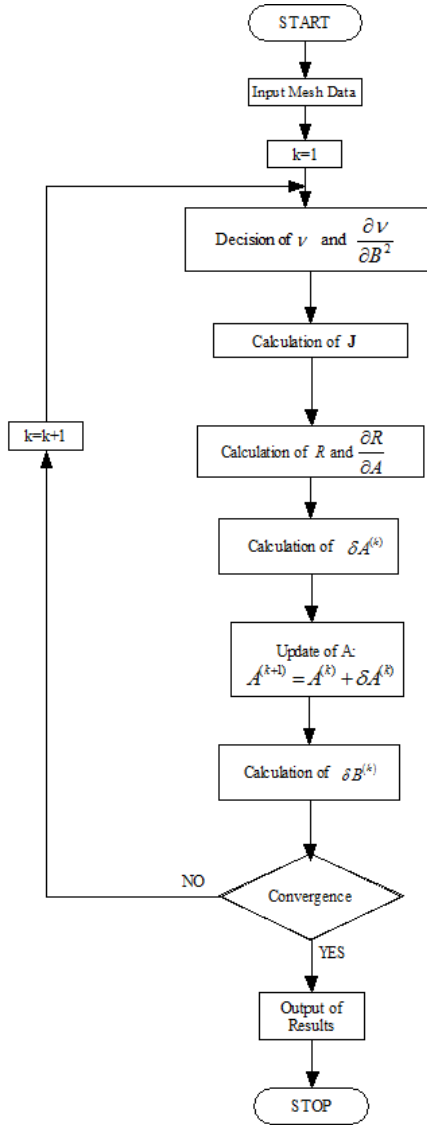
Fig. 3.3: Flow chart of Newton-Raphson method

Chapter 4

Parameter Prediction by FEM Based Virtual Prototyping

Virtual Prototyping (VP) is a technology which involves use of virtual reality and computer technologies to create digital prototype of a product under development. In a conventional product development cycle, prototype development is a costly and time consuming process, still carried out to prove design concepts, evaluate design alternatives, test product manufacturability and product conformance to the specified requirements. With the goal of replacing physical prototype digitally, a virtual prototype serves the same functions and even more of a physical prototype, regardless of which techniques are used for the virtual prototype development. A virtual prototype is used to test conformance to specifications and performance of the product in order to aid product analysis and design modifications at the machine design stage and helps improve the product development process (Wang, 2002; Lau, 2005).

Virtual prototyping shortens the product development cycle and carries out virtual testing so as to accurately predict and improve product performance as well as quality. By adopting modern virtual prototyping/analysis techniques and following simple design guidelines, the cost, in terms of time and money towards designing a custom machine is greatly reduced.

4.1 Importance of Prototyping in Electrical Machine Development Cycle

Electric machines are being used in mission critical applications throughout the world, driven by the need for greater power efficiency in the transportation, aerospace, defence and industrial automation markets. The electric machine is a very complex device being multi-domain by nature involving electro-magnetics, thermal and mechanical effects. In the face of global competition, electric machine manufacturers, like manufacturers in most industries, are searching for ways to reduce cost, optimise designs and deliver them quickly to market. Hence, designers are confronted with the task of designing machines with high power to weight ratio, high efficiency and low cost per KVA output. While designing such machines, accurate prediction of machine characteristics is essential to minimise development cost and time.

Several calculation techniques are available to predict electrical machine performance, including classical closed form analysis, lumped parameter models and non-linear time-domain finite element analysis. The choice is the trade-off among model complexity, accuracy and computing time. Analytic methods for magnetic field calculations in rotating electrical machines are based on averaging assumptions of magnetic field parameters in the air gap and in the core of the machine. The results of machine performance characteristics by analytic methods are accurate only

at steady state operation of the machine and the results are unreliable for transient operation. Hence, prototyping is necessary for the performance evaluation of any electrical machine, but, it is very expensive and time consuming to build real prototypes for rotating electrical machines as it involves investment on tool development for stator/rotor/exciter stampings each time a design modification is implemented during the machine development process. To tackle this issue, virtual prototyping is adopted to design, optimise, validate, and visualise products digitally and evaluate different design concepts before incurring the cost of physical prototypes. Present day analysis techniques include combined CAD/FEA using solid modelling and finite element magnetic simulation. This, along with first order analysis, gives accurate machine performance predictions and such evaluation techniques that do not require expensive equipments help to quickly confirm machine performance. All these techniques, applied at the alpha prototype phase, can help prove a machine design and secure resources for further development using more conventional analysis, tooling, and evaluation techniques. Thus, VP helps to evaluate whether the machines designed meet the specified requirements and if they do not, provides means to reconciling the measured performance with analysis and improve the design in future iterations.

4.2 Parameter Prediction in Brushless Alternators

Performance prediction in brushless alternators is conventionally carried out using traditional methods which combine analytical and empirical knowledge. These methods lack accuracy due to complex geometry and non-linear characteristics of magnetic materials associated with the machine. In these methods, performance characteristics of the machine such as losses, currents,

magnetisation characteristics and induced voltage are calculated based on assumptions for the magnetic field in the air gap and the core. These assumptions lead to inaccurate results of machine performance characteristics under transient operation. Hence, numerical field computation methods like finite difference method (FDM), boundary element method (BEM) and FEM have been employed for prediction and analysis of machine characteristics (Brauer, 2006; Okafor *et al.*, 2009) by electro-magnetic field analysis. Out of these techniques, FEM is increasingly used by designers due to its ability to handle complex geometry and presence of non-linear magnetic materials. Due to the advancements in computational capabilities over recent years virtual prototyping by FEM has become an attractive alternative to conventional semi-analytical and empirical design methods as well as to the still popular trial and error approach (Yilmaz and Krein, 2008; Guptha *et al.*, 2009), for prediction of machine characteristics during the design and development process.

4.3   Virtual Prototyping by FEM

Finite element model is the magnetic field model of the alternator that determines the electrical performance directly from magnetic field distribution in the active parts (stator, air gap and rotor) of the generator. The magnetic field distribution across the machine geometry is determined from Ampere's law, which is appropriately formulated using the geometrical data, material properties, winding data, the boundary conditions and period of symmetry.

The brushless alternator under study is analysed with a 2D field model. Virtual prototyping of the machine is done by modelling using FEM software, Ansys Maxwell 2D. By FEM, governing equation of electro-magnetic field existing in the geometry of

the machine is solved for MVP having component only along z-axis, from which magnetic flux density having components in the (x, y) plane is computed. Applying basic principles of electromagnetics, from the calculated value of B, all field values are computed and the machine parameters are predicted.

4.3.1 Calculation of Geometry and Material Property Assignment

Basic design of an electrical machine, *i.e.*, the dimensioning of magnetic and electric circuits, is carried out by applying conventional design methodology, using analytical equations and empirical formulae. The material for different parts are chosen based on the operating point and permissible losses.

4.3.2 Winding Data

The brushless alternator under study is provided with a 3-phase, full pitched concentric winding which is a simple, single layer winding designed for 4-poles. The winding layout is shown in Figure 4.1.

The 3-phase stator winding is having two parallel paths per phase and each coil in the concentric winding is provided with 25 turns of $1.12\,mm$ copper wire. The phase windings can be either star or delta connected as required by the customer.

4.3.3 Boundary Conditions

Conditions that express the behaviour of field on boundaries are called boundary conditions. Among these conditions, a constant value for the field variable along boundary, known as the
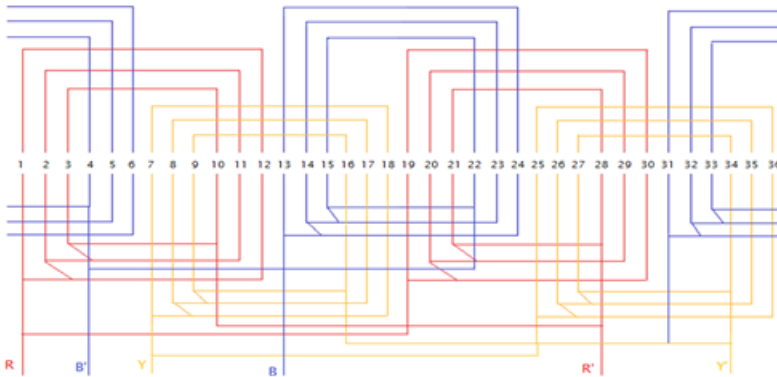
Fig. 4.1: Winding layout of 45 KVA full pitched brushless alternator

Dirichlet's condition, or a given value for the derivative of field variable normal to the boundary, known as Neumann's condition, can be assigned. In the machine structure under consideration, no flux lines cross the outer boundary since flux lines are tangential to outer boundary. Hence, the homogeneous Dirichlets condition is assigned, fixing MVP, $A_z = 0$ along the outer boundary.

The periodic condition exploits repetitive features of magnetic field inside the machine, and relates the values of A_z on two boundaries. Structure of the brushless alternator under study has symmetry along the computational domain since geometry and magnetic phenomena of the machine structure are repeated identically under pole pairs. The machine being of 4-pole, the domain under analysis during no-load condition is reduced to one fourth on account of periodic symmetry of field pattern, which reduces computational time for field analysis. Therefore, along axes of periodic symmetry, periodic boundary conditions are applied. Since flux density components cannot be discontinuous across the symmetry axis, the flux lines must be normal to the axis. Hence the Neumann's boundary condition, *i.e.*, $\frac{\partial A}{\partial n} = 0$ is

applied along the symmetry axes.

4.4 Determination of Important Parameters of the Brushless Alternator

Finite element solution of the field problem computes MVP, A at the nodes and using this information, the machine parameters such as flux, flux density, leakage flux, saturation factor, winding inductance, d and q-axes reactances and open circuit characteristics (OCC) are computed by post-processing (Salon, 1995; Bianchi, 2005).

4.4.1 Computation of Flux

The term, total flux, as applied to synchronous generators, is defined as the flux generated due to excitation winding, in the present case, the flux generated in the rotor. In magneto-static solutions, amount of flux passing a prescribed line per unit axial depth is obtained as the line integral of flux density along the line. Application of this method on a line described over a pole pitch inside the rotor body of the machine yields the flux generated per unit axial length of the machine. This quantity, further multiplied by the net iron length, results in total flux per pole in the machine. From basics of electro-magnetics, flux is computed by the formula,

$$\phi = \oint_S B \cdot dS = \oint_S (\nabla \times A)\,dS \qquad (4.1)$$

Applying Stokes theorem, $\phi = \oint_l A \cdot dl$ where the closed line integral path encloses the surface S. Therefore, the magnetic flux crossing a surface of effective length l_e and spanning between the points (x_1, y_1) and (x_2, y_2) is,

$$\phi = l_e(A_z(x_1, y_1) - A_z(x_2, y_2)) \tag{4.2}$$

Useful flux is defined as the flux linking the stator winding and causing the induced voltage. This flux is lesser than the total flux by the amount of leakage flux. On similar lines as the computation of total flux, the useful flux can also be derived. However, the line for integration now lies at the mean airgap diameter. *i.e.,* Useful flux per pole is the integral of radial value of air gap flux density over one pole pitch given by the equation,

$$\phi_U = \int_{airgapline} B_{rad} \cdot dl \tag{4.3}$$

4.4.2 Computation of Air Gap Flux Density

From the computed value of MVP, the flux density is computed by,

$$B = \nabla \times A \tag{4.4}$$

Since magnetic vector potential A has components only in z-direction, flux density vector B has components in x-y plane only. Therefore,

$$B_x = \frac{\partial A_z}{\partial y} \tag{4.5}$$

$$B_y = -\frac{\partial A_z}{\partial x} \tag{4.6}$$

$$B_z = 0 \tag{4.7}$$

4.4.3 Computation of Leakage Coefficient

Leakage coefficient is defined as the ratio of the total flux to the useful flux at a given field excitation and is computed using the

expression,

$$C_l = \frac{\phi_T}{\phi_U} \tag{4.8}$$

This coefficient is of greater significance in salient pole constructions. Largely, it reflects saturation in the stator teeth on d-axis.

4.4.4   Computation of Flux Linkage

Flux linkage ψ of an arbitrary machine winding is calculated as,

$$\psi = \frac{l_e}{S} \left(\sum_{n+} \int_{S+} A_z \, dS - \sum_{n-} \int_{S-} A_z \, dS \right) \tag{4.9}$$

where $n+$ and $n-$ are the total number of positively and negatively oriented winding conductors respectively, and $S+$ and $S-$ are corresponding conductor areas.

4.4.5   Computation of Induced EMF

The induced winding EMF is derived from flux linkage as,

$$e_w = -\frac{d\psi}{dt} \tag{4.10}$$

For AC voltages of frequency f Hz, this can be written as,

$$V = -j2\pi f \psi \tag{4.11}$$

In AC analysis, the angular frequency (rad/s) $= 2\pi f$, and thus,

$$V = -j\omega\psi \tag{4.12}$$

4.4.6 Computation of Winding Inductance

The field winding inductance can be computed through a magneto-static simulation with the armature open circuited and the field energised as in the no-load case. The conventional definition of inductance is given as flux linkages per unit current. Since the flux linking all the turns is not the same, values computed using this approach could be erroneous. A better and accurate value of inductance is obtained using the formula,

$$L = \int\int_S \frac{A \cdot \delta\, dS}{I^2} L_i \qquad (4.13)$$

4.4.7 Computation of Direct Axis Inductance

The air gap in synchronous machines of salient pole construction is non-uniform, much larger at the quadrature axis than at the direct axis and hence flux produced along direct axis is greater than that along the quadrature axis resulting in the direct axis synchronous reactance X_d having a higher value than the quadrature axis synchronous reactance X_q.

The synchronous direct axis inductance is defined as the inductance of that phase whose axis coincides with polar axis, when the 3-phase windings are simultaneously fed. In computation of the direct axis inductance L_d, the magnetising current is set to be zero and stator windings are fed in such a way as to obtain a MMF distribution with maximum value coincident with direct axis. Since magnetic field is synchronous with the rotor, a magneto-static simulation is possible. The boundary conditions are assigned to constrain the flux lines to be tangential along polar axis and normal to the inter polar axis. Once the distribution of winding is fixed, the 3-phase currents are chosen so that maximum of the MMF distribution coincides with polar axis (d-axis). This corresponds to setting $I_d = I_m$ and $I_q = 0$.

At this moment, currents satisfy the relation,

$$I_a = I_m \tag{4.14}$$

$$I_b = -\frac{I_m}{2} \tag{4.15}$$

$$I_c = -\frac{I_m}{2} \tag{4.16}$$

Then, the magnetic field axis is same as the phase axis, and direct axis of rotor is lined with the phase axis. Performing 2D magneto-static analysis, the direct axis synchronous inductance, L_d is computed by,

$$L_d = \frac{\psi_a}{I_a} = \frac{\psi_d}{I_m} \tag{4.17}$$

4.4.8 Computation of Quadrature Axis Inductance

The phase currents and the winding distribution are so chosen as to have a MMF distribution with maximum value coincident to the inter-polar axis. *i.e.*, the q-axis. The phase currents are then,

$$I_a = 0 \tag{4.18}$$

$$I_b = -\frac{\sqrt{3}}{2} I_m \tag{4.19}$$

$$I_c = \frac{\sqrt{3}}{2} I_m \tag{4.20}$$

which in turn gives $I_d = 0, I_q = I_m$.

The inductance is then calculated by,

$$L_q = \frac{\psi_q}{I_q} = \frac{\psi_q}{I_m} \tag{4.21}$$

4.4.9   Pre-determination of Machine Characteristics

FEM is used to simulate steady state operation of synchronous generator. During steady state, the 3-phase currents and voltages vary sinusoidal with time. The simulation is carried out as follows:

Input quantities:

- A constant synchronous speed is considered, and then the operating electrical frequency is $p\omega_m$.

- Rotor speed is fixed.

- Magnetising current I_f is fixed.

Open Circuit Characteristic (OCC) and Air Gap Line

In the FE model of brushless alternator, field winding formed by N_f turns is fed by a constant current I_f. The armature windings are open circuited so that they do not carry any current and considered to have null conductivity. Stator and rotor magnetic material is described by appropriate B-H characteristics.

Boundary conditions are assigned, considering that the flux lines of half a pole are mirrored flux lines of other half of the pole. Then, a value of MVP is fixed along the polar axis (Dirichlet's condition), while a normal flux density vector is assigned along the inter-polar axis (Neumann's condition). Since flux lines do not exit from the yoke, a null MVP is assigned along the external circumference of the stator.

Field winding composed by N_f turns and carrying the excitation current I_f is modelled by an equivalent conductive bar carrying total current $N_f I_f$. Once the field problem is solved, the z-axis component of MVP, $A_z(x, y)$ is obtained at each point of the

analysis domain. Then, flux linkages with each of the 3-phase windings are estimated and the rms line-to-line voltage is computed by the formula,

$$E_{L-L} = \omega\sqrt{\psi_A^2 + \psi_B^2 + \psi_C^2} \qquad (4.22)$$

4.5   Results

Virtual prototyping of a 45 KVA, 415 V, 3-phase, 4-pole brushless alternator is done by modelling the machine using Ansys Maxwell 2D. A brief listing of the machine specifications and design parameters used for modelling is provided in Table 4.1. The computer system used for simulation is having Intel i5 processor, 3.3 GHz with 4 GB RAM. Two dimensional non-linear parametric FE analysis of the machine in steady state regime of operation is carried out for estimating the significant electromagnetic parameters. Simplifying assumptions and boundary conditions, generally associated with analysis of rotating electrical machines, as detailed below, are applied for modelling the machine in Maxwell 2D.

- It is assumed that the contribution to the induced voltage from the fringe field at the end of the machine is negligible. The end effects are, therefore, neglected and, hence, any 2D section along the linear length of the machine is considered representative.

- B-H characteristics of the stator and rotor iron are assumed to vary as furnished by specifications of the core material used.

- The insulation thickness surrounding strands of conductor are neglected, resulting in representation of the conductor area as uniform ampere-turn distribution.

- It is assumed that the entire flux in the stator is confined to the core region only. Hence, the stator lamination outer edge is considered as a Dirichlet boundary.

- At no-load, perfect magnetic symmetry exists along the d-axis. The excitation along this axis is also symmetric. Therefore, d-axis is considered as a Dirichlet boundary.

- Along q-axis, mirror symmetry exists at no-load. Therefore, q-axis is considered as a Neumann boundary.

Table 4.1: Geometrical data of the prototype machine

Parameter	Value
Machine capacity	45 KVA
Voltage	415 V
Speed	1500 rpm
Operating temperature	$75^o C$
Rated p.f.	0.8
Winding connection	Star
Inner diameter of stator	240 mm
Outer diameter of stator	356 mm
Core length	130 mm
Number of stator slots	36
Inner diameter of rotor	90 mm
Outer diameter of rotor	238.2 mm
Pole arc offset	4.7 mm
Pole shoe width	123 mm
Pole body width	87 mm
Pole body height	54 mm
Stator conductor	1.12 mm copper
Rotor conductor	4.5 x 2.24 mm
Core material	M 43 C4

The software employed in the analysis has adaptive mesh generation algorithm, which iteratively increases the mesh density

to keep the error due to discretisation within the specified norm. The specification of the error norm for adaptive meshing is more heuristic than logical. In such situations, when change in the computed parameter due to increase in meshes become saturated, the iteration is terminated, since any further increase in elements will produce nearly no change in the terminal quantities of interest. The 2D parametric analysis feature in the Maxwell software allows definition of one or more quantities as variable(s) and evaluation of the end-study parameter as a function of the variable. The variable(s) can be any one or all of the following:

- model dimensions, component displacement or angular rotation

- material properties

- excitations

- boundary conditions

The results of the parametric analysis are viewed and compared using plots or tables to determine how each design variation affects the performance of the machine. In the virtual prototype of the machine under investigation, rotation is implemented by parametrics, varying the rotor angle in steps, each time computing the machine parameters of interest, by magneto-static solution.

Figure 4.2 shows finite element model of the alternator developed in Ansys Maxwell 2D software. Core material used in the machine model is M43C4 and field excitation is input as field ampere turns. Number of turns of field winding around each pole being 48 having only one parallel path, and field excitation chosen as 25 A, field ampere turns is input as $48 \times 25 = 1200$. Flux plot obtained by simulation of FE model at 25 A field excitation is shown in Figure 4.3. As the number of stator slots/teeth under both halves of a pole is equal, the flux lines are symmetrically
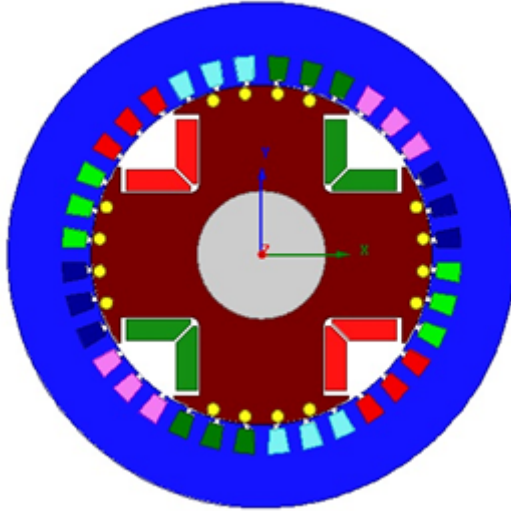
Fig. 4.2: Finite element model of the alternator

distributed. Flux density distribution and the flux density vector plot across the machine geometry are given in Figures 4.4 and 4.5 respectively.

Inter-polar leakage flux of the salient poles under no-load conditions is plotted in Figure 4.6. As a stator slot is aligned with inter-polar axis, the reluctance is maximum along that axis and hence flux density is minimum. Moreover, since stator slots are symmetrically aligned with respect to the inter-polar axis, flux lines are symmetrically distributed.

Figure 4.7 shows the radial air gap flux density distribution under a pole pitch for 25 A field excitation. Radial component of the air gap flux density is computed by calculating normal component of flux density vector in the air gap. The component of B_{airgap} normal to the air gap line drawn over a pole pitch is calculated by the fields calculator of Maxwell software and is plotted over a pole
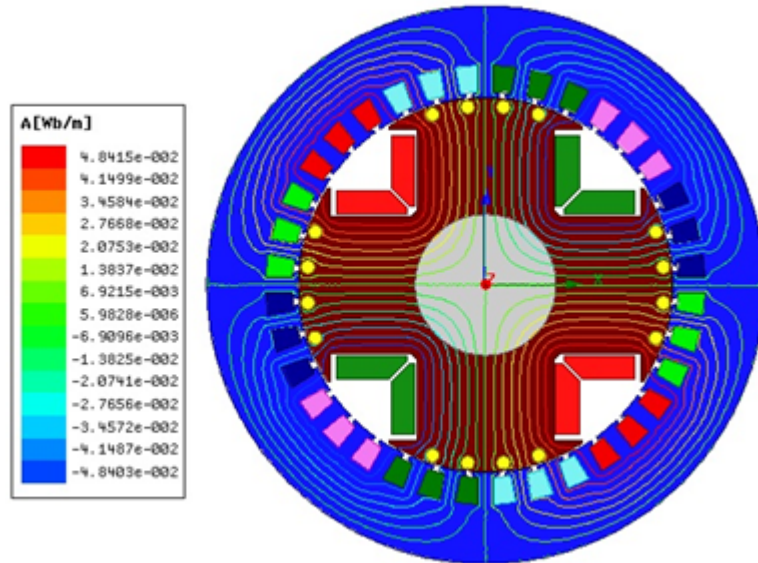
Fig. 4.3: Flux plot at 25 A field excitation

pitch. Since the machine under analysis has periodic symmetry, the same distribution of B_{rad} is repeated under remaining three poles.

Figure 4.8 shows the growth of radial component of air gap flux density B_{rad} over two pole pitches as field excitation is varied from 0 to 80 A. As inferred from the figure, the effect of stator slotting on radial flux density is becoming severe with increased field excitation, due to saturation.

In Figure 4.9, the distribution of tangential component of air gap flux density vector, *i.e.*, B_{tan} over a pole pitch is plotted and Figure 4.10 shows the growth of B_{tan} over two pole pitches, with field excitation varying from 0 to 80 A. As seen in the figure, saturation effects become severe with increased excitation.
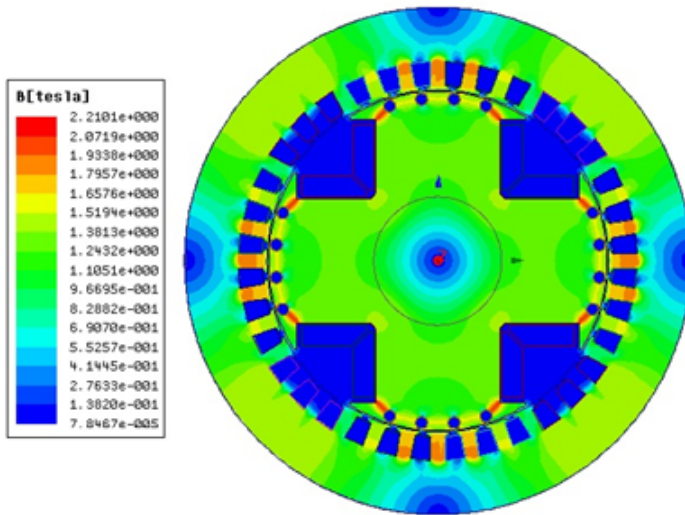
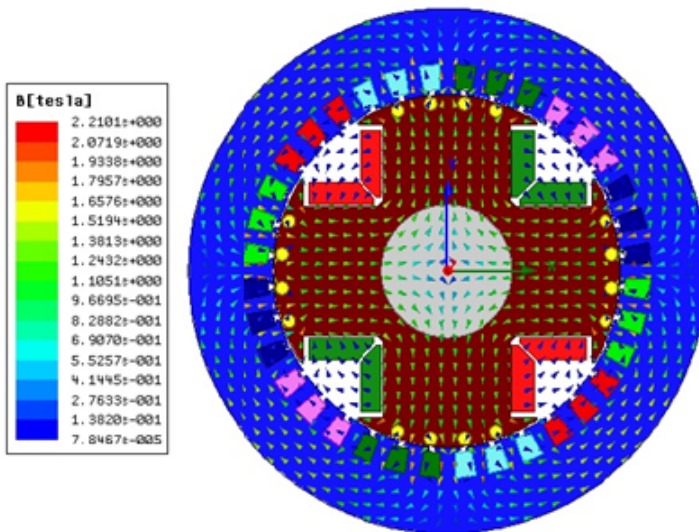**Fig. 4.4:** Flux density distribution at 25 A field excitation

Fig. 4.5: Flux density vector plot at 25 A field excitation
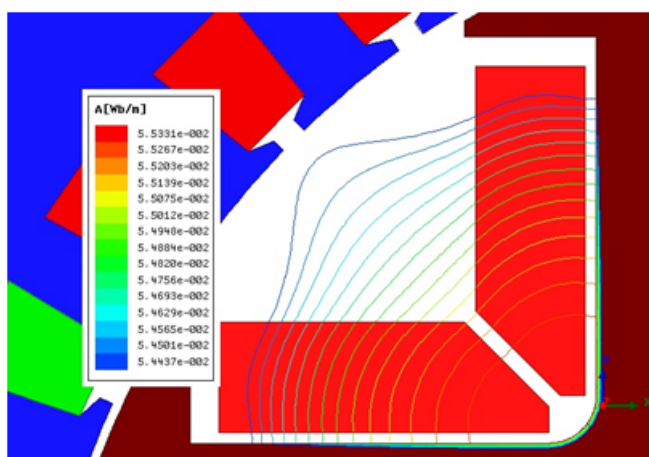
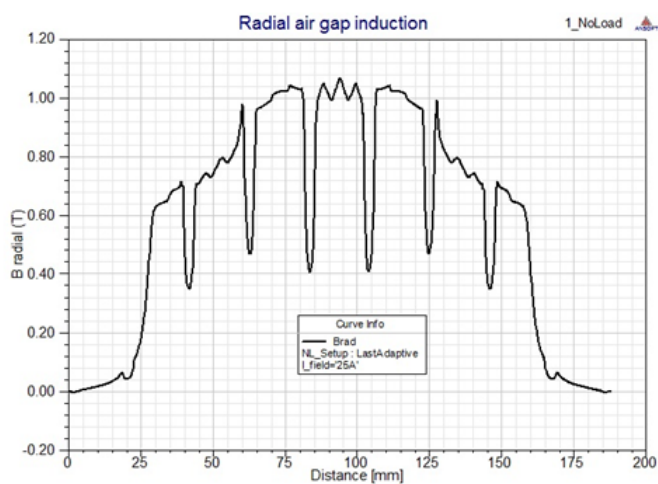**Fig. 4.6:** Inter-polar leakage flux of the salient pole structure

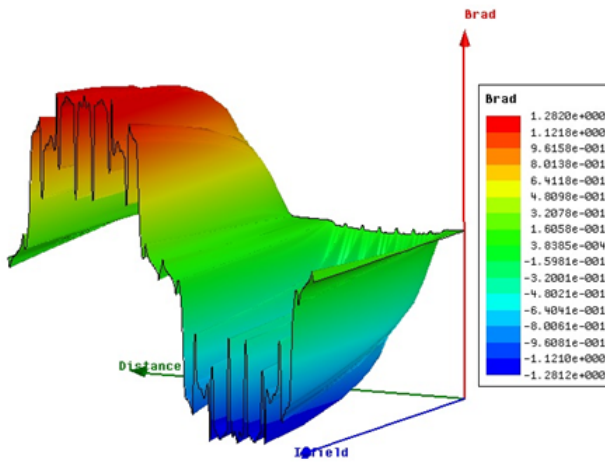**Fig. 4.7:** Radial air gap induction at 25 A field excitation

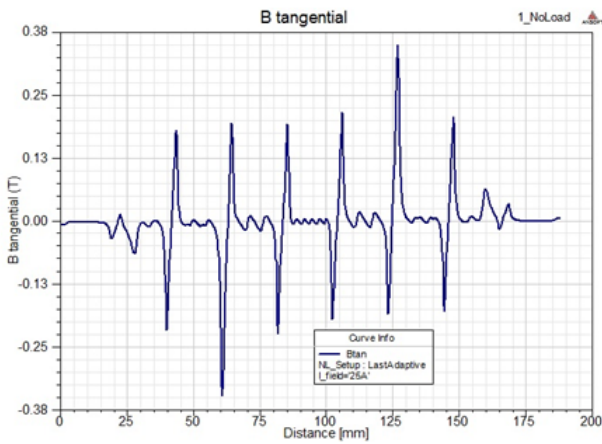**Fig. 4.8:** Growth of B_{rad} with excitation over two pole pitches

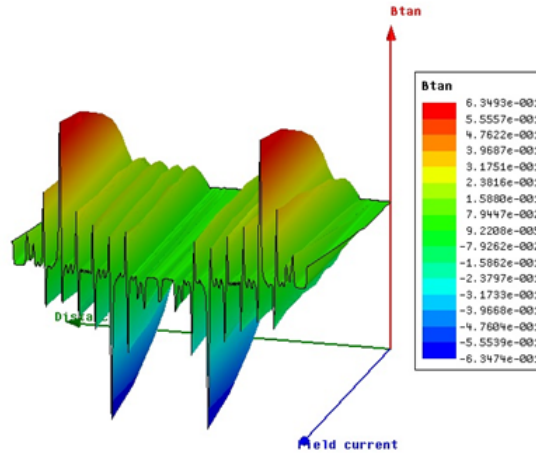**Fig. 4.9:** Tangential air gap induction at 25 A field excitation

Fig. 4.10: Growth of B_{tan} with excitation over two pole pitches

As the rotor rotates, flux lines linking with stator windings are changed and due to this rate of change of flux linkage, an EMF is induced in the winding. The variation of flux linkages in the A, B and C phases of the stator winding is shown in Figure 4.11.

As field excitation of the machine is increased in steps, flux set up in the pole also increases. When field excitation is increased beyond certain values, there is no proportional increase in flux produced, due to core saturation. This is clear from Figure 4.12 which shows the variation of total and useful flux per pole with field current. Total flux ϕ_T is computed as flux passing through the pole body and useful flux ϕ_U as that actually links with the stator winding. Therefore, ϕ_U is computed from the calculated value of B_{rad}.

From the computed values of ϕ_T and ϕ_U, leakage coefficient C_l is calculated and normal desirable value of C_l for a perfectly designed machine is around 1. As observed in Figure 4.13, the maximum value of C_l is 1.041 for the machine under analysis and from the plot, it is seen that leakage flux grows with respect to
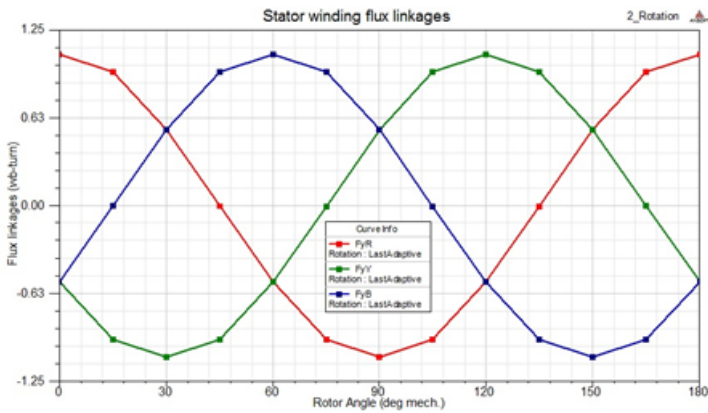
Fig. 4.11: Stator winding flux linkages with rotation of field
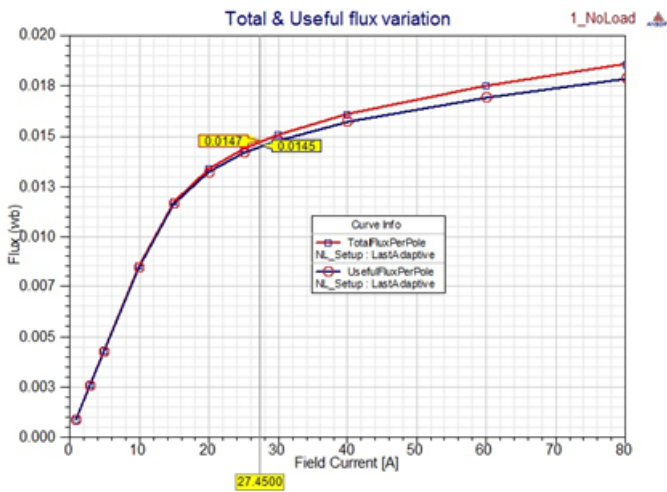
Fig. 4.12: Variation of total and useful flux per pole with field current

field excitation and becomes significant at saturation.
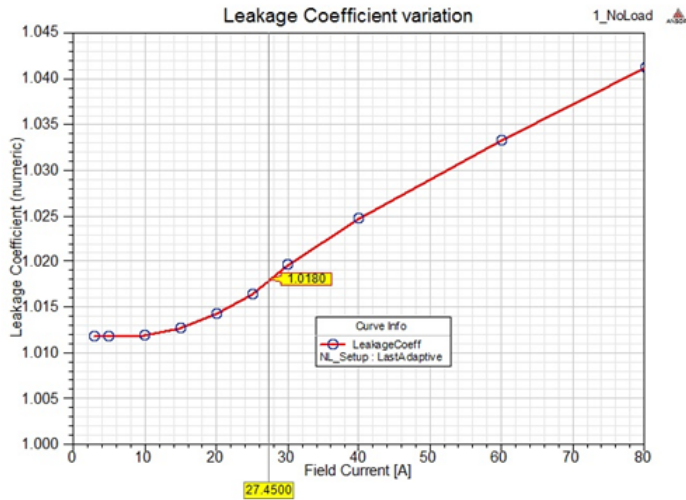
Fig. 4.13: Variation of leakage coefficient with field current

As per machine design practices, there are limiting values of B normally permitted in different parts of the machine in order to limit losses on account of core losses due to saturation. So, the designer normally makes a check of these values before finalising the design. Hence, the average values of B, *i.e.*, B_{avg} in the machine parts like stator, air gap and rotor are plotted (Figure 4.14) for different field excitations, by simulating the virtual prototype of the machine. Figure 4.15 shows plot of the maximum values of B, *i.e.*, B_{max} in different machine parts with field excitation varying from 0 to 80 A. It is ascertained that the value of B_{max} is not crossing the saturation limits for the core material selected.

As shown in Figure 4.14 , B_{avg} is minimum at the air gap, moderate in stator core and maximum in the pole body. Flux density in the pole body is kept high as it is DC flux and will not be causing eddy current losses. As shown in Figure 4.15, B_{max} is minimum at the air gap, moderate in the stator tooth and max-
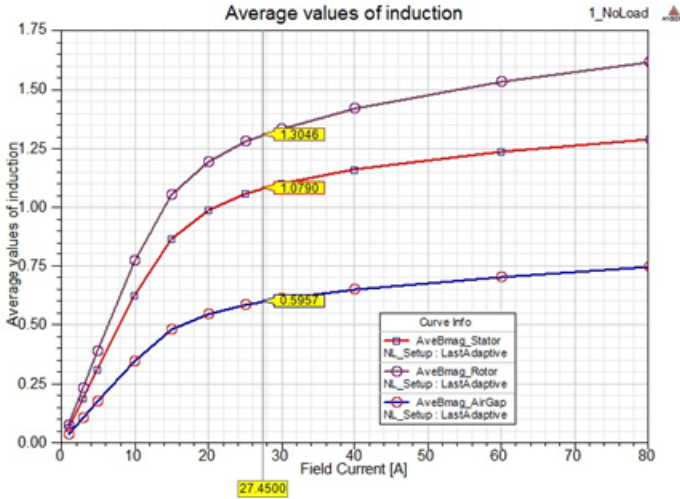
Fig. 4.14: Variation of average values of B in the machine parts

imum at the rotor tip and is not crossing saturation limits for M43C4 core material.

Figure 4.16 shows variation of field coil inductance L as a function of field current. Winding inductance is calculated by Equation (4.13) and since it varies inversely as square of current, the value of L decays exponentially with field current.

Figure 4.17 shows flux plot across geometry of the machine with only d-axis current assigned to the 3-phase stator winding and field winding assigned with zero excitation. As seen in the figure, stator MMF axis is coincident with the field direct axis. This is achieved by assigning current distribution in the 3-phase stator winding in such a way that maximum value of stator MMF coincides with the polar axis. Figure 4.18 shows variation of X_d with linear variation of stator current. At high values of stator current, the reactance X_d reduces drastically due to saturation of iron in the flux path. The saturated value of X_d per phase at rated stator current is observed to be $5.7615\,\Omega$. For prediction of
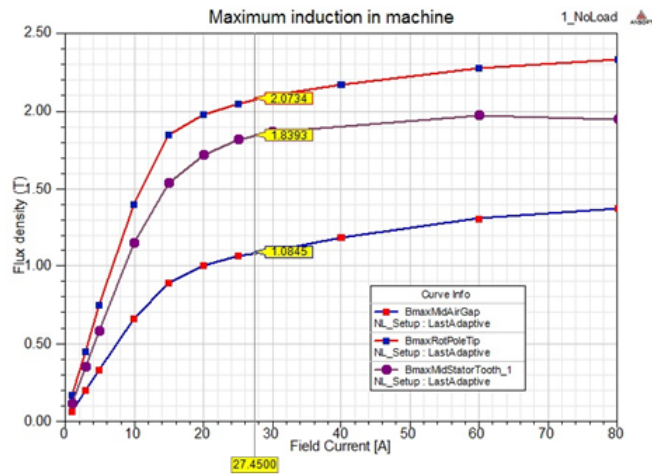
Fig. 4.15: Variation of maximum values of B in the machine parts
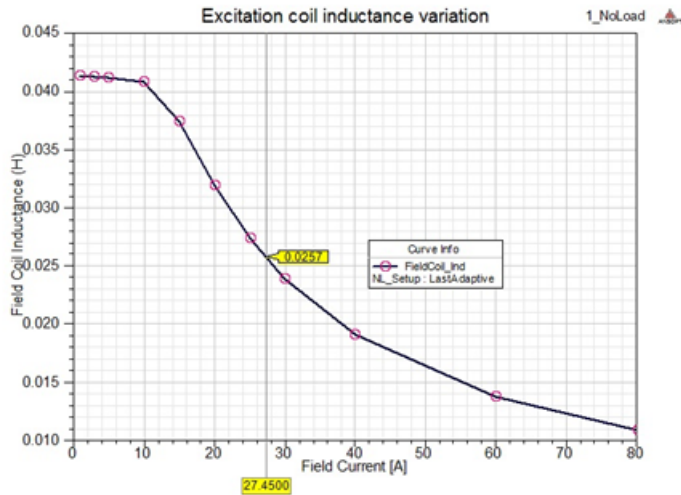
Fig. 4.16: Variation of field coil inductance with field current
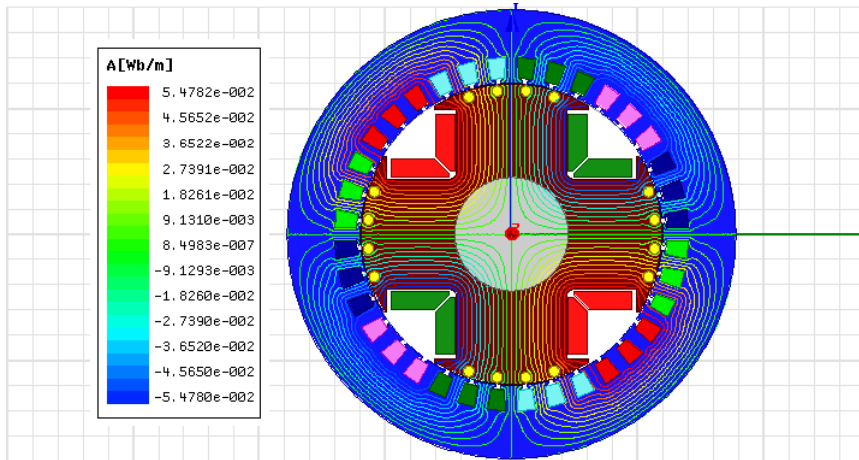
Fig. 4.17: Flux plot with only d-axis current in the stator winding
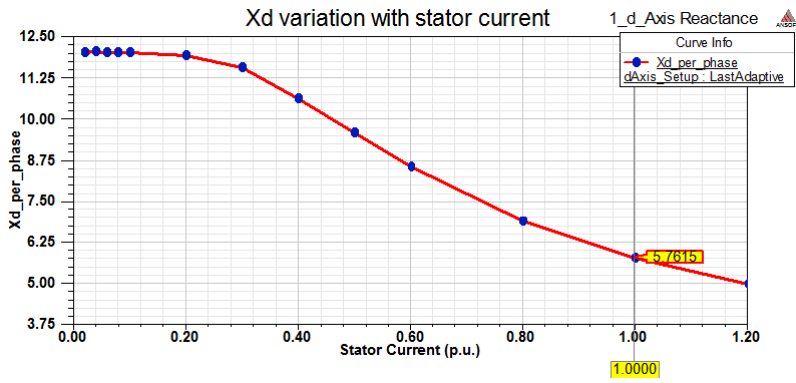
Fig. 4.18: Variation of X_d with stator current

the quadrature axis reactance of the machine, only q-axis current is assigned to the 3-phase stator winding. Figure 4.19 shows the flux distribution in the machine under this condition with field excitation made null. As seen in the flux plot, the stator MMF is in phase with the quadrature axis. This is achieved by assigning current distribution in the 3-phase stator winding in such a way that the maximum value of stator MMF coincides with the inter-polar axis. Then, the stator current is varied linearly by parametrics and variation of X_q is plotted as in Figure 4.20, which shows non-linear variation of X_q at higher values of stator current, due to saturation of iron parts in the flux path. From the plot, saturated value of X_q per phase at rated stator current is observed to be $4.3362\,\Omega$.
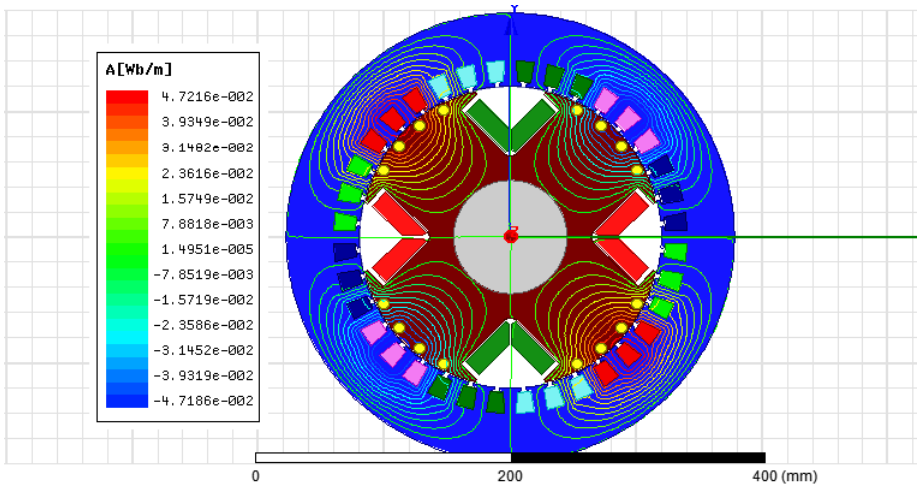
Fig. 4.19: Flux plot with only q-axis current in the stator winding

The induced phase voltage in the 3-phase synchronous machine is arrived at from the useful flux per pole, ϕ_U computed, together with the stator winding details. The open circuit characteristics obtained for the machine together with the air gap line is shown in Figure 4.21. As can be seen, OCC is a replica of the B-H
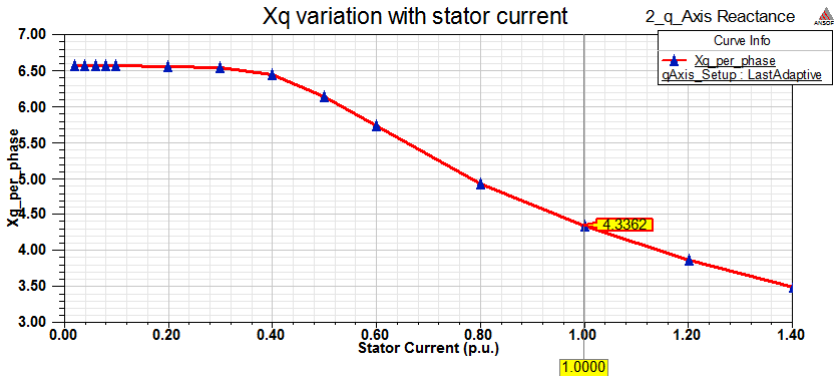
Fig. 4.20: Variation of X_q with stator current

characteristics of the core material and exhibits non-linearity at high values of field excitation due to saturation effects. From OCC, the no-load excitation requirement of the machine is read as $27.45\,A$.

Saturation factor is the ratio of voltage on the air gap line to voltage on the OCC for a given excitation. Saturation curve is an indication of level of saturation in the machine and same for the generator under investigation is shown in Figure 4.22. The value of saturation factor at rated excitation of the machine under analysis is 1.6326.

Normally, operating point of the machine is chosen based on machine parameters and characteristics plotted by simulation of the virtual prototype. By judging characteristics and the parameters predicted, the designer can judiciously select operating point of the machine. If parameters deviate from typical design values, modifications can be incorporated in the virtual prototype by changing the dimensions/ geometry/material used, which saves time and cost incurred towards design and development of machines.
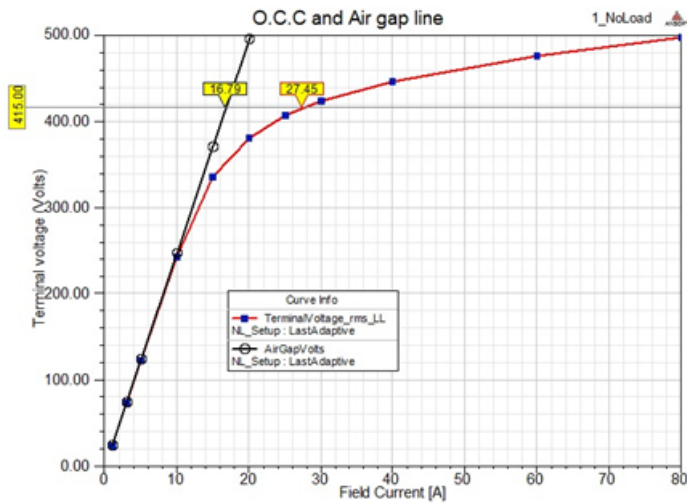
Fig. 4.21: OCC and Air Gap Line
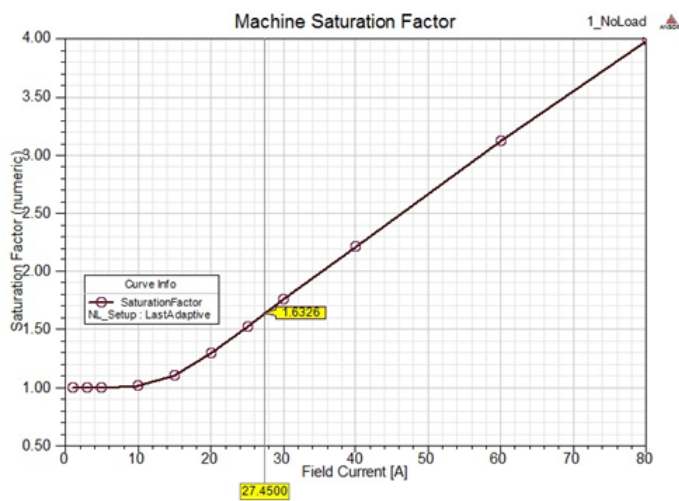
Fig. 4.22: Variation of Machine Saturation factor

4.6　Conclusion

In this chapter, a simple, fast and efficient method based on 2D FEM for predicting the performance characteristics of a salient pole brushless alternator is presented. FEM together with computer is used to investigate effect of various parameters on the machine performance, to gain a better understanding of the machine being analysed. It is cost effective and saves time on account of material resources for the multitude of physical experiments needed to gain the same level of understanding, in laboratory environments.

FEM with its inherent ability to accurately represent complex geometries without any simplification of the original machine structure, is used to evaluate magnetic field distributions in the brushless alternator. Accurate evaluation of the magnetic field distribution, in-turn, leads to accurate estimation of field related machine parameters, such as, induced voltages, voltage waveforms, harmonic magnitudes, machine reactances, leakage coefficients, induction and saturation effects. Evaluation of these parameters is significant when a comparison of design options is sought.

Chapter 5

Improved Excitation System for Brushless Alternators

5.1   Introduction

Low voltage brushless alternators are provided with excitation systems designed to keep terminal voltage of the alternator within specified tolerance band of the rated value, under all load conditions. The excitation current should be increased to overcome the internal voltage drop within the machine, under loaded conditions. In brushless alternators, power supply for the exciter field is conventionally obtained in one of the following ways:

- from a separate 3-phase permanent magnet generator (PMG).

- from the output terminals of the alternator itself, by means of a step down transformer.

- from an auxiliary stator winding located in the same slots as the main stator winding.

These excitation systems have certain disadvantages like increased cost for PMG, delay in response and difficulties experienced in generating sufficient residual voltage on start up. Disadvantages of the conventional excitation methods are surmounted by third harmonic excitation (THE) system attempted in the present study. In this method, machine provided with two auxiliary windings embedded in the main stator slots but electrically isolated from the main winding, are used for providing excitation current to the exciter field winding (Darabi, 2005; Podgornovs and Zviedris, 2007). In this compound excitation system, the combined effect of one auxiliary winding with $2/3^{rd}$ pitch and another third harmonic auxiliary winding with $1/3^{rd}$ pitch, ensure good voltage regulation without an electronic AVR and greatly reduces the total harmonic content in the output voltage cost effectively.

5.2   Overview of Practical Excitation Systems

Practical excitation systems for low voltage brushless alternators may be divided into three generic groups:

1. Static excitation which consists entirely of static equipments, *i.e.*, no rotating machines are involved other than the generator itself. The field excitation of the machine is derived from its own armature terminals, through an assembly of static components, such as current and voltage transformer and rectifiers. The excitation current is fed to the alternator field coil mounted on the rotor through slip rings and brushes.

2. DC excitation which employs a rotating DC exciter, with or without an AC or DC pilot exciter.

3. AC excitation employing a rotating AC exciter, with or without a pilot exciter.

In modern machines, especially in the power range under the scope of this study, it is established that systems employing separate excitation through shaft driven DC exciters are no longer in use (Mahon, 1992). In practice, systems either use direct self-excitation or some form of AC or brushless excitation (indirect self-excitation) or separate excitation with permanent magnet pilot exciter.

5.2.1   Direct Self Excitation

Direct self excitation system provides very fast modification of excitation following load changes because it gives direct control of main field of the generator without having to work through an intermediate exciter field. Hence this system is suitable for generators with frequent load changes, but it requires slip rings and brush gear to carry large excitation current to the rotor main field winding. Also, AVR must include some provision for building up the terminal voltage from residual magnetism of the field poles.

5.2.2   Indirect Self Excitation

In this scheme, AVR is required to supply current to the exciter field and not directly to the main field winding. Hence, the output of AVR can be smaller, but response will not be as fast compared to the direct self excitation system.

5.2.3   Separate Excitation

This system provides excitation power from a source independent of the power output. It makes use of a permanent magnet

generator coupled to the common generator and main AC exciter shaft. Since the permanent magnet pilot exciter provides near constant power excitation under all operating conditions, performance under starting and short circuit conditions tends to be superior, but the exciter response is more due to presence of exciter time constants.

5.3   Third Harmonic Excitation System

Conventional excitation system for an alternator is a shunt excitation system in which excitation power is taken from alternator main terminals through a step down transformer. In this system, when alternator is loaded with non-linear loads, the output voltage waveform gets distorted and this distorted power fed to AVR causes erratic functioning of the AVR. Also during a 3-phase short circuit at the terminal, power to AVR become zero and excitation system collapses. A good excitation system should provide some amount of excitation to the alternator even during short circuit at the terminal, so that 2 to 3 times rated current is maintained through the short circuit to ensure positive tripping of protective relays. Also any failure of the AVR causes complete breakdown of generator set since excitation is fed through the electronic AVR.

Diesel engine driven brushless alternators with full pitched main winding when used for powering single phase loads, have high harmonic content across line and neutral. Hence, single phase loads connected across such machines are affected by triplen harmonics. To circumvent this problem, conventionally, the main winding is wound at $2/3^{rd}$ pitch which introduces complexity in winding, additional insulation requirements in slots as well as in winding overhang and reduces KVA due to poor winding factor leading to increase in size by about 13%. The disadvantage of

high harmonic content in the output phase voltage of brushless alternator with full pitched main winding is overcome by resorting to an improved excitation system utilising third harmonic power, still preserving the advantages of having a full pitched main winding in the machine. In this method, the machine with full pitched main winding provided with two auxiliary windings embedded in stator slots and electrically isolated from the main winding, is used for providing excitation current for exciter field winding. In this compound excitation system, the combined effect of one auxiliary winding with $2/3^{rd}$ pitch and another third harmonic auxiliary winding with $1/3^{rd}$ pitch, ensure voltage regulation and reduces the total harmonic content in the output phase voltage.

In the third harmonic excitation system implemented, a voltage proportional to output voltage is induced in main auxiliary winding with $2/3^{rd}$ pitch. Second auxiliary winding is designed in such a way that only triplen harmonic flux produced in the air gap during loading of the alternator links with it. The triplen harmonic flux produced in the air gap vary linearly with percentage loading of the alternator and by suitably selecting number of turns of this auxiliary winding, the voltage induced in the winding is made exactly equal to the additional excitation required to compensate armature reaction produced by the load. Rectified voltages from these two windings are fed to two different windings on each pole of the exciter field, so that MMF produced by main auxiliary winding is strengthened by the third harmonic auxiliary winding. When flux produced by these two windings are additively fed to exciter field air gap, output of the alternator is maintained within permitted voltage tolerance band from no-load to full-load conditions. To achieve fine voltage control, an optional AVR is also added. The scheme of this excitation system is shown in Figure 5.1.
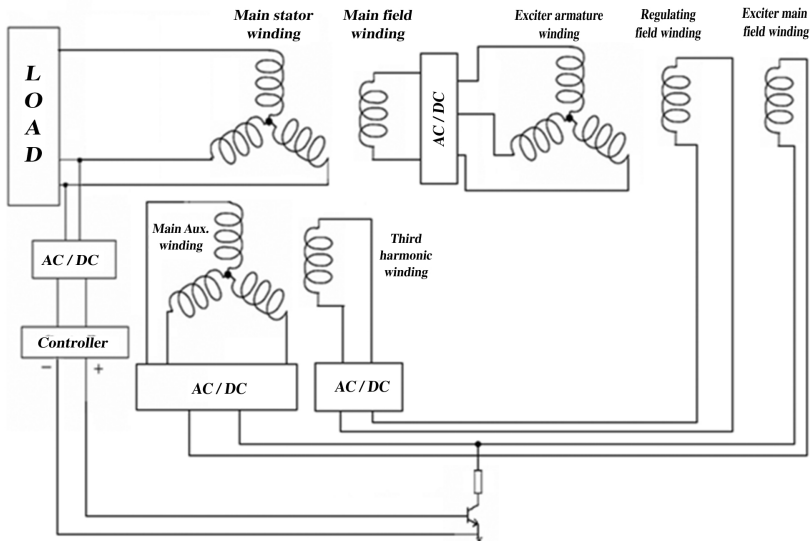
Fig. 5.1: Block diagram of third harmonic excitation system

5.4   Triplen Harmonics in Generated Voltage

The output voltage waveform of a practical AC generator is not perfectly sinusoidal. The time variation of the induced EMF in a conductor of the stator winding in an AC generator has the same form as the space distribution of flux density in the air gap. Therefore, only a sinusoidal air gap flux density can result in a sinusoidal induced EMF. Several factors such as shape of the rotor pole face, core saturation, slotting and style of coil disposition render realisation of a sinusoidal air gap flux wave impossible (Premkumar, 2006).

5.4.1   Flux Density Harmonics

Non-sinusoidal distribution of winding and permeance variations over the air gap cause production of air gap flux density

harmonics in alternators . The main field winding of the machine is concentrated around salient poles, which causes MMF in the air gap due to field winding to be non-sinusoidal. The permeance variations in the air gap are caused by slot openings in the stator, saliency in the rotor poles, damper bars in the rotor pole face, saturation of the core and eccentricity of the rotor (Langsdorf, 1955; Jokinen, 1973; Arkkio, 2007).

Magnetic flux in air gap is the product of air gap MMF and air gap permeance. The flux density is given by,

$$B = \frac{\upsilon \Lambda}{\tau_p L_i} \tag{5.1}$$

where $\tau_p L_i$ is the area of one pole through which the flux flows.

The flux density harmonics arise from harmonic contents in both the MMF and permeance. The total air gap MMF is the sum of MMFs due to currents in both the stator winding and field winding in the rotor. The most important source of permeance variations is the saliency of the rotor poles. The three sources of flux density harmonics are analysed in the following sections limiting the analysis to the fundamental and third harmonic flux density components.

5.4.2   Harmonics due to Stator Winding

In the stator frame of reference, MMF caused by a m-phase stator winding with a current I is a function of time and angle θ along the stator frame. The distance x along the stator frame is given by,

$$x = \frac{d_s}{2}\theta = \frac{p\tau_p}{\pi}\theta$$

where d_s is the diameter of stator bore and p is the number of pole pairs. When the MMF axis is set in the middle of first coil

in a coil group as in Figure 5.2, the MMF of stator winding can be written using a Fourier cosine series as,

$$v_s = v_{s,0} + \sum_{n=1}^{\infty} \hat{v}_{s,n} \cos\left(n\pi \frac{x}{\tau_p} - \omega t - \Phi_s + \beta\right) \qquad (5.2)$$

The alternator under study has a 3-phase main winding in the
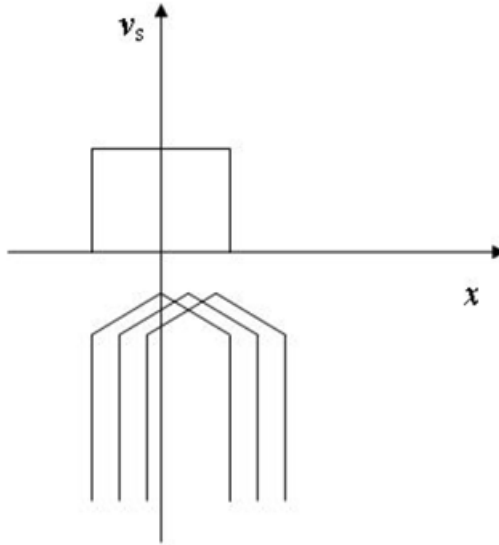
Fig. 5.2: Location of the MMF axis and MMF of the first coil (*Source: Arkkio, 2007*)

stator, and total air gap MMF due to stator winding is the vector sum of MMFs caused by the different phases. As these vectors are summed, the third harmonic components of MMF in each phase cancel each other and as such, no third harmonic MMF component is generated due to the stator current between lines. Thus, the MMF of the stator winding can be assumed to be purely sinusoidal and can be expressed as,

$$v_s = v_{s,1} \cos\left(\pi \frac{x}{\tau_p} - \omega t - \Phi_s + \beta\right) \qquad (5.3)$$

5.4.3 Harmonics due to Field Winding

To determine the MMF harmonics caused by field winding on the rotor, winding is assumed to fill the whole space between pole tip and the pole arc. The linear current density of the field winding is presented in Figure 5.3.
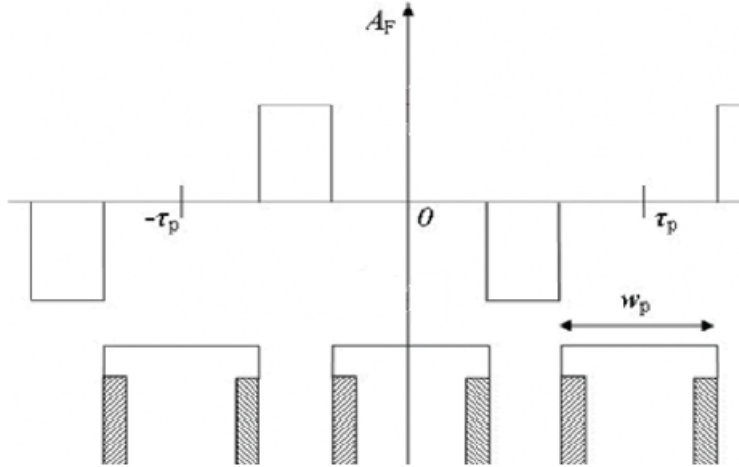
Fig. 5.3: Linear current density of the field winding (*Source: Arkkio, 2007*)

Since the linear current density axis is set in the middle of each rotor pole, current density can be expressed using a Fourier sine series. If x is the distance along rotor frame and w_p, width of the pole, linear current density in rotor frame of reference is given by,

$$A_F = \sum_{n=1}^{\infty} \hat{A}_{F,n} \sin\left(n\pi \frac{x}{\tau_p}\right) \tag{5.4}$$

Field winding MMF, v_F is obtained by integrating the linear

current density.

$$v_F = \int A_F \, dx = \sum_{n=1}^{\infty} \int \hat{A}_{F,n} \sin\left(n\pi \frac{x}{\tau_p}\right) dx$$

$$= -\sum_{n=1}^{\infty} \hat{v}_{F,n} \cos\left(n\pi \frac{x}{\tau_p}\right) \qquad (5.5)$$

where $\hat{v}_{F,n} = \hat{A}_{F,n} \frac{\tau_p}{\pi n}$.

In the stator frame of reference, the air gap MMF varies with time as the rotor rotates. The mechanical speed of the rotor being denoted by ω_m, while transforming the equations into stator frame of reference, distance x must be replaced with,

$$x \to x - \frac{d_s}{2}\omega_m t = x - \frac{2p\tau_p}{2\pi} = x - \frac{\tau_p}{\pi}\omega_m t \qquad (5.6)$$

where $\omega_m p$ is the synchronous frequency. The time and space dependent MMF in the stator frame of reference is,

$$v_F = -\sum_{n=1}^{\infty} \hat{v}_{F,n} \cos\left(n\pi \frac{x}{\tau_p} - n\omega t\right) \qquad (5.7)$$

The total MMF in the air gap of the machine is given by,

$$v = \hat{v}_{s,1} \cos\left(\pi \frac{x}{\tau_p} - \omega t - \Phi_s + \beta\right) - \sum_{n=1}^{\infty} \hat{v}_{F,n} \cos\left(n\pi \frac{x}{\tau_p} - n\omega t\right)$$
$$(5.8)$$

5.4.4 Harmonics due to Salient Rotor Poles

For analysis of the permeance harmonics caused by salient poles of the rotor, the stator surface is assumed to be smooth,

i.e., stator slotting is not taken into account. The rotor pole shoe is assumed to be cylindrical with a uniform air gap. The permeance is approximated to be constant over a pole and zero outside the pole. The approximation is shown in Figure 5.4. The
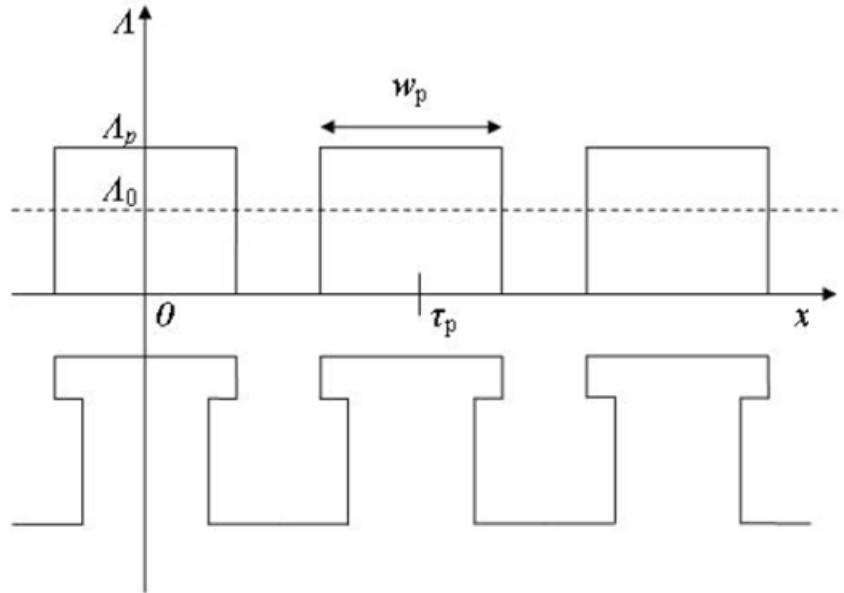
Fig. 5.4: Permeance variation due to salient rotor poles (*Source: Arkkio, 2007*)

permeance due to rotor poles can be expressed using a Fourier cosine series since the permeance axis is set in the middle of the rotor pole. Hence, the permeance is given by,

$$\Lambda = \Lambda_0 + \sum_{n=1}^{\infty} \hat{\Lambda}_n \cos\left((2n\pi\frac{x}{\tau_p}\right) \tag{5.9}$$

where $\Lambda_0 = \frac{1}{\tau_p} \int_{-\frac{\tau_p}{2}}^{+\frac{\tau_p}{2}} \Lambda \, dx = \Lambda_p \frac{1}{w_p} \int_{-\frac{w_p}{2}}^{\frac{\tau_p}{2}} dx = \Lambda_p \frac{w_p}{\tau_p}$ is the average permeance, and the amplitudes of the harmonics are given by,

$$\hat{\Lambda}_n = \frac{2}{\tau_p} \int_{-\frac{\tau_p}{2}}^{+\frac{\tau_p}{2}} \Lambda \cos\left(2n\pi \frac{x}{\tau_p}\right) dx = \frac{2}{\tau_p} \Lambda_p \int_{-\frac{w_p}{2}}^{+\frac{w_p}{2}} \cos\left(2n\pi \frac{x}{\tau_p}\right) dx$$

$$= \Lambda_p \frac{2}{\pi n} \sin\left(n\pi \frac{w_p}{\tau_p}\right) \quad (5.10)$$

When saturation is not taken into account, the constant permeance over a pole is $\Lambda_p = \mu_0 \frac{\tau_p L'}{l'_g}$, where the equivalent air gap l'_g is obtained by multiplying the actual air gap l_g with Carter's coefficient k_c. *i.e.*, $l'_g = k_c l_g$. In stator frame of reference, the permeance also varies with time in a similar manner as the field winding MMF. Using Equation (5.6), the time and space dependent permeance is,

$$\Lambda = \Lambda_0 + \sum_{n=1}^{\infty} \hat{\Lambda}_n \cos\left(\left(2n\pi \frac{x}{\tau_p} - 2n\omega t\right)\right) \quad (5.11)$$

The half waves of the permeance distribution are not symmetrical and both even and odd harmonics exist in the permeance spectrum.

Flux Density

The flux density is obtained as product of total MMF and permeance. *i.e.*,

$$
\begin{aligned}
B = \frac{1}{\tau_p L'} &\left[\hat{v}_{s,1} \cos \left(\pi \frac{x}{\tau_p} - \omega t - \Phi_s + \beta \right) \right. \\
&\left. - \sum_{n=1}^{\infty} \hat{v}_{F,n} \cos \left(n\pi \frac{x}{\tau_p} - n\omega t \right) \right] \\
&\times \left[\Lambda_0 + \sum_{n=1}^{\infty} \hat{\Lambda}_n \cos \left(2n\pi \frac{x}{\tau_p} - 2n\omega t \right) \right] \qquad (5.12)
\end{aligned}
$$

As is evident from Equation (5.12), flux density consists of both time and space harmonics. Magnitude of induced voltage is inversely proportional to frequency of the harmonic component and thus lower order time harmonics induce higher voltages in the auxiliary winding.

Since harmonics in both MMF and permeance are co-sinusoidal, the harmonic frequencies in the flux density are obtained as sum and difference of frequencies in the MMF and permeance. As amplitudes of MMF and permeance harmonics are inversely proportional to their number of order, only the lowest order harmonics have significant effect on total flux density. Hence, main and third harmonic auxiliary windings are designed to utilise first and third order space harmonics respectively.

Only the air gap permeance distribution has even harmonic components and thus the odd flux density harmonics can only be formed of odd MMF harmonics and even permeance harmonics. Since the permeance varies periodically with a fundamental period of one pole pair, flux density space fundamental can be obtained either as the product of MMF fundamental and constant permeance or as product of the third MMF harmonic and

second permeance harmonic. Therefore, fundamental component of the flux density is given by,

$$
\begin{aligned}
B_1 = {} & \frac{v_{s,1}\hat{\Lambda}_0}{\tau_p L'} \cos\left(\pi\frac{x}{\tau_p} - \omega t - \Phi_s + \beta\right) \\
& - \frac{\hat{v}_{F,1}\Lambda_0}{\tau_p L'} \cos\left(\pi\frac{x}{\tau_p} - \omega t\right) \\
& - \frac{\hat{v}_{F,3}\Lambda_2}{2\tau_p L'} \cos\left(\pi\frac{x}{\tau_p} - \omega t\right)
\end{aligned}
\tag{5.13}
$$

The third space harmonic can be obtained either as product of the third MMF harmonic and constant permeance or the MMF fundamental and second permeance harmonic. Combining these yields,

$$
\begin{aligned}
B_3 = {} & \frac{v_{s,1}\hat{\Lambda}_2}{2\tau_p L'} \cos\left(3\pi\frac{x}{\tau_p} - 3\omega t + \Phi_s - \beta\right) \\
& - \frac{\hat{v}_{F,3}\Lambda_0}{\tau_p L'} \cos\left(3\pi\frac{x}{\tau_p} - 3\omega t\right) \\
& - \frac{\hat{v}_{F,1}\Lambda_2}{2\tau_p L'} \cos\left(3\pi\frac{x}{\tau_p} - 3\omega t\right)
\end{aligned}
\tag{5.14}
$$

The previous study gave an approximation for the magnetic flux density in the air gap taking into account MMF caused by stator winding as well as field winding and the permeance variations due to salient rotor poles.

5.5   Design of Third Harmonic Winding

Design of third harmonic winding by analytic methods demands accurate calculation of third harmonic flux density in the air gap of the machine. Estimating amplitude of third harmonic flux in air gap of a machine accurately by conventional design

procedures is difficult due to complex geometry of the machine and non-linear characteristics of the magnetic materials. Hence design of third harmonic winding is done by finite element based virtual prototyping.

5.5.1 FEM Based Virtual Prototyping of the Machine with Third Harmonic Winding

Virtual prototype of the machine is developed by modelling using Ansys Maxwell 2D (Ansys Maxwell 2D V14 documentation manual). FEM modelling of the synchronous machine is done using the geometrical data, material properties, winding data, period of symmetry and the boundary conditions. Winding data are prepared separately for conventional full pitched machine and the full pitched machine with THE winding. Design settings in Maxwell software for the parametric analysis of the machine is given in Table 5.1. FEM models of the two configurations are analysed separately for harmonic content in the output phase voltage to ascertain the effect of third harmonic excitation winding on triplen harmonics. The virtual prototype of the machine with third harmonic winding (THW) is subjected to detailed analysis for the EMF induced per turn of THW and based on this, the number of turns of THW is selected.

By conventional design procedures, the no load exciter field current of the machine estimated is 0.9 A and that at full load, 0.8 p.f. is 2.2 A. With an exciter field winding having $9\,\Omega$ resistance, the voltage required from main auxiliary winding under no-load and that required from third harmonic auxiliary winding under loaded conditions are estimated. Combining these data with simulation results of induced EMF per turn in the main and the third harmonic auxiliary windings, the numbers of turns of auxiliary windings are calculated.

Table 5.1: Design settings in Maxwell 2D for parametric analysis

Variable Name	Value
VA	$45000\,VA$
$Voltage$	$415\,V$
$PowerFactor$	0.8
$Frequency$	$50\,Hz$
$NoOfPoles$	4
$RotorRadius$	$119.1\,mm$
$AirGap$	$0.9\,mm$
$StatorBoreRadius$	$(RotorRadius + AirGap)$
$StatorCoreWidth$	$58\,mm$
$StatorOuterRadius$	$(StatorBoreRadius + StatorCoreWidth)$
spu	1
rpu	1
$StParPath$	2
$PotorParPath$	1
I_{phase}	$spu * VA/(sqrt(3) * Voltage)$
$Theeta$	$120 * Pi/180$
w	$2 * Pi * Frequency$
$I_{ParPath}$	$I_{phase}/StParPath$
Cur_A	$I_{ParPath} * cos(w * t)$
Cur_B	$I_{ParPath} * cos(w * t - Theeta)$
Cur_C	$I_{ParPath} * cos(w * t + Theeta)$
$StatorTurns$	25
Aph_{AT}	$Cur_A * StatorTurns$
Bph_{AT}	$Cur_B * StatorTurns$
Cph_{AT}	$Cur_C * StatorTurns$
$FieldTurns$	48
I_{Field}	75
$Field_{AT}$	$rpu * FieldTurns * I_{Field}$
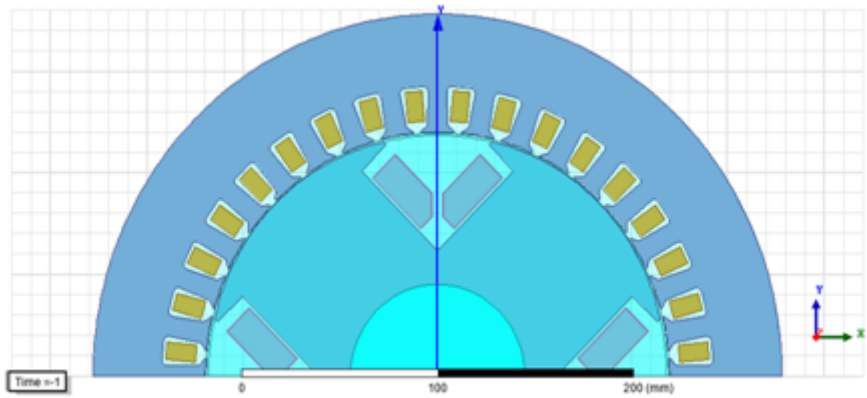
Fig. 5.5: FEM model of 45 KVA alternator with full pitch winding
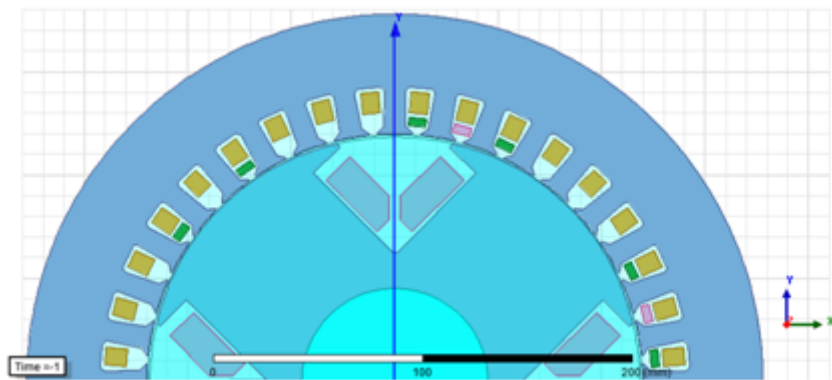
Fig. 5.6: FEM model of 45 KVA alternator with third harmonic and fundamental auxiliary windings

FE models of two configurations of the generators with the two different winding layouts are shown in Figures 5.5 to 5.6 and flux density plots in Figures 5.7 to 5.8.
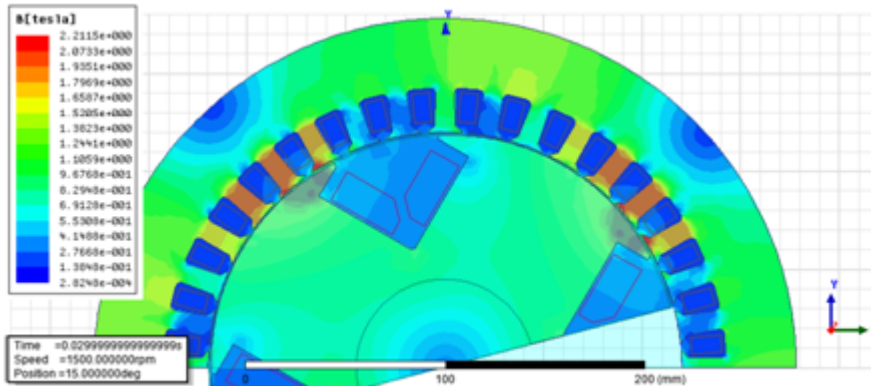
Fig. 5.7: Flux density plot of 45 KVA full pitched alternator with rotor rotated through 15°

On simulation of the machine models, it is observed that the induced voltage per turn of the fundamental auxiliary winding is 8.5 V and that of the THW is 3.2 V as evident in Figure 5.9. Based on the exciter field resistance and the voltage per turn developed in the auxiliary windings, the number of turns of the main auxiliary and the third harmonic windings are designed to keep the terminal voltage under no load and loaded conditions of the machine within tolerance limits.

The voltage induced in the third harmonic winding under different load conditions are also plotted (Figure 5.10). For this, the stator current is varied from 0.2 to 1.4 p.u. and it is observed that voltage induced in THW increases with increase in load current. This ensures suitability of the third harmonic winding in meeting the additional excitation power during loaded conditions of the machine.
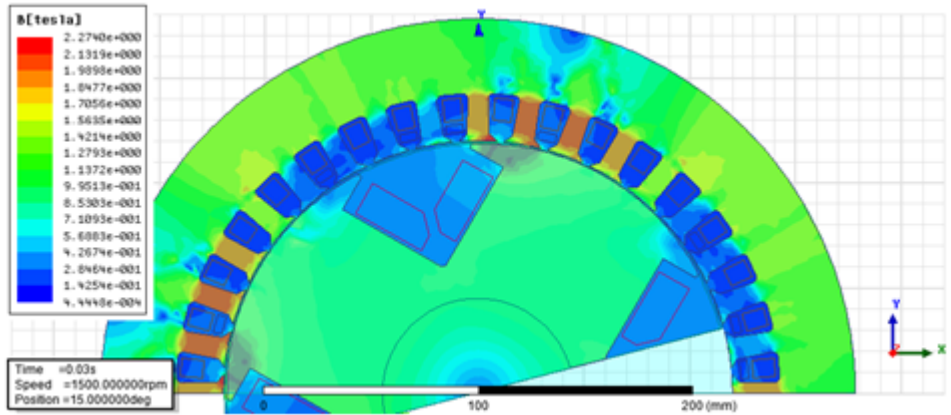
Fig. 5.8: Flux density plot of 45 KVA alternator with THE winding and rotor rotated through 15°

5.6   Experimental Machine

In the third harmonic excitation system implemented, additional excitation power to compensate for armature reaction effect during loaded conditions of the alternator is taken from the air gap flux density harmonics using THW embedded in stator slots of the alternator. Similar to the way the flux density fundamental induces a voltage into the main winding of the machine, the flux density harmonics induce voltages in the auxiliary windings as well. In the improved excitation system, the fundamental and third harmonic flux components are utilised to produce the excitation power under no-load and loaded conditions. The auxiliary windings are wound into the stator slots together with the main winding and located on top of the slot between main winding and the air gap.

In synchronous machines, the synchronous speed, $n = \frac{60 \times f}{p}$, where f is the frequency and p is the number of pair of poles of the machine. The third harmonics of the magnetic field ro-
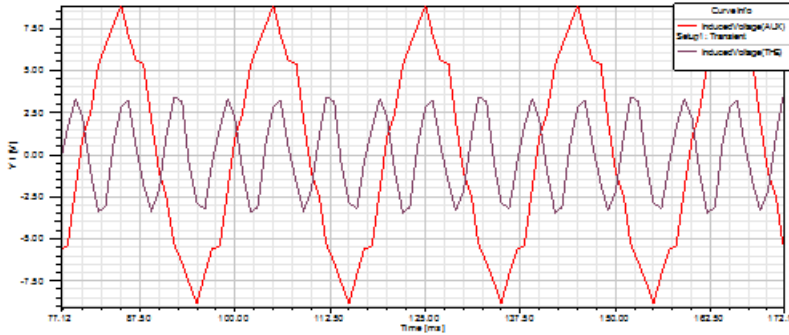
Fig. 5.9: Induced voltage waveforms of fundamental auxiliary winding and third harmonic winding

tate with synchronous rotating frequency of $n_3 = \frac{60 \times f_3}{p}$, where f_3 is the third harmonic frequency. The number of poles, $2p_3$ is three times higher in comparison with number of poles, $2p$ of the fundamental. Therefore, THW is wound for $2p_3 = 6p$ number of poles with winding pitch $y_3 = \frac{S}{6p}$, where S is the number of stator slots. The third harmonic excitation is implemented in a 45 KVA, 415 V, 3-phase, 4 pole synchronous brushless alternator. The main winding is a full pitched concentric winding and THW is wound for $1/3^{rd}$ pitch so that only third harmonic voltage is induced in it. The winding layout of the 45 KVA machine with third harmonic excitation system is shown in Figure 5.11.

The excitation requirement for the machine is estimated as 2.2 A maximum, at 10 V. For third harmonic winding, two turns of 1 mm dia. round copper wire per harmonic pole is wound. These additional turns are accommodated in the stator slots having 112 conductors of 1.12 mm dia. of main winding. As area of additional turns is only 6% of main winding copper area, this could be easily accommodated in the same stator slot. Wound stator of the experimental machine with main winding and auxiliary winding is shown in Figure 5.12.
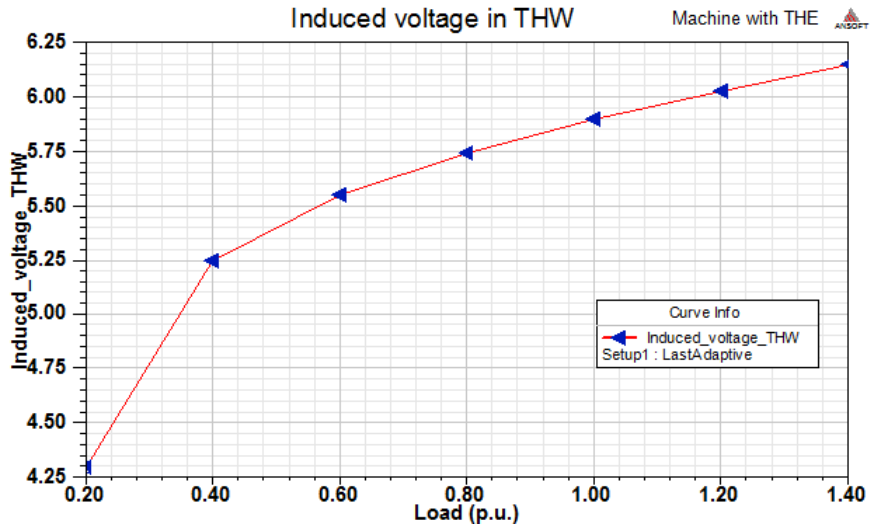
Fig. 5.10: Voltage induced in THW for varying load conditions

The third harmonic excitation system of the experimental machine is shown in Figure 5.13 and the assembled machine with THE system is shown in Figure 5.14.

The induced voltages in the main auxiliary and the third harmonic windings are shown in Figure 5.15. In order to ascertain the capability of the THW to meet excitation requirements during loaded conditions, experiments were conducted on the prototype machine under different load conditions. The excitation voltage produced by the THW under different load conditions for both resistive (R) and resistive-inductive (RL) loads are given in Table 5.2. The tabulations show that excitation voltage produced by THW vary linearly with the load applied on the alternator and hence is capable of providing additional excitation during loaded conditions of the alternator, compensating the armature reaction effect.
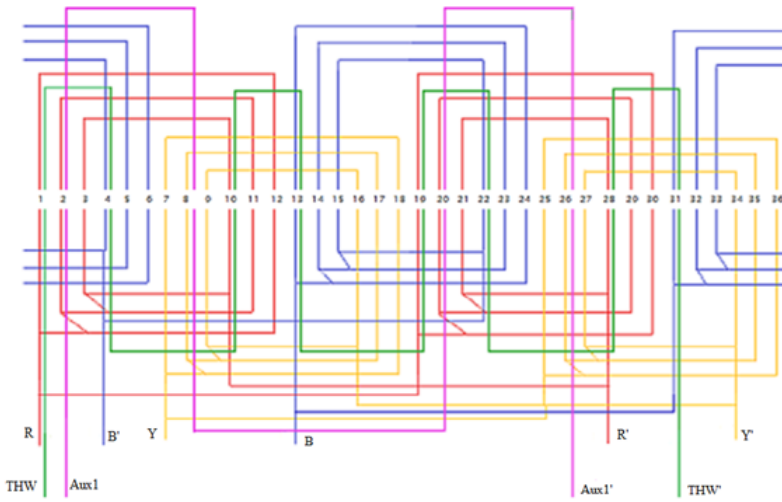
Fig. 5.11: Winding layout of the 45 KVA brushless alternator with third harmonic excitation

Fig. 5.12: Main and auxiliary windings in the stator
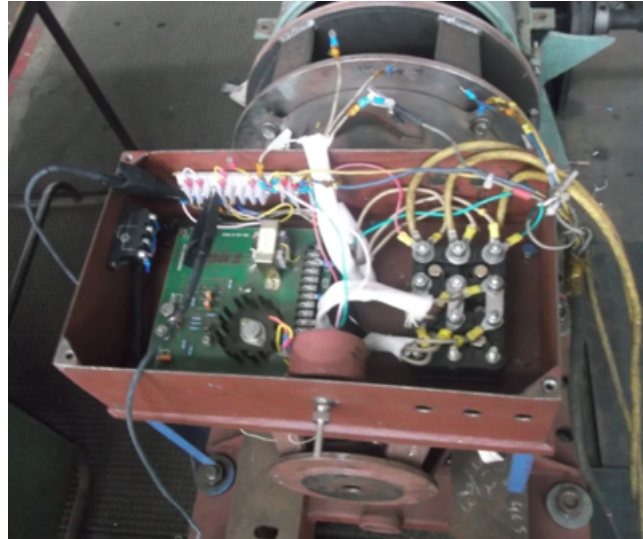
Fig. 5.13: The third harmonic excitation system of the experimental machine

Fig. 5.14: The 45 KVA experimental machine with third harmonic excitation system
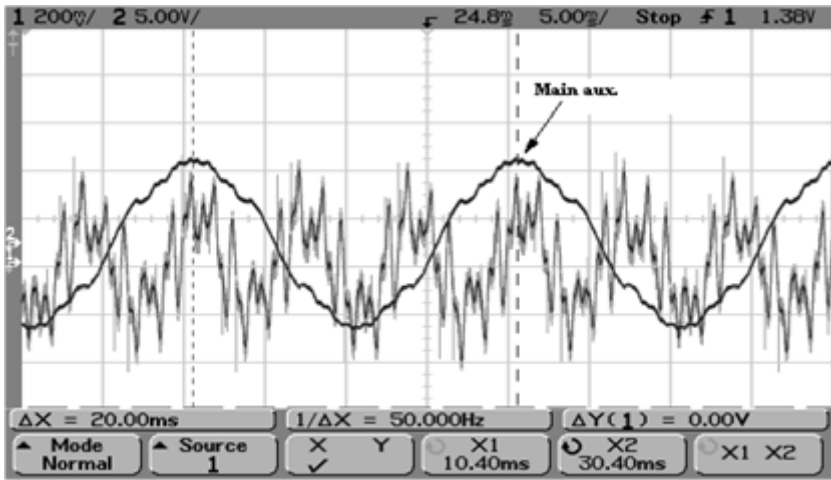
Fig. 5.15: Induced voltage waveforms of fundamental auxiliary winding and third harmonic winding in the experimental machine

Table 5.2: Generated voltage across third harmonic winding at different load conditions

Nature of load	Load p.f.	% Load	Induced voltage in THW(V)
(R)	UPF	25%	6.4
	UPF	50%	6.82
	UPF	75%	8.48
	UPF	100%	8.75
(RL)	0.8 pf	25%	5.38
	0.8 pf	50%	6.39
	0.8 pf	75%	7.852
	0.8 pf	100%	8.766

5.7 Conclusion

In this chapter, a simple, reliable and cost effective excitation system for low voltage brushless alternators is presented with two auxiliary windings embedded into the stator slots. The winding layout of the third harmonic winding is designed for $1/3^{rd}$ pitch so that only third harmonic flux in the air gap links with it. To finalise the number of turns and conductor dimensions of the third harmonic winding, it is necessary to predict third harmonic flux in the air gap of the machine. Since calculation of third harmonic flux by analytic methods is inaccurate, the prediction is done by virtually prototyping the machine using FEM. Based on the FEM results, the design of the THW is finalised and an experimental machine with THE system is developed.

On measuring the voltage induced in the third harmonic auxiliary and the fundamental auxiliary windings of the prototype machine, it is observed that the experimental results are in close agreement with the simulation results.

Chapter 6

Impact of Third Harmonic Excitation System on Voltage Regulation and Output Voltage Harmonics

6.1 Introduction

The basic function of excitation systems in brushless alternators is to provide necessary direct current to the field winding of the synchronous generator, to maintain the required terminal voltage, even under varying load conditions. Thus, excitation systems have a powerful impact on generator dynamic performance ensuring quality of energy delivered to the consumers.

Present study focussed on the design and development of a brushless alternator with third harmonic excitation which utilizes third harmonic flux generated under load conditions, in the air gap of the machine, for excitation purposes. The experimental machine with THE was tested for voltage regulation to check the effec-

tiveness of the new excitation system. Since the novel excitation system utilizes third harmonic flux for generating exciting power, the suitability of the same as a damper of triplen harmonics in the output phase voltage was also verified.

6.2 Impact of THE on Voltage Regulation

The excitation system of a brushless alternator should be capable of keeping the voltage regulation of the machine within prescribed limits, under all load conditions. The specified voltage regulation of the machine under study being $\pm 1\%$, effectiveness of third harmonic excitation system was verified by measuring voltage regulation of the experimental machine under various load conditions, with R load and RL load separately. The results are given in Table 6.1.

Table 6.1: Voltage regulation of the alternator under different load conditions

Nature of load	Load p.f.	% Load	Output voltage (line to line)					
			AB (V)	VR(%)	BC (V)	VR(%)	AC (V)	VR(%)
R	UPF	25%	415	0	413.88	0.27	411.23	0.91
	UPF	50%	414.25	0.18	416.36	-0.33	418.85	-0.93
	UPF	75%	411.22	0.91	417.41	-0.58	417.12	-0.51
	UPF	100%	413.79	0.29	411.15	0.93	413.11	0.45
RL	0.8	25%	415.95	-0.23	418.57	-0.86	419.11	-0.99
	0.8	50%	411.97	0.73	411.22	0.91	412.18	0.68
	0.8	75%	413.49	0.36	414.25	0.18	418.02	-0.73
	0.8	100%	413.49	0.36	414.4	0.15	412.81	0.53

Experimental results show that the THE system implemented in 45 KVA alternator is capable of limiting the voltage regulation within the prescribed limits, thereby proving effectiveness of the system under different load conditions.

6.3 Output Voltage Harmonics

FEM models of 45 KVA machine with the two different winding layouts were simulated for 0.8 p.f., full load, and output voltage harmonics were analysed in each case. A prototype machine rated for 45 KVA with THE system was developed, and experiments were conducted to validate the simulation results.

6.3.1 Simulation Results

Virtual prototypes of synchronous generator with different winding layouts are modelled in FEM software Ansys Maxwell 2D and analysed for output voltage harmonics. Output phase volt-
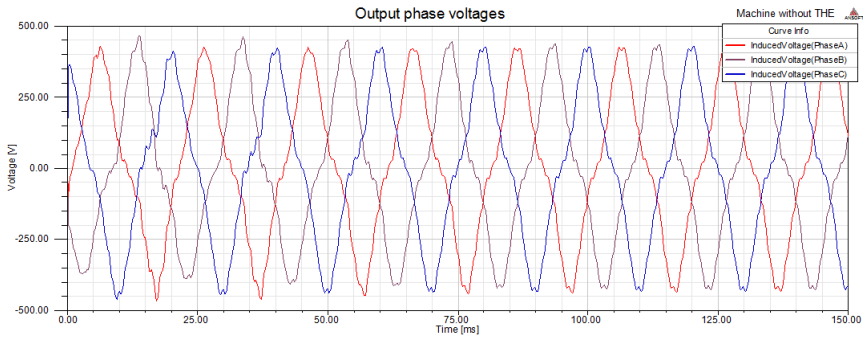
Fig. 6.1: Output voltage waveform of 45 KVA full pitched generator

age waveforms and their harmonic distribution for the machine with conventional excitation system and that with THE system are compared. Figure 6.1 shows the voltage in the three output phases A, B and C of the machine with full pitched main winding having conventional excitation system. The phase voltage is distorted due to high triplen harmonic content and the harmonic content in the phase voltage is computed by FFT analysis and Figure 6.2 shows the harmonic spectra. As observed, presence of
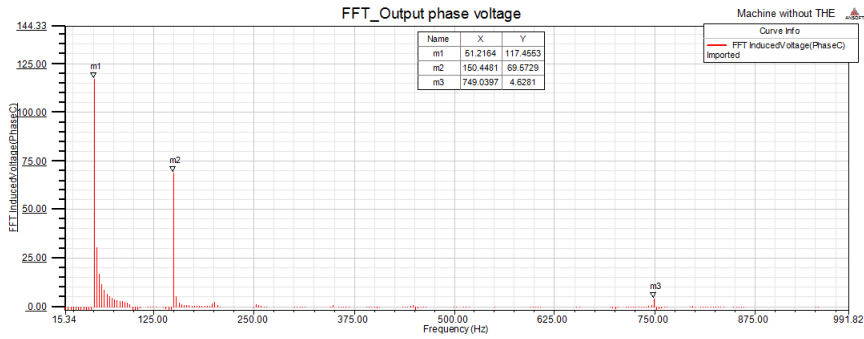
Fig. 6.2: Harmonic spectra of the output voltage waveform of the full pitched generator
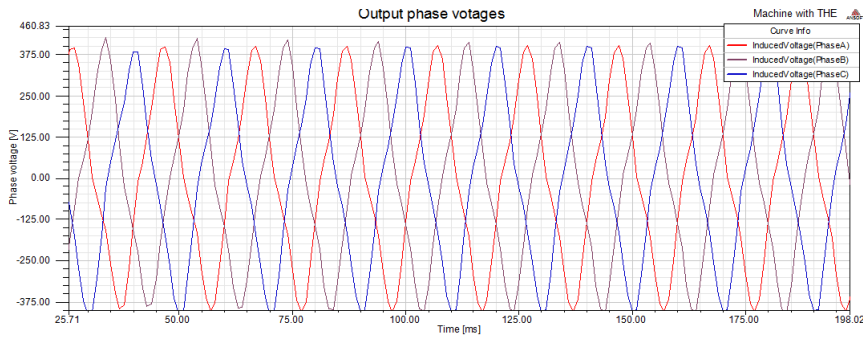
Fig. 6.3: Output voltage waveform of full pitched generator with THE

3rd and 5th harmonics in the phase voltage is significant. Voltage in the three output phases of the machine with THE is shown in Figure 6.3. The harmonic content in the phase voltages are significantly reduced due to the effect of third harmonic winding. The harmonic spectra of the phase voltage (Figure 6.4) shows that 5th harmonics is completely eliminated and there is reduction in 3rd harmonic content by 17.1%. On comparing the harmonic spectra of the output voltages, as shown in Figures 6.2 and 6.4, it is clear that, by adopting THE in the full pitched machine, the
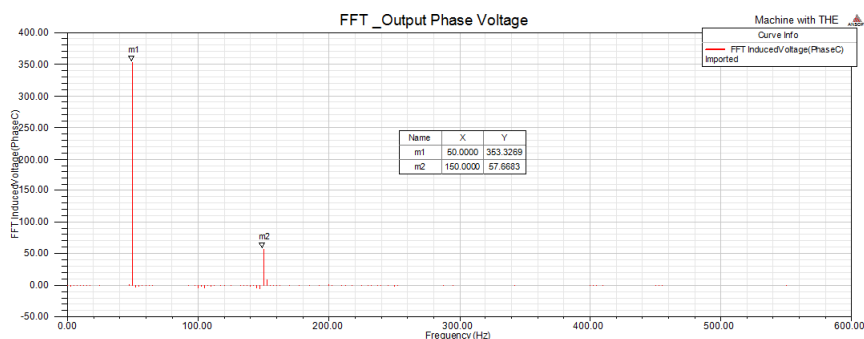
Fig. 6.4: Harmonic spectra of the output voltage waveform of the full pitched generator with THE

triplen harmonics are reduced which confirms the suitability of third harmonic winding as damper of triplen harmonics in the output phase voltage.

6.3.2 Experimental Results

Experiments were conducted on the 45 KVA prototype machine with the third harmonic excitation system and output voltage waveforms were analysed for total harmonic distortion. The output voltage waveform for 0.8 p.f., full load applied on the machine without THE is shown in Figure 6.5 and output voltage waveform of the machine with THE is shown in Figure 6.6. THD of the output voltages were obtained as 7.116% and 4.886% respectively, for the conventional machine and the machine with THE. Analysis of output voltage harmonics of the generator with THE confirmed reduction in total harmonic distortion as compared to that in generator without THE. This is attributed to the reduction in triplen harmonics under loaded conditions utilising third harmonic power for excitation.
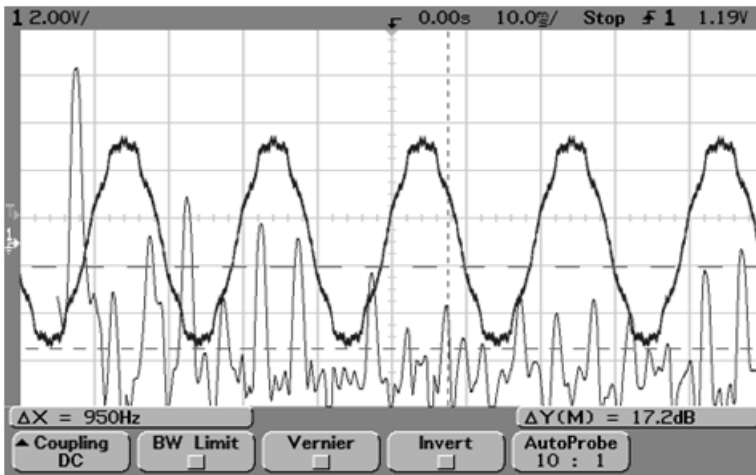
Fig. 6.5: Output voltage waveform (line to neutral) of experimental machine without THE, at full load, 0.8 p.f.
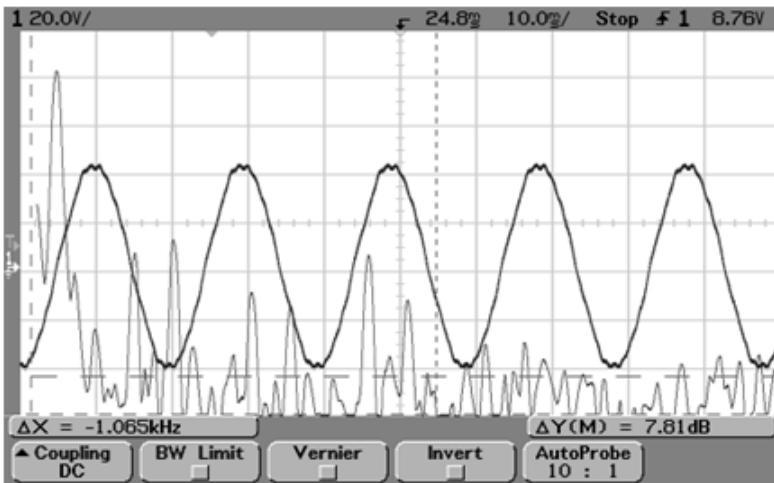
Fig. 6.6: Output voltage waveform (line to neutral) of experimental machine with THE, at full load, 0.8 p.f.

6.4   Conclusion

The compound excitation system using third harmonic winding helps to eliminate use of expensive compounding transformer or shunt AVR otherwise required, reducing overall cost of the machine at the same time enhancing reliability of the system. Simulation results show that, by utilising third harmonic flux in the air gap for excitation purposes during loaded conditions, triplen harmonics in the output phase voltage are reduced. Prototype of the experimental machine with THE system designed and developed based on FEM analysis proved effective in keeping the voltage regulation within specified limits and has added advantage of reduced harmonics in output phase voltage.

Chapter 7

Summary, Conclusion and Future Scope

7.1 Summary

Chapter 1 introduces the background of the research problem followed by Chapter 2 which presents a thorough review of literature available on the topic. The essence of the research work is incorporated in Chapters 3 to 6. The finite element formulation of the field problem in brushless alternators is explained in chapter 3. FEM based virtual prototyping for parameter prediction in synchronous generators is discussed in chapter 4 and the parameters of the machine predicted by simulation of the virtual prototype are analysed. Chapter 5 describes the design and implementation of an improved excitation system for brushless alternators utilising third harmonic flux in the air gap of the machine. Chapter 6 discusses the influence of the THE system on the voltage regulation and THD in the output phase voltage of the machine.

139

7.1.1 FE Formulation of the Field Problem

The magnetic field distribution along the cross section of the brushless alternator is described by Poisson's equation. The field properties of the machine are invariant along z-axis and hence 2D FEM formulation is sufficient for analysis of the machine thereby considerably reducing the computational time. The field variables computed in the problem domain by FEM, are used for deriving the machine parameters, by post-processing.

To improve the accuracy of computation, the quadratic triangular elements are used where field variable at the six nodes of each element in the problem domain are computed and then interpolated to compute the field variable at each and every point in the analysis domain. Iso-parametric elements used for discretisation help modelling the complex geometry of the machine accurately.

7.1.2 Parameter Prediction by FEM based Virtual Prototyping

Virtual prototyping of the machine is done by modelling the machine using FEM software, Ansys Maxwell 2D. The FE modelling of a brushless alternator of 45 KVA capacity is done using geometrical data, material properties, winding data, period of symmetry and the boundary conditions. Simulation of the virtual prototype of the alternator is carried out and based on electromagnetic field analysis, the machine parameters are predicted. FEM proves to be an efficient numerical tool for prediction of performance characteristics of electrical machines in the design stage thus saving development time and cost by avoiding expensive and time consuming prototyping.

7.1.3 Improved Excitation System for Brushless Alternators

A third harmonic excitation system for brushless alternators is designed with two auxiliary windings embedded in the stator slots, electrically isolated from the main winding. In the fundamental auxiliary winding, a voltage proportional to the output voltage is induced. The third harmonic auxiliary winding is designed in such a way that only triplen harmonic flux produced in air gap of the alternator links with the winding. Triplen harmonic flux produced in the air gap vary linearly with percentage loading of alternator and by suitably selecting the number of turns of THW, voltage induced in the winding is made exactly equal to the additional excitation required to compensate armature reaction caused by the load. Rectified voltages of both the auxiliary windings are fed to two different windings on each pole of the exciter field, so that MMF produced by fundamental auxiliary winding is strengthened by the third harmonic auxiliary winding under loaded conditions. When flux produced by these two windings are additively fed to the exciter field, output of the alternator is maintained within permitted voltage tolerance band from no load to full load conditions.

A finite element model of the machine with THE is simulated for predicting the induced EMF per turn in the fundamental and the third harmonic auxiliary windings, thereby calculating the numbers of turns of the auxiliary windings. The voltage induced in the third harmonic winding for different load conditions are also plotted and it shows that the induced voltage in THW is sufficient for providing additional excitation for the machine under loaded conditions. A prototype brushless alternator of 45 KVA, 415 V, 3-phase, 4 pole with THE is developed and experimented to validate the simulation results.

7.1.4 Impact of THE System on Voltage regulation and Output Voltage Harmonics

In the compound excitation system using third harmonic winding, the combined effect of the fundamental auxiliary winding with $2/3^{rd}$ pitch and the third harmonic auxiliary winding with $1/3^{rd}$ pitch, ensures desired voltage regulation and reduces the total harmonic content in the output phase voltage. Experiments conducted on the 45 KVA prototype machine with THE system and the output phase voltage waveforms analysed for THD exhibited considerable reduction as compared to that in generator without THE. This is attributed to the reduction in triplen harmonics under loaded conditions, by utilising third harmonic power for excitation. The compound excitation system using THE system eliminate use of expensive compounding transformer or shunt AVR otherwise required, thereby drastically reducing overall cost of the machine, at the same time enhancing reliability of the system.

7.2 Conclusion

The present investigation successfully designed and implemented a simple, reliable and cost effective excitation system for low voltage brushless alternators, with two auxiliary windings embedded into the stator slots. Since the number of turns of auxiliary windings are very small compared to main winding of the machine, same could be accommodated in the stator slots. To finalise the number of turns and conductor dimensions of THW, it is necessary to predict third harmonic flux in the air gap of the machine. Since calculation of third harmonic flux by analytic methods is inaccurate, the prediction is done by virtually prototyping the machine using FEM. Based on the simulation results, the design of THW is finalised and an experimental machine with

THE system is developed.

Analysis of THD in the output phase voltage of the alternator with THE exhibited reduction in total harmonic distortion as compared to that in generator without THE. The compound excitation system using THW eliminates use of expensive compounding transformer or shunt AVR thereby reducing the overall cost of the machine, at the same time reliability of the system is enhanced.

FEM proves to be an efficient numerical tool for virtual prototyping for prediction of performance characteristics of electrical machines in the design stage thereby avoiding expensive and time consuming prototyping. The numerical test platform based on FEM can replace costly and hazardous tests conducted in conventional test beds.

7.3   Suggestions for Future Reaearch

- Field analysis of synchronous machines is of multi-physics nature which includes electric, magnetic, thermal and mechanical aspects. The work presented here is restricted only to analysis of electric and magnetic phenomena within the machine structure.

- The present work is limited to the study of impact of THE system on voltage regulation and THD of output phase voltage. There is scope for extending the investigation to other important performance criteria of brushless alternators like TVD/TVR and Short circuit characteristics.

- From results of the present study it is obvious that fifth harmonics is also a predominant component in the generator output voltage. Therefore, by suitably changing pitch of the harmonic auxiliary winding, fifth harmonic flux can

also be utilised for generating excitation power, so that to-
tal harmonic content in the output phase voltage of the
alternator can further be reduced.

- Present study is limited to the parameter prediction by
  magneto-static analysis together with parametric investi-
  gation of the machine model. The transient parameters
  of the machine can also be predicted by resorting to tran-
  sient analysis where movement modelling of the rotor also
  is considered.

List of Publications

International / National Conferences

- Jiji K. S., Jayadas N. H. and C. A. Babu, "An Improved Excitation System for Low Voltage Salient Pole Synchronous Generators Utilizing Third Harmonic Power", The EE Centenary Conference , IISc, Bangalore. December 2012.

- Jiji K. S., Jayadas N. H. and C. A. Babu, "Prediction of Performance characteristics of Salient pole Synchronous Generators by Finite Element Method", Proceedings of International Conference on Emerging Trends in Manufacturing technology, Kochi, September 2012.

- Jiji K. S., Jayadas N. H. and C. A. Babu, "FEM based design of Third harmonic Excitation System for Low Voltage Salient Synchronous Generators", Proceedings of International Conference on Electrical Machines and Systems (ICEMS 2012), Sapporo, JAPAN, October 2012.

International Journals

- Jiji K. S., Jayadas N. H. and C. A. Babu, "FEM based Virtual Prototyping and Design of Third Harmonic Excitation System for Low Voltage Salient Pole Synchronous Generators", IEEE Transactions on Industry Applications, pp. $1829 - 1834$, Vol. 50, Issue 3, May/June 2014.

- Jiji K. S., Jayadas N. H. and C. A. Babu, "Prediction of Steady State Parameters of Synchronous Generators by Finite Element Method", Wiley International Journal of Numerical Modelling, Communicated.

Bibliography

[1] *IS 4722: Specification for electrical machines (Second revision).* 2001.

[2] *IEC 60034-1: Rotating electrical machines - Part 1.* 2004.

[3] *Ansys Maxwell 2D V14 Documentation manual.* Ansys, 2011.

[4] ABDULLAH, B., FARIS, M., BAHARUDIN, Z., HAMID, B., AND HISHAM, N. "The Third Harmonic Model for Salient Pole Synchronous Generator Under Balanced Load". *Energy Conversion, IEEE Transactions on 29*, 2 (2014), 519–526.

[5] ADKINS, B. *"The general theory of electrical machines"*. Chapman & Hall, 1957.

[6] AMAYA, M., COSTA, A., PALACIOS, J., AND CADAVID, H. "Identification of the synchronous machine parameters by the simulation of time domain tests using finite-elements method". In *Proc. of the Int. Conf. on Electric Machines and Drives (IEMDC'03)*.

[7] ANGST, G., AND OLDENKAMP, J. "Third-harmonic voltage generation in salient-pole synchronous machines". *Transactions of the American Institute of Electrical Engi-*

neers. *Part III: Power Apparatus and Systems 3*, 75 (1956), 434–441.

[8] Arjona, L., and Macdonald, D. "A new lumped steady-state synchronous machine model derived from finite element analysis". *Energy Conversion, IEEE Transactions on 14*, 1 (1999), 1–7.

[9] Arkkio, A. *Low-voltage Synchronous Generator Excitation Optimization and Design*. PhD thesis, HELSINKI UNIVERSITY OF TECHNOLOGY, 2007.

[10] Ashtiani, C., and Lowther, D. "The use of finite elements in the simulation of the steady state operation of a synchronous generator with a known terminal loading condition". *Magnetics, IEEE Transactions on 19*, 6 (1983), 2381–2384.

[11] Bargallo, R. "Finite elements for electrical engineering". *Electrical Engineering Department of Universitat Politécnica de Catalunya* (2006).

[12] Bastos, J. P. A., and Sadowski, N. *"Electromagnetic modeling by finite element methods"*. CRC press, 2003.

[13] Behrend, B. A. *"The induction motor and other alternating current motors: their theory and principles of design"*. McGraw-Hill, 1921.

[14] Belforte, P., and Chiampi, M. "A finite element formulation for electromagnetic devices supplied by alternating voltages". *COMPEL: The International Journal for Computation and Mathematics in Electrical and Electronic Engineering 3*, 1 (1984), 1–15.

[15] Bianchi, N. *"Electrical machine analysis using finite elements"*. CRC press, 2005.

[16] BIDDLECOMBE, C., SIMKIN, J., JAY, A., SYKULSKI, J., AND LEPAUL, S. "Transient electromagnetic analysis coupled to electric circuits and motion". *Magnetics, IEEE Transactions on 34*, 5 (1998), 3182–3185.

[17] BLONDEL, A., AND ADAMS, C. A. *"Synchronous motors and converters: theory and methods of calculation and testing"*. McGraw-Hill Book Company, 1913.

[18] BOLDEA, I. *"Synchronous generators"*. CRC Press, 2005.

[19] BRAUER, J. *"What every engineer should know about finite element analysis"*. CRC Press, 1993.

[20] BROWN, N., AND HAYDOCK, L. "New brushless synchronous alternator". *IEE Proceedings-Electric Power Applications 150*, 6 (2003), 629–635.

[21] CALVANO, F., DAL MUT, G., FERRAIOLI, F., FORMISANO, A., MARIGNETTI, F., MARTONE, R., RUBINACCI, G., TAMBURRINO, A., AND VENTRE, S. "A novel technique based on integral formulation to treat the motion in the analysis of electric machinery". *International Journal of Applied Electromagnetics and Mechanics 39*, 1 (2012), 637–643.

[22] CALVANO, F., DAL MUT, G., FERRAIOLI, F., FORMISANO, A., MARIGNETTI, F., MARTONE, R., RUBINACCI, G., TAMBURRINO, A., AND VENTRE, S. "Computation of end-winding inductances of rotating electrical machinery through three-dimensional magnetostatic integral FEM formulation". *COMPEL: The International Journal for Computation and Mathematics in Electrical and Electronic Engineering 32*, 5 (2013), 1539–1551.

[23] CENTNER, M., AND HANITSCH, R. "Fractional slot-winding with asymmetrical stator slot-layout". In *Power Electronics, Electrical Drives, Automation and Mo-*

tion, 2006. SPEEDAM 2006. International Symposium on (2006), IEEE, pp. 108–110.

[24] CHAN, T., LAI, L., AND YAN, L. "Analysis of a stand-alone permanent magnet synchronous generator using a time stepping coupled field circuit method". *IEE Proc. Electr. Power Appl. 152* (2005), 1459–1467.

[25] CHAN, T., AND LAI, L. L. "A novel single-phase self-regulated self-excited induction generator using a three-phase machine". *Energy Conversion, IEEE Transactions on 16*, 2 (2001), 204–208.

[26] CHAN, T., WANG, W., AND LAI, L. "Analysis and performance of a permanent-magnet synchronous generator supplying an isolated load". *IET electric power applications 4*, 3 (2010), 169–176.

[27] CHANG, L., AND MUSZYNSKI, J. J. "Design of a 5-phase permanent magnet brushless DC motor for automobiles". In *Vehicular Technology Conference, 2003. VTC 2003-Fall. 2003 IEEE 58th* (2003), vol. 5, IEEE, pp. 3197–3201.

[28] CHARI, M. "Electromagnetic modeling of electrical machinery for design applications". In *Industrial Electromagnetics Modelling*. Springer, 1983, pp. 3–14.

[29] CHARI, M., CSENDES, Z., SILVESTER, P., KONRAD, A., AND PALMO, M. "Three-dimensional magnetostatic field analysis of electrical machinery by the finite-element method". *Power Apparatus and Systems, IEEE Transactions on*, 8 (1981), 4007–4019.

[30] CHARI, M., KONRAD, A., PALMO, M., AND D'ANGELO, J. "Three-dimensional vector potential analysis for machine field problems". *Magnetics, IEEE Transactions on 18*, 2 (1982), 436–446.

[31] Chari, M., Minnich, S., Csendes, Z., Berkery, J., and Tandon, S. "Load characteristics of synchronous generators by the finite-element method". *Power Apparatus and Systems, IEEE Transactions on*, 1 (1981), 1–13.

[32] Chari, M., and Silvester, P. "Analysis of turboalternator magnetic fields by finite elements". *Power Apparatus and Systems, IEEE Transactions on*, 2 (1971), 454–464.

[33] Chari, M., and Silvester, P. P. *"Finite elements in electrical and magnetic field problems"*. John Wiley & Sons Incorporated, 1980.

[34] Chebak, A., Viarouge, P., and Cros, J. "Optimal design of a high-speed slotless permanent magnet synchronous generator with soft magnetic composite stator yoke and rectifier". *Mathematics and Computers in Simulation (MATCOM) 81* (2010), 239–251.

[35] Chicco, G., Postolache, P., and Toader, C. "Triplen harmonics: myths and reality". *Elsevier Journal of Electric Power System Research 81* (2011), 1541–1549.

[36] Chiricozzi, E., and Di Napoli, A. "Saturation effect on the magnetic field distribution in tooth region of electric machines". *Magnetics, IEEE Transactions on 14*, 5 (1978), 473–475.

[37] Comanescu, M., Keyhani, A., and Dai, M. "Design and analysis of 42-V permanent-magnet generator for automotive applications". *Energy Conversion, IEEE Transactions on 18*, 1 (2003), 107–112.

[38] Ćosović, M., Smaka, S., Maaić, Š., Steinhart, H., et al. "Design of wound rotor low-voltage synchronous generator". In *Information, Communication and Automation Technologies (ICAT), 2011 XXIII International Symposium on* (2011), IEEE, pp. 1–5.

151

[39] DARABI, A. "Auxiliary windings, supplying the AVR of a brushless synchronous generator". In *Proc. of 8th International Conference on Electrical Machines and Systems (ICEMS 2005)*.

[40] DARABI, A., AND TINDALL, C. . "Brushless exciter modelling for small salient pole alternators using finite elements". *IEEE transactions on energy conversion 17* (2002), 306–312.

[41] DARABI, A., AND TINDALL, C. "Analogue AVR model for use in real time transient simulation of small salient pole alternators". In *Power Electronics, Machines and Drives, 2002. International Conference on (Conf. Publ. No. 487)* (2002), IET, pp. 451–455.

[42] DARABI, A., AND TINDALL, C. "Damper cages in genset alternators: FE simulation and measurement". *Energy Conversion, IEEE Transactions on 19*, 1 (2004), 73–80.

[43] DARABI, A., TINDALL, C., AND FERGUSON, S. "Finite element time step coupled generator, load, AVR and brushless exciter modeling". *IEEE Trans. Energy Convers. 19* (2004), 258–264.

[44] DEMERDASH, N., AND LAU, N. "Flux penetration and losses in solid nonlinear ferromagnetics using state space techniques applied to electrical machines". *Magnetics, IEEE Transactions on 12*, 6 (1976), 1039–1041.

[45] DEMERDASH, N., AND NEHL, T. "An evaluation of the methods of finite elements and finite differences in the solution of nonlinear electromagnetic fields in electrical machines". *Power Apparatus and Systems, IEEE Transactions on*, 1 (1979), 74–87.

[46] DOHERTY, R., AND NICKLE, C. "Synchronous machines I : an extension of blondel's two-reaction theory". *Amer-*

ican Institute of Electrical Engineers, Transactions of the 45 (1926), 912–947.

[47] DOHERTY, R., AND NICKLE, C. "Synchronous machines-III: Torque angle characteristics under transient conditions". *American Institute of Electrical Engineers, Transactions of the 46* (1927), 1–18.

[48] DOHERTY, R., AND NICKLE, C. "Three-phase short circuit synchronous machines - V". *American Institute of Electrical Engineers, Transactions of the 49*, 2 (1930), 700–714.

[49] ELENA OTILIA VIRJOGHE, DIANA ENESCU, M.-F. S., AND IONEL, M. *Finite Element Analysis - New Trends and Developments.* InTech, 2012.

[50] ERCEG, G., ERCEG, R., AND IDZOTIC, T. "Using digital signal processor for excitation system of brushless synchronous generator". In *Industrial Electronics Society, 1999. IECON'99 Proceedings. The 25th Annual Conference of the IEEE* (1999), vol. 3, IEEE, pp. 1355–1360.

[51] FINLAYSON, B., AND SCRIVEN, L. "The method of weighted residuals - a review". *Appl. Mech. Rev 19*, 9 (1966), 735–748.

[52] FINLAYSON, B. A. *"The method of weighted residuals and variational principles"*, vol. 73. SIAM, 2013.

[53] FITZGERALD, A. E., KINGSLEY, C., UMANS, S. D., AND JAMES, B. *"Electric machinery"*. McGraw-Hill New York, 1983.

[54] FORTESCUE, C. L. "Method of symmetrical co-ordinates applied to the solution of polyphase networks". *American Institute of Electrical Engineers, Transactions of the 37*, 2 (1918), 1027–1140.

[55] Fu, W., and Ho, S. "Extension of the Concept of Windings in Magnetic Field Electric Circuit Coupled Finite Element Method". *Magnetics, IEEE Transactions on 46*, 6 (2010), 2119–2123.

[56] Fu, W., Zhou, P., Lin, D., Stanton, S., and Cendes, Z. "Modeling of solid conductors in two-dimensional transient finite-element analysis and its application to electric machines". *Magnetics, IEEE Transactions on 40*, 2 (2004), 426–434.

[57] Fuchs, E., Fuchs, H., and Masoum, M. "Power quality of electric machines and power systems". In *Proceedings of the Eighth IASTED International Conference* (2008), vol. 608, p. 35.

[58] Fuchs, E., and Masoum, M. A. *"Power quality in power systems and electrical machines"*. Academic press, 2011.

[59] Fuchs, E. F., and Erdelyi, E. A. "Non-linear theory of turbo-alternators Part II: Load dependent synchronous reactances". *Power Apparatus and Systems, IEEE Transactions on*, 2 (1973), 592–599.

[60] Godhwani, A., and Basler, M. "A digital excitation control system for use on brushless excited synchronous generators". *Energy Conversion, IEEE Transactions on 11*, 3 (1996), 616–620.

[61] Grabner, C., and Schmidt, E. "Novel insights into the nonlinear dependency of the airgap magnetic flux density of synchronous generators with fractional slot windings in case of various operational states". In *Canadian Conference on Electrical and Computer Engineering CCECE 2003*.

[62] Griffo, A., Wrobel, R., Mellor, P. H., and Yon, J. M. "Design and characterization of a three-phase brush-

154

less exciter for aircraft starter generator". *Industry Applications, IEEE Transactions on 49*, 5 (2013), 2106–2115.

[63] GUPTHA, C., MARWAHA, S., AND MANNA, M. S. "Finite element method as an aid to machine design: A computational tool". In *Proc. of COMSOL Conference, Bangalore, India, (COMSOL 2009)*.

[64] HAMEYER, K., HENROTTE, F., SANDE, H. V., DELIÈGE, G., AND DE GERSEM, H. "Finite element models in electrical machine design". In *Vth Congresso Brasileiro de Electromagnetismo CBMag 2002* (2002).

[65] HARGREAVES, P., MECROW, B., AND HALL, R. "Open circuit voltage distortion in salient pole synchronous generators with damper windings". In *Power Electronics, Machines and Drives (PEMD 2010), 5th IET International Conference on* (2010), IET, pp. 1–6.

[66] HECHT, F., AND MARROCCO, A. "A finite element simulation of an alternator connected to a nonlinear external circuit". *Magnetics, IEEE Transactions on 26*, 2 (1990), 964–967.

[67] HEYLAND, A. "*A graphical treatment of the induction motor*". McGraw Publishing Company, 1906.

[68] HOOLE, S. "*Computer aided analysis and design of electromagnetic devices*". Elsevier, 1989.

[69] HUANG, S., WANG, L., AND XIA, Y. "Calculation of winding voltage of permanent magnet synchronous generator based on tooth flux method". In *Proc. of the Int. Conf. on Electrical Machines and Systems (ICEMS 2008)*.

[70] HUGHES, T., AND LIU, W. "Implicit-explicit finite elements in transient analysis: stability theory". *Journal of applied Mechanics 45*, 2 (1978), 371–374.

[71] HUMPHRIES, S. *"Finite-element methods for electromagnetics"*. Boca Raton, USA: CRC Press, 1997.

[72] IAMAMURA, B., LE MENACH, Y., TOUNZI, A., SADOWSKI, N., GUILLOT, E., JACQ, T., AND LANGLET, J. "Study of synchronous generator static eccentricities-FEM results and measurements". In *Electrical Machines (ICEM), 2012 XXth International Conference on* (2012), IEEE, pp. 1829–1835.

[73] IDE, K., TAKAHASHI, M., SATO, M., TSUJI, E., AND NISHIZAWA, H. "Higher harmonics calculation of synchronous generators on the basis of magnetic field analysis considering rotor movement". *Magnetics, IEEE Transactions on 28*, 2 (1992), 1359–1362.

[74] INOUE, K., YAMASHITA, H., NAKAMAE, E., AND FUJIKAWA, T. "A brushless self-exciting three-phase synchronous generator utilizing the 5th-space harmonic component of magneto motive force through armature currents". *Energy Conversion, IEEE Transactions on 7*, 3 (1992), 517–524.

[75] JI, Z., YINGLI, L., AND MINGXIU, W. "Determination of power angle curves of synchronous machines considering cross-magnetizing saturation effect". In *Power Engineering Society Winter Meeting, 2000. IEEE* (2000), vol. 1, IEEE, pp. 228–232.

[76] JIN, J. *"The finite element method in electromagnetics"*. John Wiley & Sons, 2014.

[77] JOKINEN, T., ET AL. *Utilization of harmonics for self-excitation of a synchronous generator by placing an auxiliary winding in the rotor*. Finnish Academy of Technical Sciences, 1973.

[78] KABIR, S., AND SHUTTLEWORTH, R. "Brushless exciter model". *IEE Proceedings-Generation, Transmission and Distribution 141*, 1 (1994), 61–67.

[79] KARAYAKA, H. B., KEYHANI, A., HEYDT, G. T., AGRAWAL, B. L., AND SELIN, D. A. "Synchronous generator model identification and parameter estimation from operating data". *Energy Conversion, IEEE Transactions on 18*, 1 (2003), 121–126.

[80] KARMAKER, H., AND KNIGHT, A. M. "Investigation and simulation of fields in large salient-pole synchronous machines with skewed stator slots". *Energy Conversion, IEEE Transactions on 20*, 3 (2005), 604–610.

[81] KELLER, S., XUAN, T. M., AND SIMOND, J. J. "Computation of the no-load voltage waveform of laminated salient pole synchronous generators". *IEEE Trans. Ind. Appl. 42* (2006), 681–687.

[82] KIM, C. E., AND SYKULSKI, J. K. "Harmonic analysis of output voltage in synchronous generator using finite element method taking account of the movement". *IEEE Trans. Magn. 38* (2002), 1249–1252.

[83] KNIGHT, A., KARMAKER, H., AND WEBER, K. "Use of a permeance model to predict force harmonic components and damper winding effects in salient-pole synchronous machines". *IEEE Trans. Energy Convers. 17* (2002), 478–484.

[84] KNIGHT, A. M., AND KARMAKER, H. "Investigation and simulation of fields in large salient pole synchronous machines with skewed stator slots". *IEEE transactions on energy conversion 20* (2005), 604–610.

[85] KNIGHT, A. M., TROITSKAIA, S., STRANGES, N., AND MERKHOUF, A. "Analysis of large synchronous machines with axial skew, part 1: flux density and open-circuit volt-

age harmonics". *Electric Power Applications, IET 3*, 5 (2009), 389–397.

[86] KNIGHT, A. M., TROITSKAIA, S., STRANGES, N., AND MERKHOUF, A. "Analysis of large synchronous machines with axial skew, part 2: inter-bar resistance, skew and losses". *IET electric power applications 3*, 5 (2009), 398–406.

[87] KOCABAS, D. A. "Novel winding and core design for maximum reduction of harmonic magnetomotive force in AC motors". *IEEE Trans. on Magn. 45* (2009), 735–746.

[88] KOLONDZOVSKI, Z., AND PETKOVSKA, L. "Analysis of the synchronous machine reactance and methods for their determination". In *MAKOCIGRE Symp., Ohrid* (2004).

[89] KOLONDZOVSKI, Z., AND PETKOVSKA, L. "Determination of a synchronous generator characteristics via finite element analysis". *Serbian Journal of Electrical Engineering 2* (2005), 157–162.

[90] KOSTENKO, M. *"Electrical machines"*. Foreign languages publishing house, 1962.

[91] KRAUSE, P. C., WASYNCZUK, O., SUDHOFF, S. D., AND PEKAREK, S. *Analysis of electric machinery and drive systems*, vol. 75. John Wiley & Sons, 2013.

[92] KRON, G. *"The application of tensors to the analysis of rotating electrical machinery"*. General electric review, 1938.

[93] KRON, G. *"A short course in tensor analysis for electrical engineers"*. John Wiley & Sons, 1942.

[94] KRUG, K., DAREVSKII, A., ZEVEKE, G., IONKIN, P., LOMONOSOV, V. Y., NETUSHIL, A., AND STRAKHOV, S. "Fundamentals of electrical engineering". *Gosdnergoizdat, Moscow* (1952).

[95] Kumbhar, G., Kulkarni, S., Escarela-Perez, R., and Campero-Littlewood, E. "Applications of coupled field formulations to electrical machinery". *COMPEL: The International Journal for Computation and Mathematics in Electrical and Electronic Engineering 26*, 2 (2007), 489–523.

[96] Langsdorf, A. S. *Theory of alternating current machinery*. Tata McGraw-Hill Education, 1955.

[97] Lau, G.-K. "Design Optimization of Actuators Using ANSYS".

[98] Lawrenson, P., and Miller, T. "Transient solution of the diffusion equation by discrete fourier transformation". *Finite Elements in Electrical and Magnetic Field Problems* (1978).

[99] Lidenholm, J., and Lundin, U. "Estimation of hydropower generators parameters through field simulations of standard tests". *IEEE Trans. Energy Convers. 25* (2010), 931–939.

[100] Lombard, P., and Meunier, G. "A general purpose method for electric and magnetic combined problems for 2D, axisymmetric and transient systems". *Magnetics, IEEE Transactions on 29*, 2 (1993), 1737–1740.

[101] Longley, F. "The calculation of alternator swing curves: The step-by-step method". *American Institute of Electrical Engineers, Transactions of the 49*, 3 (1930), 1129–1150.

[102] Lyon, W. V. *"Applications of the method of symmetrical components"*. McGraw-Hill book company, inc., 1937.

[103] Ma, L., Sanada, M., Morimoto, S., and Takeda, Y. "Prediction of iron loss in rotating machines with rotational loss included". *IEEE Trans. Magn. 39* (2003), 2036–2041.

159

[104] MAGNUSSEN, F., CHIN, Y.-K., SOULARD, J., BROD-
      DEFALK, A., ERIKSSON, S., AND SADARANGANI, C.
      ”Iron losses in salient permanent magnet machines at field-
      weakening operation”. In *Industry Applications Confer-
      ence, 2004. 39th IAS Annual Meeting. Conference Record
      of the 2004 IEEE* (2004), vol. 1, IEEE.

[105] MAHON, L. *”Diesel generator handbook”*. Butterworth-
      Heinemann, 1992.

[106] MERKHOUF, A., GUILLOT, E., HUDON, C., DESNOY-
      ERS, M., AGUIAR, A. B., AND AL-HADDAD, K. ”Electro-
      magnetic loss computation in large hydro electrical genera-
      tor using different existing models”. In *Electrical Machines
      (ICEM), 2012 XXth International Conference on* (2012),
      IEEE, pp. 238–242.

[107] MI, C., SLEMON, G. R., AND BONERT, R. ”Modeling
      of iron losses of permanent-magnet synchronous motors”.
      Industry Applications, IEEE Transactions on 39, 3 (2003),
      734–742.

[108] MONORCHIO, A., BRETONES, A., GOMEZ MARTIN, R.,
      MANARA, G., AND MITTRA, R. ”A hybrid time-domain
      technique that combines the finite element, finite difference
      and method of moment techniques to solve complex elec-
      tromagnetic problems”. *IEEE Transactions on Antennas
      and Propagation 52* (2004), 2666–2674.

[109] MUKHOPADHYAY, A. K. *”Matrix analysis of electrical ma-
      chines”*. New Age International, 2007.

[110] NAKAHARA, A., TAKAHASHI, K.AND IDE, K., KANEDA,
      J., HATTORI, K., WATANABE, T., MOGI, H., KAIDO,
      C., MINEMATSU, E., AND HANZAWA, K. ”Core loss in
      turbine generators: Analysis of no-load core loss by 3D

magnetic field calculation". In *Proc. of the XVI Int. Conf. on Electrical Machines (ICEM 2004)*.

[111] NONAKA, S., AND KAWAGUCHI, T. "A new variable-speed AC generator system using a brushless self-excited-type synchronous machine". *Industry Applications, IEEE Transactions on 28*, 2 (1992), 490–496.

[112] NONAKA, S., AND KAWAGUCHI, T. "Excitation scheme of brushless self-excited-type three-phase synchronous machine". *Industry Applications, IEEE Transactions on 28*, 6 (1992), 1322–1329.

[113] NONAKA, S., KESAMARU, K., AND HORITA, K. "Analysis of brushless four-pole three-phase synchronous generator without exciter by the finite element method". *Industry Applications, IEEE Transactions on 30*, 3 (1994), 615–620.

[114] OJO, J. O., AND LIPO, T. A. "An improved model for saturated salient pole synchronous motors". *Energy Conversion, IEEE Transactions on 4*, 1 (1989), 135–142.

[115] OKAFOR, E. N. C., OKON, P. E., AND OKORO, C. C. "Magnetic field mapping of a direct current electrical machine using finite element method". *Journal of Applied Sciences Research 5(11)* (2009), 1889–1898.

[116] PARK, R. "Definition of an ideal synchronous machine and formula for the armature flux linkages". *General Electric Review 31*, 6 (1928), 332–334.

[117] PARK, R. "Two-reaction theory of synchronous machines-II". *American Institute of Electrical Engineers, Transactions of the 52*, 2 (1933), 352–354.

[118] PARK, R. H. "Two-reaction theory of synchronous machines generalized method of analysis-part I". *American*

161

Institute of Electrical Engineers, Transactions of the 48, 3 (1929), 716–727.

[119] PETKOVSKA, L., KOLONDZOVSKI, Z., AND CVETKOVSKI, G. "FEM coupling for transient performance analysis of a salient poles synchronous generator". In *Universities Power Engineering Conference, 2008. UPEC 2008. 43rd International* (2008), IEEE, pp. 1–5.

[120] PETRINIC, M., CAR, S., AND ELEZ, A. "Iterative procedure for determination of synchronous generator load point using finite element method". In *Electrical Machines (ICEM), 2012 XXth International Conference on* (2012), IEEE, pp. 339–345.

[121] PETROV, G. "Electric machines, Part I: Induction and synchronous machines". *National Electric Power, Moscow 311* (1963).

[122] PODGORNOVS, A., AND ZVIEDRIS, A. "Characteristics of the synchronous motors determination by results of mathematical simulation of magnetic field". In *Proc. of International Conference on Compatibility in Power Electronics, 2007.*

[123] PREMKUMAR, C. "Modelling considerations in the magnetic field analysis of rotating electrical machines using the finite element method". *BHEL Journal* (2006), 60–66.

[124] PREMKUMAR, C. "Turbogenerator induced voltage waveform computation and telephone harmonic capability prediction". *BHEL Journal* (2006), 26–32.

[125] PUCHSTEIN, A. "Calculation of slot constants". *American Institute of Electrical Engineers, Transactions of the 66*, 1 (1947), 1315–1323.

[126] Pyrhonen, J., Tapani, J., and Valeria, H. "Design of rotating electrical machines". Wiley, 2009.

[127] Rabelo, B., Hofmann, W., Tilscher, M., and Basteck, A. "Voltage regulator for reactive power control on synchronous generators in wind energy power plants". In *Nordic Workshop on Power and Industrial Electronics (NORPIE). Norway* (2004), pp. 1–6.

[128] Rafinejad, P., and Sabonnadiere, J.-C. "Finite element computer programs in design of electromagnetic devices". *Magnetics, IEEE Transactions on 12*, 5 (1976), 575–578.

[129] Ranlöf, M. "Electromagnetic Analysis of Hydroelectric Generators".

[130] Ranlof, M., P. R., and U, L. "On permeance modeling of large hydrogenerators with application to voltage harmonics prediction". *IEEE Trans. on Energy Conversion 25* (2010), 1179–1186.

[131] Rapetti, F., Santandrea, L., Bouillault, F., and Razek, A. "Calculation of eddy currents in moving structures using a finite element method on non-matching grids". *COMPEL-The international journal for computation and mathematics in electrical and electronic engineering 19*, 1 (2000), 10–29.

[132] Roshen, W. "Iron loss model for permanent-magnet synchronous motors". *Magnetics, IEEE Transactions on 43*, 8 (2007), 3428–3434.

[133] Rudenberg, R. "Saturated synchronous machines under transient conditions in the pole axis". *American Institute of Electrical Engineers, Transactions of the 61*, 6 (1942), 297–306.

[134] Sadiku, M. N. *Numerical techniques in electromagnetics.* CRC press, 2000.

[135] Sadowski, N., Carly, B., Lefevre, Y., Lajoie-Mazenc, M., and Astier, S. "Finite element simulation of electrical motors fed by current inverters". *Magnetics, IEEE Transactions on 29*, 2 (1993), 1683–1688.

[136] Sadowski, N., Lefevre, Y., Lajoie-Mazenc, M., and Cros, J. "Finite element torque calculation in electrical machines while considering the movement". *Magnetics, IEEE Transactions on 28*, 2 (1992), 1410–1413.

[137] Sahm, D. "A two-axis, bond graph model of the dynamics of synchronous electrical machines". *Journal of the Franklin Institute 308*, 3 (1979), 205–218.

[138] Salon, S., and Chari, M. *"Numerical methods in electromagnetism".* Academic press, 1999.

[139] Salon, S. J. *"Finite element analysis of electrical machines"*, vol. 101. Kluwer academic publishers Boston USA, 1995.

[140] Sarma, M. S. *"Synchronous machines: their theory, stability and excitation systems".* Gordon & Breach Publishing Group, 1979.

[141] Say, M. G. *"The performance and design of alternating current machines: transformers, three-phase induction motors and synchronous machines".* Pitman, 1952.

[142] Schmidt, E., Traxler-Samek, G., and Schwery, A. *"Design improvement of large hydro-generators using high efficient numerical field calculation methods".* na, 2002.

[143] Schulz, R., Farmer, R., Bennett, S. M., Selin, D., and Sharma, D. "Benefit assessment of finite element

based generator saturation model". *IEEE transactions on Power Systems 2* (1987), 1027–1033.

[144] SCHWERY, A., TRAXLER-SAMEK, G., AND SCHMIDT, E. " Application of a transient finite element analysis with coupled circuits to calculate the voltage shape of a synchronous generator". In *Electromagnetic Field Computation (CEFC) 2002. IEEE Conference on* (2002).

[145] SHANMING, W., XIANGHENG, W., PENGSHENG, S., YU, F., WEIMING, M., AND GAIFAN, Z. "Research on voltage harmonic distortion of synchronous generators". In *Proceedings of 5th International Conference on Electrical Machines and Systems (ICEMS 2001)*.

[146] SHAOGANG, H., YONGHONG, X., AND SHANCAI, Q. "Calculation of the third harmonic excitation of synchronous generator using tooth flux method". In *Proc. of International Conference on Electrical Machines and Systems (ICEMS 2007)*.

[147] SHAOGONG, H., SHANCAI, Q., AND YONGHONG, X. "Design method for third harmonic excitation system based on computation of electromagnetic field". In *Proc. of International Conference on Electrical Machines and Systems (ICEMS 2007)*.

[148] SHIBATA, F., AND KOHRIN, T. "A brushless, self-excited polyphase synchronous generator". *Power Apparatus and Systems, IEEE Transactions on*, 8 (1983), 2413–2419.

[149] SHIBATA, F., AND NAOE, N. "Characteristics of brushless and exciterless, self-excited synchronous generators". In *Industry Applications Society Annual Meeting, 1990., Conference Record of the 1990 IEEE* (1990), IEEE, pp. 293–300.

[150] SHIMA, K., IDE, K., AND TAKAHASHI, M. "Finite-element calculation of leakage inductances of a saturated salient-pole synchronous machine with damper circuits". *Energy Conversion, IEEE Transactions on 17*, 4 (2002), 463–470.

[151] SHIMA, K., IDE, K., AND TAKAHASHI, M. "Analysis of leakage flux distributions in a salient-pole synchronous machine using finite elements". *Energy Conversion, IEEE Transactions on 18*, 1 (2003), 63–70.

[152] SILVESTER, P., AND CHARI, M. "Finite element solution of saturable magnetic field problems". *Power Apparatus and Systems, IEEE Transactions on*, 7 (1970), 1642–1651.

[153] SILVESTER, P. P., AND FERRARI, R. L. *"Finite elements for electrical engineers"*. Cambridge university press, 1996.

[154] SINGH, B., AND RAVI, J. "Design and analysis of a 3 KVA, 28 V permanent magnet brushless alternator for light combat aircraft". In *Proc. of the International Conference on Power electronics, Drives and Energy systems (PEDES 2006)*.

[155] SINGH, M., SINGH, S. P., SINGH, B., PANDEY, A. S., DIXIT, R., AND MITTAL, N. "Stand alone power generation by 3φ asynchronous generator: A comprehensive survey". In *Power, Control and Embedded Systems (ICPCES), 2012 2nd International Conference on* (2012), IEEE, pp. 1–14.

[156] SPOONER, E., AND WILLIAMSON, A. "Direct coupled, permanent magnet generators for wind turbine applications". *IEE Proceedings-Electric Power Applications 143*, 1 (1996), 1–8.

[157] STEINMETZ, C. P. *"Theory and calculation of alternating current phenomena"*, vol. 4. McGraw-Hill Book Company, Incorporated, 1916.

[158] SUSNJIC, L. *"Finite-element simulation of a synchronous generator under the case of symmetrical sudden short-circuit in Q-axis"*. In *Electric Machines and Drives Conference Record, 1997. IEEE International* (1997), IEEE, pp. MC1–7.

[159] SYKULSKI, J. K. *"Field Simulation as an Aid to Machine Design: the State of the Art"*. In *Power Electrocnics and Motion Control Conference, 2006. EPE-PEMC 2006. 12th International* (2006), IEEE, pp. 1937–1942.

[160] TANDON, S., ARMOR, A., AND CHARI, M. *"Nonlinear transient finite element field computation for electrical machines and devices"*. *Power Apparatus and Systems, IEEE Transactions on*, 5 (1983), 1089–1096.

[161] TANDON, S., RICHTER, E., AND CHARI, M. *"Finite elements and electrical machine design"*. *IEEE transactions on Magnetics 16* (1980), 1020–1022.

[162] TESSAROLO, A., BASSI, C., AND GIULIVO, D. *"Time-stepping finite-element analysis of a 14-MVA salient-pole shipboard alternator for different damper winding design solutions"*. *Industrial Electronics, IEEE Transactions on 59*, 6 (2012), 2524–2535.

[163] TROWBRIDGE, C., AND SYKULSKI, J. *"Some key developments in computational electromagnetic and their attribution"*. *IEEE transactions on Magnetics 42* (2006), 503–508.

[164] TROWBRIDGE, C. W. *"An Introduction to computer aided electromagnetic analysis"*. Vector Fields, 1990.

[165] TSUKERMAN, I. "Application of multilevel preconditioners to finite element magnetostatic problems". *Magnetics, IEEE Transactions on 30*, 5 (1994), 3562–3565.

[166] VAANANEN, J. "Circuit theoretical approach to couple two-dimensional finite element models with external circuit equations". *Magnetics, IEEE Transactions on 32*, 2 (1996), 400–410.

[167] WAIT, R. *"The numerical solution of algebraic equations"*. Wiley New York, 1979.

[168] WAKILEH, G. J. "Harmonics in rotating machines". *Electric Power Systems Research 66*, 1 (2003), 31–37.

[169] WAMKEUE, R., KAMWA, I., AND CHACHA, M. "Line to line short circuit based finite element performance and parameter predictions of large hydrogenerators". *IEEE Transactions on Energy Conversion 18* (2003), 370–378.

[170] WANG, G. G. "Definition and review of virtual prototyping". *Journal of Computing and Information Science in engineering 2*, 3 (2002), 232–236.

[171] WELCHKO, B. A., JAHNS, T. M., SOONG, W. L., AND NAGASHIMA, J. M. "IPM synchronous machine drive response to symmetrical and asymmetrical short circuit faults". *Energy Conversion, IEEE Transactions on 18*, 2 (2003), 291–298.

[172] WHITE, D., AND WOODSON, H. "Electromagnetic energy conversion". *New-York: John Willey & Sons, Inc 528* (1959).

[173] WILLIAMSON, S., FLACK, T. J., AND VOLSCHENK, A. F. "Representation of skew in time-stepped two-dimensional finite-element models of electrical machines". *Industry Applications, IEEE Transactions on 31*, 5 (1995), 1009–1015.

[174] WILLIAMSON, S., AND VOLSCHENK, A. "Time-stepping finite element analysis for a synchronous generator feeding a rectifier load". *IEE Proceedings-Electric Power Applications 142*, 1 (1995), 50–56.

[175] YAMAZAKI, K., AND SETO, Y. "Iron loss analysis of interior permanent-magnet synchronous motors-variation of main loss factors due to driving condition". *Industry Applications, IEEE Transactions on 42*, 4 (2006), 1045–1052.

[176] YILMAZ, M., AND KREIN, P. T. "Capabilities of finite element analysis and magnetic equivalent circuits for electrical machine analysis and design". In *Proc. of the Power Electronics Specialists Conference, 2008.*

[177] YONGHONG, X., SHAOGANG, H., AIGANG, G., JIN, R., AND PING, Z. "Analysis of the no load harmonic electromagnetic field of synchronous generator using tooth flux method". In *Proc. of the International Conference on Electrical Machines and Systems (ICEMS 2008).*

[178] ZHAN, Y., AND KNIGHT, A. M. "Parallel time-stepped analysis of induction machines with Newton–Raphson iteration and domain decomposition". *Magnetics, IEEE Transactions on 44*, 6 (2008), 1546–1549.

[179] ZHOU, P.-B. *Numerical analysis of electromagnetic fields.* Springer Science & Business Media, 2012.

169